

**IDENTIFICATION OF PROCESS DYNAMICS USING RELAY WITH
HYSTERESIS**



BAJARANGBALI

IDENTIFICATION OF PROCESS DYNAMICS USING RELAY WITH HYSTERESIS

A

*Thesis Submitted
in Partial Fulfilment of the Requirements
for the Degree of*

DOCTOR OF PHILOSOPHY

By

BAJARANGBALI



Department of Electronics and Electrical Engineering

Indian Institute of Technology Guwahati

Guwahati - 781 039, INDIA.

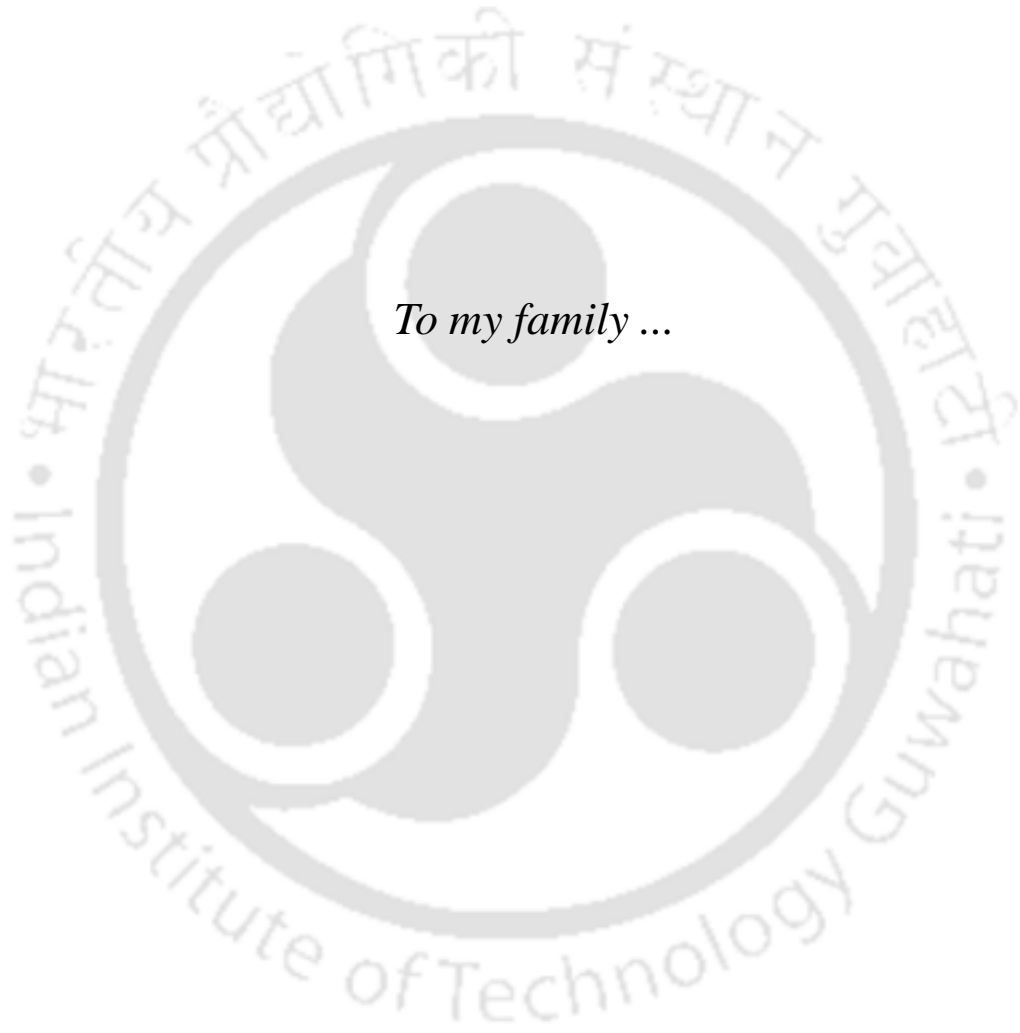
February, 2015

Certificate

This is to certify that the thesis entitled “**IDENTIFICATION OF PROCESS DYNAMICS USING RELAY WITH HYSTERESIS**”, submitted by **Bajarangbali** (11610222), a research scholar in the *Department of Electronics & Electrical Engineering, Indian Institute of Technology Guwahati*, for the award of the degree of **Doctor of Philosophy**, has been carried out by him under my supervision and guidance. The thesis has fulfilled all requirements as per the regulations of the institute and in my opinion has reached the standard needed for submission. The results embodied in this thesis have not been submitted to any other University or Institute for the award of any degree or diploma.

Dated:
Guwahati.

Prof. Somanath Majhi
Dept. of Electronics & Electrical Engg.
Indian Institute of Technology Guwahati
Guwahati - 781039, Assam, India.



Acknowledgements

At the outset, I would like to express my whole hearted and deep sense of gratitude to my supervisor, Prof. Somanath Majhi, for his excellent guidance and support throughout the course for this work. My heartfelt thanks to him for the unlimited support and patience shown to me. I am highly grateful to him for patiently and carefully checking all my manuscripts and thesis. This thesis would not have been possible without his bounteous effort.

I would like to thank my doctoral committee members Prof. C. Mahanta, Dr. Praveen Kumar and Dr. Praveen Tripathy for sparing their precious time to evaluate the progress of my work. Their suggestions have been valuable. I would also like to thank the Head of the Department, Prof. R. Bhattacharjee and other faculty members for their kind help carried out during my academic studies. My special thanks to Mr. Sanjib, Mr. Sidananda, Mr. Goswami and all the members of the Control & Instrumentation Laboratory for maintaining an excellent computing facility and providing various resources useful for the research work.

I am highly grateful to PES Institute of Technology, Bangalore South Campus, Karnataka, India for deputing me to study at Indian Institute of Technology Guwahati (IITG), a prestigious institute in India and providing me with financial assistance. I sincerely thank Dr. J. Suryaprasad, Director, PESIT South Campus, Bangalore for his help and support.

I had a great time with my many friends at IIT Guwahati, including (but not limited to) Saurabh, Mridul, Arghya, Ankit, Tousif, Sanjoy, Ramesh, Dola Gobinda and Mehta. I thank them for their support and encouragement. Among those deserving of a special mention is my wife Seema, who had extended her wholeheartedly support to bring this work into existence. She has been able to take care of my daughter extremely well. I thank my daughter Sanvi for keeping me energetic and reducing my worries. Again, I am grateful to my parents, in-laws, sisters and brothers, whose love and encouragement made this research possible.

I am thankful to AICTE, Govt. of India for financing my studies under QIP scheme at IIT Guwahati. Finally, I would like to thank the Almighty God for bestowing me this opportunity and showering his blessings on me to come out successful against all odds.

(Bajarangbali)

Abstract

In recent years, many research work on relay based process identification have been reported. Still there is much scope for improvements and extensions of this method. Relay with hysteresis has advantage of reducing the effect of noise as compared to ideal and asymmetrical relays. In our proposed method this relay with hysteresis is utilized. In this thesis using describing function technique explicit expressions are derived and using state space method improved results are obtained.

This thesis presents identification of single-input-single-output (SISO) and two-input-two-output (TITO) process dynamics using relay with hysteresis. The analytical expressions are derived based on describing function (DF) technique and state space method. The DF technique is applied to develop off-line and on-line identification methods for SISO and TITO processes whereas the state space method is applied for off-line identification of SISO processes. In case of SISO processes a generalized second order plus time delay (SOPDT) process model is realized in terms of a class of process models. The proposed DF technique is extended for identification of TITO processes in terms of two SISO process models. Even though DF technique is simple and gives explicit expressions but suffers from the limitation of approximate results.

To overcome the limitations of DF technique, firstly the state space method is applied to estimate the model parameters of SISO processes with all pole form of representation. The state space method is further extended to SISO non-minimum phase (NMP) processes where a SOPDT NMP process model is realized in terms of a class of process models. Relay with hysteresis is used in the closed loop to generate sustained oscillations or limit cycle output whose frequency and amplitude are utilized to identify the process dynamics. As relay with hysteresis has advantage of mitigating the effect of measurement noise. Further, noise elimination is carried out with the help of Fourier series based curve fitting technique which is applied during identification of processes using DF technique. As the curve fitting technique is an off-line

method hence, for state space based identification a closed loop structure consisting of the process, relay with hysteresis and a denoising block is proposed for online mitigation of noise. The combined effect of this denoising block and relay with hysteresis gives good results in the face of measurement noise. The proposed state space method shows significant improvement in results as compared with the conventional relay feedback technique. In present work the identification algorithms are developed for linear time invariant (LTI) process models.



CONTENTS

List of Figures	iv
List of Tables	vi
Nomenclature	viii
Mathematical Notations	ix
List of Publications	xi
1 Introduction	1
1.1 Research Background	1
1.2 Motivation	7
1.3 Contributions of this Thesis	8
1.4 Thesis Organization	9
2 Off-line and on-line identification of SISO processes	11
2.1 Introduction	11
2.2 Identification method and analytical expressions	12
2.3 Issue of measurement noise and load disturbance	17
2.4 Process identification	18
2.4.1 FOPDT process model	18
2.4.2 SOPDT process model	23
2.4.3 Underdamped SOPDT process model	30
2.4.4 Critically damped SOPDT process model	36
2.5 Generalized analytical expressions	39

2.5.1	Expressions for SOPDT process model	40
2.5.2	Expressions for FOPDT process model	41
2.6	Summary	42
3	Off-line and on-line identification of TITO processes	44
3.1	Introduction	44
3.2	Identification method	45
3.3	Estimation of process model parameters	48
3.4	Simulation results	50
3.5	Summary	57
4	Relay with hysteresis and state space based identification	58
4.1	Introduction	58
4.2	Identification method	60
4.2.1	Measurement noise and denoising	61
4.3	Derivation of analytical expressions	63
4.3.1	Expression for ε	65
4.3.2	Expression for t_p	66
4.3.3	Expression for A_p	67
4.3.4	Estimation of δ	68
4.4	Process identification	68
4.4.1	SOPDT process model	68
4.4.2	FOPDT process model	73
4.4.3	Underdamped SOPDT process model	77
4.4.4	Critically damped SOPDT process model	79
4.4.5	Integrating SOPDT process model	81
4.5	Implementation of proposed method in real plants	84
4.6	Summary	86

5	Identification of processes with non-minimum phase characteristics	87
5.1	Introduction	87
5.1.1	Contributions compared to the reference [1]	89
5.2	Identification method	89
5.3	Analytical expressions for parametric estimation	90
5.4	Process identification	94
5.4.1	FOPDT NMP process model	94
5.4.2	Overdamped SOPDT NMP process model	96
5.4.3	Underdamped SOPDT NMP process model	98
5.4.4	Critically damped SOPDT NMP process model	101
5.4.5	Integrating SOPDT NMP process model	103
5.5	Summary	106
6	Conclusions and Future Work	107
6.1	Conclusions	107
6.2	Suggestions for further work	108
A	Supplementary Materials	110
A.1	Detailed derivation of the expression (2.1)	110
A.2	Detailed derivation of the expressions (4.7) and (4.8)	112
A.3	Detailed derivation of the expressions (5.11) and (5.12)	114
A.4	Procedure to use <i>fsolve</i> function	115
	References	118

LIST OF FIGURES

2.1	Conventional off-line identification scheme	13
2.2	Conventional on-line identification scheme	13
2.3	Equivalent representation of Fig. 2.2	14
2.4	Symmetrical relay diagrams	14
2.5	Process output and input signals for ideal relay	15
2.6	Process output and input signals for relay with hysteresis	15
2.7	Relay and limit cycle outputs	21
2.8	Noisy and denoised limit cycle outputs	23
2.9	Limit cycle and its second derivative output	28
2.10	Limit cycle output	30
2.11	Nyquist plots for Example 4: (a) Actual process, (b) identified model (off-line) and (c) model proposed by Lavanya et al. [2]	33
2.12	Low frequency noisy signal and denoised limit cycle outputs	34
2.13	Nyquist plots for Example 6: (a) Actual process, (b) identified model (off-line), (c) identified model (on-line) and (d) model proposed by Thyagarajan & Yu [3]	38
3.1	Conventional TITO system with relay and controller	46
3.2	Equivalent representation of Fig. 3.1	47
3.3	Limit cycle output from loop 1	51
3.4	Noisy and denoised limit cycle outputs from loop 1	52
3.5	Nyquist plots: (a) proposed model, (b) proposed by Padhy et al. [4] and (c) decoupled model	53

3.6	Nyquist plots: (a) proposed model, (b) proposed by Padhy et al. [4] and (c) decoupled model	54
3.7	Noisy and denoised limit cycle outputs from loop 1	56
4.1	Proposed relay feedback identification scheme	60
4.2	Denoising block	61
4.3	Limit cycle output and its second derivative for SOPDT process	63
4.4	Noisy and denoised signals	70
4.5	Nyquist plots for Example 2: (a) Actual process, (b) proposed model, (c) model proposed by Liu and Gao [5] and (d) model proposed by Vivek and Chidambaram [6]	72
4.6	Noisy and denoised signals	75
4.7	Flowchart for implementation procedure	85
5.1	Relay feedback block diagram with denoising block	90
5.2	Half limit cycle output	93
5.3	Process output	95
5.4	Noisy and denoised limitcycles	97
5.5	Noisy and denoised limitcycles	100
A.1	Nonlinear feedback scheme	110

LIST OF TABLES

2.1	Comparison of process models for Example 1	22
2.2	Comparison of process models for Example 2	29
2.3	Comparison of process models for Example 3	30
2.4	Comparison of process models for Example 4	34
2.5	Comparison of process models for Example 5	35
2.6	Effect of measurement noise on parameters in % error, for Example 5	36
2.7	Comparison of process models for Example 6	38
2.8	Effect of measurement noise on parameters in % error for Example 6	39
3.1	Error analysis using H_∞ norm	54
3.2	Error analysis for estimated parameters for Example 2	56
4.1	Comparison of process models for Example 1	71
4.2	Effect of measurement noise on parameters in % error, for Example 1	71
4.3	Comparison of process models for Example 2	73
4.4	Comparison of process models for Example 3	75
4.5	Comparison of process models for Example 4	76
4.6	Effect of measurement noise on parameters in % error, for Example 4	76
4.7	Effect of measurement noise on parameters in % error, for Example 5	79
4.8	Comparison of process models for Example 6	81
4.9	Comparison of process models for Example 7	83
5.1	Comparison of process models for Example 2	97
5.2	Comparison of model parameters in % error	98
5.3	Comparison of process models for Example 3	100

5.4	Comparison of model parameters in % error	101
5.5	Comparison of process models for Example 4	102
5.6	Comparison of model parameters in % error	103
5.7	Comparison of process models for Example 5	104
5.8	Comparison of model parameters in % error	104
5.9	Comparison of process models for Example 6	105
5.10	Comparison of model parameters in % error	105



NOMENCLATURE

DF	Describing function
FOPDT	First order plus time delay process model
FPAA	Field programmable analog array
PID	Proportional-integral-derivative controller
NMP	Non-minimum phase process model
RHP	Right half of the s-plane
SISO	Single-input-single-output process model
SOPDT	Second order plus time delay process model
SNR	Signal to noise ratio
TITO	Two-input-two-output process model

MATHEMATICAL NOTATIONS

K	Steady state gain of a process model
δ	Time delay of a process model
τ_1, τ_2	Time constants of a process model
z	Right half s-plane zero of a process model
K_P	Proportional gain
T_I	Integral time constant
T_D	Derivative time constant
h	Amplitude of a relay
ε	Hysteresis of a relay
A_p	Peak amplitude of limit cycle output
A_d	Amplitude at discontinuity in limit cycle output
T_p	Half period of symmetrical limit cycle output
t_p	Time at which peak amplitude of limit cycle occurs after zero crossing
$y(t)$	Output signal
$u(t)$	Process input
$r(t)$	Set-point / reference input
$e(t)$	Error signal
t	Time
$G(s)$	Transfer function of a process
$G_m(s)$	Transfer function of a process model
$G_c(s)$	Transfer function of a controller
N	Describing function of the relay with hysteresis

- \tilde{E} Estimation error value
- ω_{cr} Critical frequency of the process



LIST OF PUBLICATIONS

Journal Publications

1. Bajarangbali, Majhi S. and Pandey S., “Identification of FOPDT and SOPDT Process Dynamics using Closed Loop Test”, *ISA Transactions (Elsevier)*, vol. 53(4), 1223 - 1231, 2014.
2. Bajarangbali and Majhi S., “Identification of underdamped process dynamics”, *Systems Science & Control Engineering (Taylor & Francis)*, vol. 2(1), 541 - 548, 2014.
3. Bajarangbali and Majhi S., “Relay based identification of systems”, *International Journal of Scientific & Engineering Research*, vol. 3, 1 - 4, 2012.
4. Bajarangbali and Majhi S., “Identification of integrating and critically damped systems with time delay”, *Control Theory and Technology (Springer)* manuscript no. JCTA 14-0018 (accepted).
5. Bajarangbali and Majhi S., “Identification of non-minimum phase processes with time delay in the presence of measurement noise”, *ISA Transactions (Elsevier)* manuscript no. ISATRANS-D-14-00546R1 (revision submitted).
6. Bajarangbali and Majhi S., “Estimation of first and second order process model parameters”, *Proceedings of The National Academy of Sciences (Springer)* manuscript no. NASA-D-14-00152 (under review).

Conference Publications

1. Bajarangbali and Majhi S., “Modeling of Stable and Unstable Second Order Systems with Time Delay”, *IEEE INDICON*, IIT Bombay, India, 2013.

2. Bajarangbali and Majhi S., “TITO system identification using relay with hysteresis”, *IEEE International Conference on Power and Energy in NERIST, (ICPEN 2012)*, India 2012.
3. Bajarangbali and Majhi S., “Smart Relay Based Online Estimation of Process Model Parameters”, *International Conference on Soft Computing for Problem Solving (SocProS 2012)*, Jaipur, India 2012 and *Advances in Intelligent Systems and Computing*, Vol. 236, pp. 1195 - 1204, (Springer), India 2014.
4. Bajarangbali and Majhi S., “Modelling of integrating and unstable time delay processes”, *Proc. of 36th NSC, Annamalai Nagar, India 2012* and *Recent advancements in system modelling applications, Lecture Notes in Electrical Engineering*, Vol. 188, pp. 311 - 318, (Springer), India 2013.

CHAPTER 1

INTRODUCTION

1.1 Research Background

There are many methods (e.g., derivation of model equations by using first principles and then utilizing the process data to estimate the model parameters, system identification using neural networks and fuzzy logic based identification) available for identification of unknown process dynamics. Still relay based process identification has gained wide acceptance in industrial applications, as it is easy to implement and saves time. The relay feedback technique has several attractive features [7–9] as mentioned below:

1. Relay feedback technique helps in identifying the process information around the important frequency termed as the ultimate frequency (the frequency where the phase angle corresponds to $-\pi$).
2. As it is a closed loop test, the process will not drift away from the nominal operating point.
3. It is more time efficient as compared to conventional step or pulse testing, for processes having a long time constant. The experimental time is approximately two to four times the ultimate period.
4. Relay based autotuning method can be modified to deal with disturbances and perturbations in the process.

A. Process identification using describing function (DF) technique

Process identification plays a significant role for analysis of process operation and also design of model based controller. Process identification corresponds to mathematical modeling of an unknown process in terms of transfer function form, utilizing the measurements of system's input and output signals. Recently, identification of process dynamics from relay feedback technique has gained considerable attention for controller tuning in process industries. In early eighties Åström and Hägglund [10] proposed the use of relay feedback testing called autotune variation (ATV) method for estimation of unknown process model parameters using describing function (DF) technique. This ATV method identifies process information around the important frequency called the ultimate frequency. Here in DF technique, the nonlinear device relay is approximated by a gain, hence the estimated parameters will be approximate. Applications of Åström and Hägglund autotuner are found throughout the process industries and the success of this autotuner is attributed to the fact that the identification and tuning mechanisms are so simple that operators understand how it works. Subsequently many variations to the original method have been developed and used in a number of applications, like autotuning of PID (proportional-integral-derivative) controller and process identification. Later, Luyben [11] used Åström's autotune method to obtain transfer functions of nonlinear and complex processes. Luyben applied this method for obtaining a suitable linear transfer function model of nonlinear distillation column using computer simulation. Luyben proposed two transfer functions and to fit the data into these transfer functions, five different models are developed. Each model had two equations for time constant parameter. After solving the two equations, if the values are approximately equal then the predefined transfer function is used to fit the corresponding model data. Hence, this method was more time consuming. A number of relay based identification methods [10–16] using DF technique have been proposed to obtain process models in terms of transfer functions. Chang et al. [17] developed analytical expressions for identification of first order, second order and higher order processes using Z-transform method. Li et al. [18] proposed estimation of unknown process model parameters for stable and unstable processes by

using two relay tests. But use of two relay tests increases the time as the number of experiments doubled. Shen et al. [12] considered dual input describing function approach (DIDF) and an input biased relay feedback experiment to identify two points on the Nyquist curve. But this method can be applied only for stable processes. Liu et al. [19] presented a detailed tutorial review on process identification from relay or step test, including the significance of DF method, in the past three decades. Atherton [20] discussed the importance of relay in autotuning of controllers and also highlighted about DF method. Hang et al. [21] presented a tutorial review for auto-tuning of process controllers using relay feedback technique. Padhy and Majhi [14] proposed an ideal relay based identification algorithm for stable and unstable first order processes using DF method. Kumanan and Nagaraj [22] pointed out the significance of process identification for controller design and proposed tuning of PID controllers, employing firefly algorithm.

B. Extension to two-input-two-output (TITO) processes

Multivariable or MIMO (multi-input-multi-output) processes are commonly used in many process industries. Identification of these processes is a difficult task due to the interactions between the loops and system variables. Identification of multivariable processes using relay feedback testing can be done by three possible ways [23]: i) applying single relay feedback, ii) employing relay in sequence and iii) applying decentralized relay.

In single relay feedback scheme, the relay input is applied to one loop at a time while keeping the remaining loops open. In sequential relay feedback testing, the relay is applied to a loop to extract the process information later this loop is closed with a controller and the same procedure is repeated for the remaining loops. In the case of decentralized relay feedback scheme, relay inputs are simultaneously applied to all loops to acquire the process information. This decentralized relay feedback is the most preferred scheme [23] that is used for identification of multivariable process dynamics. The TITO (two-input-two-output) processes are considered as one of the most commonly used multivariable processes [24, 25]. Few researchers presented algorithms for identification of multivariable processes. Wang et al. [23] proposed identifica-

tion of TITO processes using decentralized relay feedback technique. Choi et al. [26] proposed identification of multivariable processes (TITO) using sequential loop closing method. But accurate time delay of the process can not be estimated here. Padhy and Majhi [27] have suggested on-line identification of TITO processes using relay feedback with describing function approximation. Grosdidier and Morari [28] defined a dynamic interaction measure, through which the stability of decentralized control system can be predicted along with performance loss caused by the system. Methods [29–33] are presented for automatic tuning of PI or PID controllers for multivariable processes.

C. State space based identification of SISO processes

Åström and Eykhoff [34] had given a detailed survey on process identification and also mentioned about the importance of identification for designing a control strategy. The parameters estimated by describing function method are approximate hence researchers started working towards development of exact expressions so that more accurate parameters could be estimated. For SISO processes, Wang et al. [35] developed exact expressions for time period and amplitude of the limit cycle under relay feedback for a first order plus time delay (FOPDT) process model. Initially the authors used biased relay to get oscillatory waveforms to identify the process. But using biased relay caused larger disturbances than unbiased relay, hence later the authors used unbiased relay to improve the results. Jahanmiri and Fallahi [36] proposed algorithms for identification of SOPDT processes based on the open loop test and step input variable. Majhi and Atherton [37] and Majhi [38], [39] developed relay based identification algorithms using state space approach along with ideal relay. Majhi and Mahanta [40] have extended the work of [37] and proposed novel identification method and control strategy for SOPDT integrating processes. Srinivasan and Chidambaram [41] used Laplace transform approach and modified asymmetrical relay feedback method to get improved FOPDT model parameters. But this method requires appropriate selection of an extra parameter γ (displacement in the relay height) for accurate calculation of process gain and ultimate frequency. Vivek and Chidambaram [42] also proposed

improved identification algorithms using Laplace transform method and single symmetric relay feedback test. Thyagarajan and Yu [3] and Panda and Yu [43] proposed waveform factor of relay feedback response to estimate unknown process model parameters applying ideal relay feedback. Panda [44] proposed time domain approach for estimation of SOPDT underdamped processes using relay feedback test. Mehta and Majhi [45] have proposed on-line identification of cascade control systems using relay with hysteresis. Using state space method and single relay feedback test Majhi and Atherton [46] developed exact expressions and suggested on-line tuning of process controllers for an unstable FOPDT systems. Marchetti et al. [13] used two relay tests for identification of open loop unstable processes. Liu and Gao [47] used Newton-Raphson iteration method for obtaining exact expressions for integrating and unstable process models. Recently Panda et al. [48] used single relay feedback test to estimate the process model parameters of integrating and time delay processes. Fedele [49] suggested step response test to obtain the FOPDT process model. Analytical expressions are proposed [50] to identify second order underdamped processes, considering rectangular pulse inputs. Mei and Li [51] suggested algorithms for identification of integrating processes with the help of step input test. Liu and Gao [52] used closed loop step response test to identify the process dynamics of integrating and unstable processes. But relay feedback method is more time efficient as compared to step or pulse input test [7]. Mehta and Majhi [53] used state space technique to estimate the nonlinear process model parameters. Recently Padhan and Majhi [54] utilized relay feedback method to identify the process dynamics of power system and suggested model based PID load frequency controller. Vivek and Chidambaram [55] used an ideal relay to extract the process information which is utilized to estimate the model parameters of critically damped SOPDT processes. Ananth and Chidambaram [56] proposed step response based identification algorithms to estimate the parameters of an unstable FOPDT process model using the PID controller. This method suffers from the stability problem which is pointed out by Cheres [57]. To overcome the stability problem in [56], Padma Sree and Chidambaram [58] proposed modifications to the method suggested in [56]. Luyben [59] presented identification of stable and unstable FOPDT processes using shape factor technique and relay input. Boiko [60] suggested identification of

FOPDT process dynamics using the locus of a perturbed relay system method. Sivakumar et al. [61] used a saturation relay feedback test to identify the process dynamics of first order and higher order processes with large time delay.

D. Extension to non-minimum phase processes

Relay feedback testing has gained wide acceptance for estimating unknown parameters of transfer function models of industrial processes and their control. The processes consisting of zero on the right half of the s-plane (RHP) are termed as non-minimum phase (NMP) processes. The NMP characteristics can be observed in some complex chemical systems [62], Zhang et al. [63] described ship's path control system in restricted waters as NMP system. Shen et al. [64] presented frequency domain analysis for prediction of the existence of sustained oscillations for processes with RHP poles and zeros. Balaguer et al. [65] used step response to identify the inverse response models. Wang et al. [66] proposed identification of minimum and non-minimum phase second and higher order process dynamics by applying fast Fourier transform (FFT) technique to find the frequency response of the process and inverse fast Fourier transform (IFFT) to construct the step response of the process. But relay feedback testing has got the advantage [7] of more time efficient for processes with long time constant. Panda et al. [48] presented relay based algorithms for model parameter estimation of integrating processes with time delay and also addressed about the transient response of the process with a zero in the numerator. Atherton and Majhi [62] used asymmetrical relay feedback technique to estimate the process model parameters, considering a second order system with zero in terms of a class of process models. Majhi [1] proposed algorithms for identification of NMP process dynamics using state space method. The author used ideal relay to extract the process information and to remove the effect of measurement noise, Fourier series based curve fitting technique is applied. Liu and Gao [67] considered asymmetrical relay with hysteresis for identification of NMP processes with time delay. The identification methods proposed by Majhi [1] and Liu and Gao [67] can be applied to either FOPDT NMP processes or higher order NMP

processes with repeated poles. Ramakrishnan and Chidambaram [68] applied an asymmetrical relay test and Laplace transform technique to derive the analytical expressions for estimation of process model parameters, considering a second order NMP process without time delay as one of the case studies. Vivek and Chidambaram [69] used asymmetrical relay and Laplace transform method to identify the process dynamics of an unstable SOPDT process with a zero in the numerator.

1.2 Motivation

Relay feedback method is widely used for identification of various types of process models in the process industry, still there is a scope for improvement. In the literature many authors used ideal relay or biased relay for identification of process dynamics, with or without noise. Use of biased relay generates an asymmetrical process output where it will be difficult to make out the presence of load disturbance at the process input so, an unbiased or ideal relay is suggested. As measurement noise is a common issue in practice, use of an ideal relay suffers from chattering leading to incorrect relay switching. To avoid this relay switching at wrong instants, relay with hysteresis is generally preferred. Hence, in proposed work we are using this relay with hysteresis. Most reported methods employing DF technique, derived analytical expressions for particular type of process model. This motivated us to develop the analytical expressions using DF technique for a particular process model as well as generalized model which is realized in terms of a class of process models. As DF technique gives approximate results hence expressions are derived using state space method to estimate the model parameters of a class of processes accurately. The state space method is extended to identify the process dynamics of various types of NMP process models. In the literature many identification methods are available for SISO processes, few authors proposed algorithms for identification of TITO processes using conventional relay. An attempt has been made to identify the process dynamics of TITO processes using DF method. Since relay with hysteresis has the advantage of reducing the effect of measurement noise, the identification methods are proposed using this relay. In process con-

trol, the majority of the processes with time delay are often assumed to be stable and unstable FOPDT or SOPDT process models. Hence, these process models are considered in proposed identification method.

1.3 Contributions of this Thesis

Although relay feedback technique for process identification has been widely addressed, there still exists a lot of scope to improve the results. In particular, in this thesis we have investigated and contributed to the following areas:

I. Off-line and on-line identification of SISO processes

Simple analytical expressions based on describing function (DF) technique are derived for identification of the class of processes in terms of transfer function models. The explicit expressions are derived by considering individual process models as well as generalized process model. A single relay with hysteresis is used in closed loop, to extract process information and to reduce the effect of measurement noise. Explicit expressions are derived for off-line and on-line estimation of stable and unstable process model parameters. Since measurement noise is a critical issue in process industries, validity of the proposed method is illustrated under noisy environment. As relay with hysteresis reduces the effect of noise, Fourier series based curve fitting technique is appended to obtain noise free process output.

II. Off-line and on-line identification of TITO processes

The DF technique used earlier for identification of SISO processes is extended to identify the process dynamics of TITO processes in terms of two SISO process models. The DF based expressions are derived for on-line method which can also be modified for off-line mode of operation. For denoising Fourier series based curve fitting technique is utilized.

III. Relay with hysteresis and state space based identification

As DF technique gives approximate results hence, state space method is used for off-line identification of accurate process dynamics for SISO stable or unstable FOPDT and SOPDT process models. A generalized SOPDT process model is realized in terms of a class of process models and state space method is applied to derive the mathematical expressions. Relay with hysteresis is used to extract the process information through limit cycle. The limit cycle quantities are utilized in the analytical expressions to estimate the process model parameters. The relay with hysteresis helps in generating sustained oscillations and also reduces effect of measurement noise, which is an important issue in process identification. Different types of processes in the form of transfer function models are considered to show the efficacy of the proposed method and results are compared with available methods in the literature with and without noise effect. To reduce the effect of measurement noise a denoising block is proposed in the closed loop along with the process and relay with hysteresis.

IV. Identification of processes with non-minimum phase characteristics

As the time domain based state space method gives improved identification results, the same is extended to derive the analytical expressions for estimation of NMP process model parameters. A generalized stable SOPDT NMP process model is realized in terms of a class of NMP process models like FOPDT, SOPDT overdamped, underdamped, critically damped and integrating process models. The denoising block proposed earlier is modified to recover the noise free process output.

1.4 Thesis Organization

This thesis is divided into six chapters. A brief description of each chapter is presented in this section.

- **Chapter 2:** In this chapter methods are proposed for off-line and on-line identification of SISO process dynamics, employing simple and effective DF technique. The nonlinear device relay with hysteresis is used to extract process information that helps in estimating

the unknown process model parameters. Another advantage of relay with hysteresis is that it reduces the effect of measurement noise. The validity of proposed method is illustrated with the help of typical process transfer function models from the literature. To test the robustness of the method, process dynamics are identified for different relay settings. Results with and without noise are compared using Nyquist plots and estimation errors.

- **Chapter 3:** In this chapter the DF technique is extended to identify the process dynamics of TITO processes in terms of two SISO process models. The expressions are derived for both on-line and off-line mode of operation. Simulation results are illustrated to show the usefulness of the proposed method even in the presence of measurement noise.
- **Chapter 4:** In this chapter state space based mathematical expressions are derived for a generalized SISO SOPDT process model which is realized in terms of stable or unstable FOPDT, SOPDT overdamped, underdamped, critically damped and integrating process models. The method proposed in this chapter gives accurate process model parameters. Effect of measurement noise is reduced using relay with hysteresis and a denoising block is proposed to further mitigate the noise effect. Well known examples are considered to show the general usefulness of the proposed method. Results are compared using estimation error values and Nyquist plots.
- **Chapter 5:** In this chapter state space method is extended to identify the process dynamics of SISO NMP process models during off-line mode of operation. The mathematical expressions derived for a stable SOPDT NMP process model are realized for a class of process models. The denoising block proposed earlier is modified to obtain noise free limit cycle output. Simulation results are illustrated to validate the proposed method and results are compared with recent methods.
- **Chapter 6:** In this chapter conclusions from the research work are drawn and suggestions for further work are documented.

CHAPTER 2

OFF-LINE AND ON-LINE IDENTIFICATION OF SISO PROCESSES

2.1 Introduction

Process identification plays an important role in automatic tuning of controllers in industries. In early eighties, Åström and Hägglund [10] proposed the use of relay feedback combined with describing function (DF) approximation as a simple means to determine the ultimate gain and ultimate frequency. Luyben [11] pioneered the use of relay feedback tests and describing function analysis for process identification. Many authors used DF method to develop the analytical expressions for estimation of process model parameters. Li et al. [18] proposed algorithms for identification of stable and unstable process dynamics using two relay tests which takes more time as the number of experiments doubled. Shen et al. [12] suggested an input biased relay test to find out two important points on the Nyquist curve by applying dual input describing function (DIDF) approach for the estimation of stable process model parameters. Marchetti et al. [13] employed an ideal relay to identify unstable processes. Lee et al. [70] used relay with hysteresis and DF method to obtain the process dynamics of stable FOPDT processes. Padhy and Majhi [14] derived analytical expressions based on DF method to calculate the process model parameters of stable and unstable FOPDT processes employing ideal relay. As in DF technique the nonlinear device relay is approximated by a nonlinear gain (N) hence, the estimated process model parameters are approximate. So, many identification methods are proposed to obtain accurate process dynamics. Vivek and Chidambaram [6] employed Laplace

transform approach for estimation of FOPDT process model parameters using symmetrical relay test. Thyagarajan and Yu [3] proposed shape factor analysis of relay feedback response to estimate unknown process model parameters. Majhi and Atherton [37, 46] and Majhi [39] developed relay based identification algorithms for different types of processes using ideal relay and state space method. These techniques give accurate results but involve extensive calculation and need to solve set of nonlinear equations simultaneously. In the literature, process identification methods are available for particular type of processes in general and few authors have considered the effect of noise. Under noisy environment an ideal relay is subjected to chattering hence, to avoid incorrect relay switching, relay with hysteresis is applied for process identification [19, 70]. Relay with hysteresis reduces the effect of measurement noise and further noise elimination is carried out with the help of Fourier series based curve fitting technique [1, 39]. Generally, the hysteresis width is selected as twice the standard deviation of noise [7].

In this chapter, explicit expressions are derived based on DF technique to estimate the unknown process model parameters of SISO processes during off-line and on-line mode of operation. In relay based process identification, DF method is widely adopted because of the ease of computation involved and general usefulness of the method. Initially the expressions are derived separately for stable or unstable FOPDT and SOPDT process models including underdamped and critically damped process models. Later it is shown that these expressions can be obtained by generalizing the expressions derived for SOPDT process model. The process information is extracted using relay with hysteresis. Validity of the presented method, with and without measurement noise, is demonstrated through simulation results which are compared with available methods in the literature.

2.2 Identification method and analytical expressions

This section presents the procedures for identification of FOPDT and SOPDT processes by off-line and on-line relay based closed loop tests. The conventional off-line identification structure

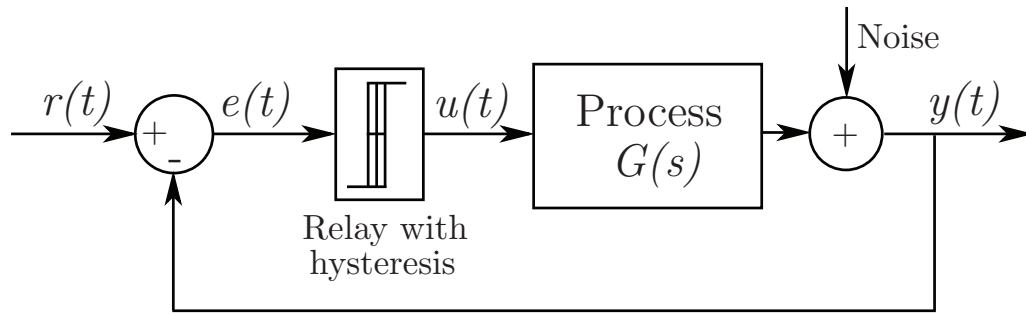


Figure 2.1: Conventional off-line identification scheme

is shown in Fig. 2.1, which consists of a relay with hysteresis and the process $G(s)$ in the closed loop. In figure, $r(t)$ is the reference or setpoint input, $e(t)$ is input to the relay and $u(t)$ and $y(t)$ are process input and output, respectively. It is assumed that the measurement noise appears at the process output. During process identification, the reference input $r(t)$ is made zero so that the system generates sustained oscillations or limit cycles. As shown in Fig. 2.2, the on-line identification structure consists of a PID controller connected in parallel with the relay in the loop, the equivalent representation of this figure is shown in Fig. 2.3. It is apparent from Fig. 2.3 that the relay sees a fictitious process $\bar{G}(s)$ ($G(s)$) coupled with the inner loop controller $G_c(s)$ in the loop. The process gets stabilizing signal from the inner feedback controller thereby improving its stability during identification. Under noisy environment the conventional relay experiment employing an ideal relay induces chattering in the process output which is not preferred in real time applications. Hence, a relay with hysteresis is applied to

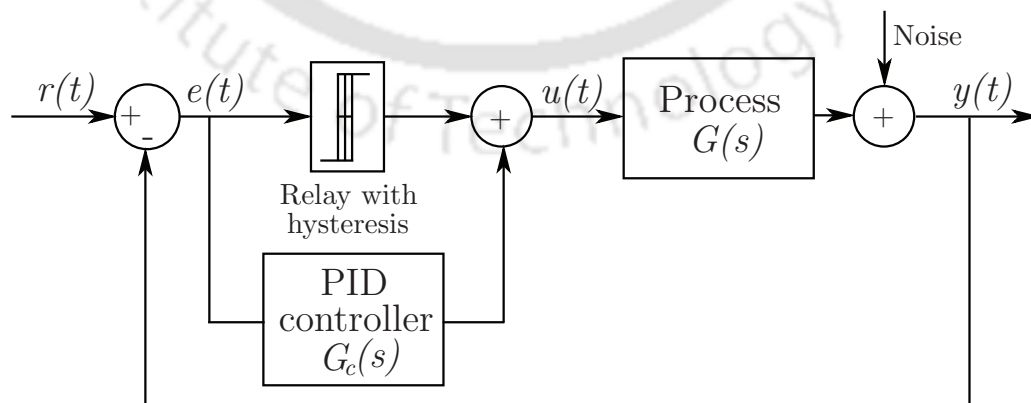


Figure 2.2: Conventional on-line identification scheme

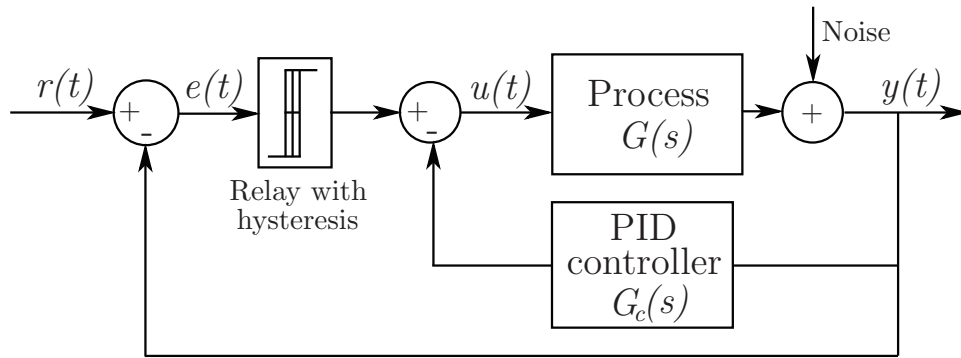


Figure 2.3: Equivalent representation of Fig. 2.2

minimize the correlation with high frequency noise. Therefore, to trigger the relay switching, the feedback error must shift beyond the zero crossing line by substantial quantity relative to the noise level.

The typical diagram of an ideal relay and relay with hysteresis is shown in Fig. 2.4 where $\pm h$ indicates relay height or amplitude and $\pm \epsilon$ is the hysteresis width which is generally set to twice the calculated standard deviation of noise. Figs. 2.5 and 2.6 show the relay responses to the process output for an ideal relay and relay with hysteresis, respectively.

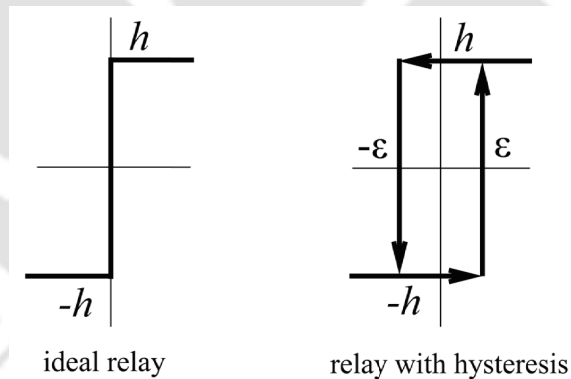


Figure 2.4: Symmetrical relay diagrams

In DF method the nonlinear device relay with hysteresis is approximated by a gain (N) as

$$N = \frac{4h \left(\sqrt{A_p^2 - \epsilon^2} - j\epsilon \right)}{\pi A_p^2} \quad (2.1)$$

(The detailed proof of (2.1) is given in Appendix A.1)

where A_p is peak amplitude of limit cycle.

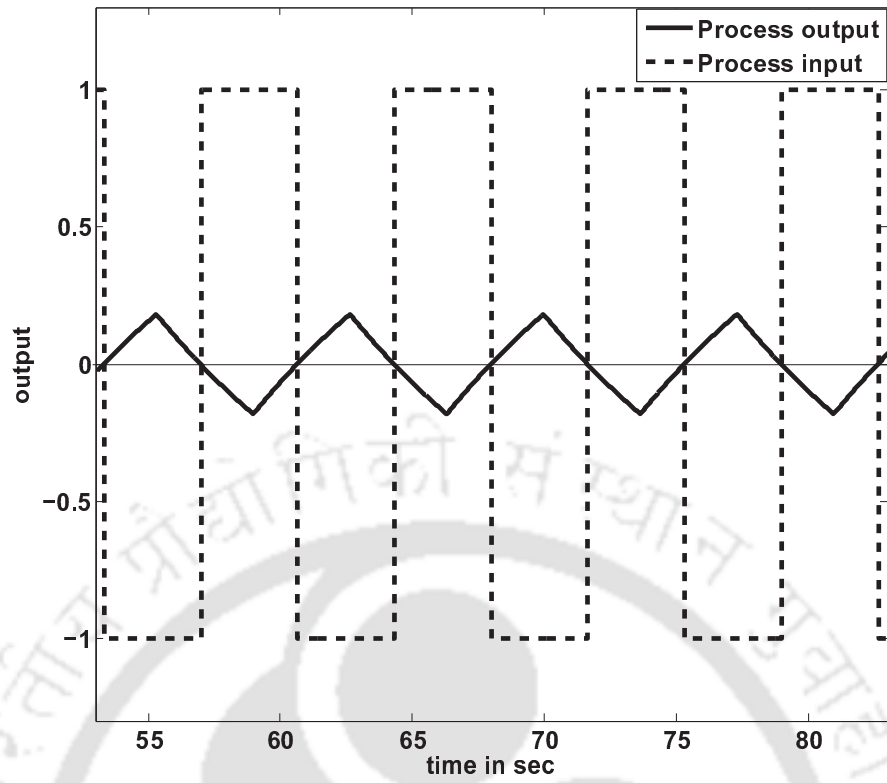


Figure 2.5: Process output and input signals for ideal relay

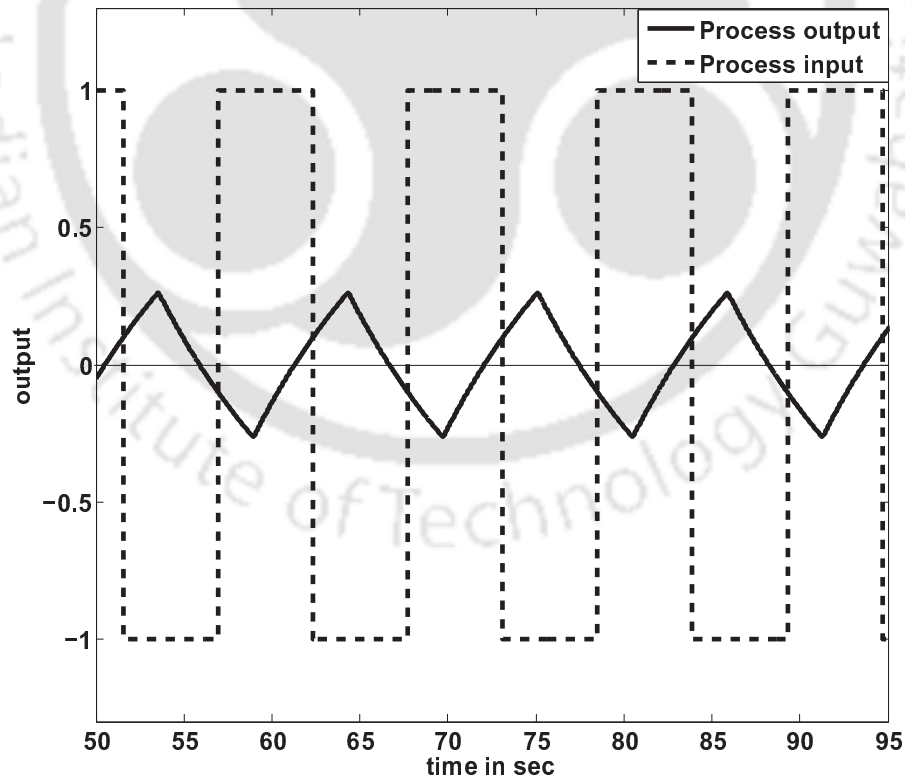


Figure 2.6: Process output and input signals for relay with hysteresis

The condition to obtain sustained oscillations during off-line identification is

$$NG_m(j\omega) = -1 \quad (2.2)$$

where $G_m(j\omega)$ is the process model in frequency domain.

Let the form of PID controller be

$$G_c(s) = K_P \left(1 + \frac{1}{T_I s} + \frac{T_D s}{\alpha T_D s + 1} \right) \quad (2.3)$$

where K_P , T_I , T_D and α are the proportional gain, integral time constant, derivative time constant and derivative filter constant, respectively. Normally, α is very small so, the derivative filter term in (2.3) is neglected in the following derivations for ease in analysis. Hence, (2.3) is reduced to

$$G_c(s) = K_P \left(1 + \frac{1}{T_I s} + T_D s \right) \quad (2.4)$$

Rewriting the above equation in frequency domain

$$G_c(j\omega) = K_P \left(1 + \frac{1}{j\omega T_I} + j\omega T_D \right) \quad (2.5)$$

Now, for on-line identification the condition to get a stable limit cycle is

$$N\tilde{G}_m(j\omega) = -1 \quad (2.6)$$

where $\tilde{G}_m(j\omega)$ is the fictitious process model in frequency domain, which is represented as

$$\tilde{G}_m(j\omega) = \frac{G_m(j\omega)}{1 + G_m(j\omega)G_c(j\omega)} \quad (2.7)$$

The following expression is obtained by using (2.7) in (2.6)

$$G_m(j\omega) [N + G_c(j\omega)] = -1 \quad (2.8)$$

Eqs. (2.2) and (2.8) are utilized in Sections 2.4 and 2.5 to derive analytical expressions to estimate the unknown process model parameters.

During on-line identification test to obtain the sustained oscillations the initial controller parameters $K_P = 0.01$ (for stable processes) and 0.001 (for unstable processes), $T_I = 0.5$ and $T_D = 0.125$ are chosen. The choice is decided from a number of simulation results.

2.3 Issue of measurement noise and load disturbance

In process control systems, irrespective of accurate sensors, the process output is corrupted with measurement noise generated from control valves, measuring devices or the process itself. This noise causes multiple switching of relay at the zero crossing. Due to multiple switching at the process input, the limit cycle will have number of measurements for time period and amplitude, leading to inaccurate estimation of process model parameters. So, it is essential to eliminate the effects of measurement noise. Therefore, to reduce chattering in the process output, a relay with hysteresis is applied in the proposed identification method. To illustrate the effect of noise in simulations, a white Gaussian noise of zero mean and certain variance ($0, \sigma_n^2$) is injected to the output signal which induces noisy oscillations. The noise power is quantified by signal to noise ratio (SNR) given by

$$SNR = 10 \log \left(\frac{\sigma_y^2}{\sigma_N^2} \right) \quad (2.9)$$

measured in decibel (dB), where σ_y^2 is the variance of the process output signal and σ_N^2 the noise variance. To recover the noise free process output, Fourier series based curve fitting technique [1, 39] is employed. Any practical or noisy periodic signal is assumed to be represented by its equivalent Fourier series expression which can be written as

$$D(t) = \sum_{g=0}^8 \zeta_{1g} \cos(g\omega t) + \sum_{g=0}^8 \zeta_{2g} \sin(g\omega t) \quad (2.10)$$

where ζ_{1g} and ζ_{2g} (for $g = 0, 1, 2, \dots$) are the Fourier coefficients, g is the number of terms, ω is the frequency of the fitted signal and $D(t)$ is denoised output signal. Here the value of g is restricted to 8 for computational complexity reduction. A noisy signal can be decomposed into number of signals oscillating with multiples of fundamental frequency. From these number of signals, one clean signal corresponding to the noisy signal is obtained.

To verify the efficacy of the proposed method under realistic conditions, process model parameters are estimated even in the presence of measurement noise. The proposed method is also tested for noise with low frequency in fourth example. Simulations are not carried out with several noise patterns but in real time scenarios the noise can be of various forms. Practical is-

sues such as noise, effect of neglected dynamics etc. play a major role in model based controller design. Our identification method provides a tool for model based controller design not aiming at achieving a very accurate model at any working condition but just at those frequencies that are interesting for control purposes.

In the presence of static load disturbance of magnitude L , both the relay output and load disturbance serve as process input leading to a significant shifting in the limit cycle output. In order to recover the original limit cycle a bias of magnitude $-\hat{L}$ (as suggested in [39]) may be added to relay amplitudes to nullify the shifting occurred in limit cycle output.

2.4 Process identification

2.4.1 FOPDT process model

Let the process in the off-line identification structure shown in Fig. 2.1 be represented by the stable or unstable FOPDT process transfer function model

$$G_m(s) = \frac{Ke^{-\delta s}}{\tau_1 s \pm 1} \quad (2.11)$$

The above transfer function model in frequency domain becomes

$$G_m(j\omega) = \frac{Ke^{-j\omega\delta}}{j\omega\tau_1 \pm 1} \quad (2.12)$$

where the unknown parameters K , τ_1 and δ are the steady state gain, the time constant and the time delay of the process model, respectively. From the measurements of peak amplitude (A_p) and time period (T_p) of the limit cycle output, the process model parameters τ_1 and δ are estimated for any non-zero settings of the relay. Substituting $G_m(j\omega)$ from (2.12) and N from (2.1) in (2.2) results in

$$\frac{4h \left(\sqrt{A_p^2 - \varepsilon^2} - j\varepsilon \right) Ke^{-j\omega\delta}}{\pi A_p^2 (j\omega\tau_1 \pm 1)} = -1 \quad (2.13)$$

Equating the magnitude on both sides of (2.13), one obtains

$$\frac{4hK}{\pi A_p \sqrt{(\omega \tau_1)^2 + 1}} = 1 \quad (2.14)$$

The above equation is further solved to obtain the following expression for stable or unstable process model

$$\tau_1 = \frac{1}{\omega} \sqrt{\left(\frac{4hK}{\pi A_p}\right)^2 - 1} \quad (2.15)$$

Now, equating the phase angle on both sides of (2.13) for stable process we get

$$-\omega \delta - \tan^{-1}(\omega \tau_1) - \tan^{-1}\left(\frac{\varepsilon}{\sqrt{A_p^2 - \varepsilon^2}}\right) = -\pi \quad (2.16)$$

which is reduced to

$$\delta = \frac{1}{\omega} \left[\pi - \tan^{-1}\left(\frac{\omega \tau_1 \sqrt{A_p^2 - \varepsilon^2} + \varepsilon}{\sqrt{A_p^2 - \varepsilon^2} - \varepsilon \omega \tau_1}\right) \right] \quad (2.17)$$

Similarly, equating the phase angle on both sides of (2.13) for unstable process

$$-\omega \delta + \tan^{-1}(\omega \tau_1) - \tan^{-1}\left(\frac{\varepsilon}{\sqrt{A_p^2 - \varepsilon^2}}\right) = 0 \quad (2.18)$$

on further solving we get

$$\delta = \frac{1}{\omega} \left[\tan^{-1}\left(\frac{\omega \tau_1 \sqrt{A_p^2 - \varepsilon^2} - \varepsilon}{\sqrt{A_p^2 - \varepsilon^2} + \varepsilon \omega \tau_1}\right) \right] \quad (2.19)$$

where $\omega = \pi/T_p$. Due to symmetrical relay input, the limit cycle output generated is also symmetrical hence, the time period (T_p) is measured from half limit cycle output.

Using the explicit Eqs. (2.15) and (2.17) and measurements made on the half limit cycle, the process model parameters τ_1 and δ of the stable process are estimated during off-line mode of operation similarly, to estimate the parameters of unstable process model, Eqs. (2.15) and (2.19) are utilized.

For on-line identification, substitution of $G_m(j\omega)$, N and $G_c(j\omega)$ given in (2.12), (2.1) and (2.5) into (2.8) results in

$$\frac{Ke^{-j\omega\delta}(u + jv)}{(j\omega\tau_1 \pm 1)} = -1 \quad (2.20)$$

where

$$u = K_P + \frac{4h\sqrt{A_p^2 - \varepsilon^2}}{\pi A_p^2} \quad (2.21)$$

and

$$v = K_P\omega T_D - \frac{K_P}{\omega T_I} - \frac{4h\varepsilon}{\pi A_p^2} \quad (2.22)$$

Similar to off-line method, equating the magnitude and phase angle on both sides of (2.20) and solving the following expressions are obtained

$$\tau_1 = \frac{1}{\omega} \left[\sqrt{K^2(u^2 + v^2) - 1} \right] \quad (2.23)$$

for stable or unstable processes.

$$\delta = \frac{1}{\omega} \left[\pi + \tan^{-1} \left(\frac{v - u\omega\tau_1}{u + v\omega\tau_1} \right) \right] \quad (2.24)$$

for stable process and

$$\delta = \frac{1}{\omega} \left[\tan^{-1} \left(\frac{v + u\omega\tau_1}{u - v\omega\tau_1} \right) \right] \quad (2.25)$$

for unstable process.

Hence, for on-line method Eqs. (2.23) and (2.24) are utilized to obtain the parameters (τ_1 and δ) of stable FOPDT process model similarly, for unstable process model Eqs. (2.23) and (2.25) are used.

As the DF technique gives expressions for two parameters for a particular process model so, the steady state gain K is assumed to be positive and estimated from steady state simulation [7] for both stable and unstable process models.

Example 1

Let us consider the following stable FOPDT process [18]

$$G(s) = \frac{e^{-2s}}{10s + 1}.$$

The relay test is conducted for off-line mode of operation using $h = 1$ and $\varepsilon = 0.025$ to generate the limit cycle output with the parameters $A_p = 0.2017$ and $T_p = 4.0909$. The relay and limit cycle outputs are as shown in Fig. 2.7. The steady state gain $K = 1.0$, is obtained from the method as mentioned in subsection 2.4.1. Substituting this value along with relay and limit cycle quantities in (2.15) and (2.17) the remaining process model parameters $\tau_1 = 8.1167$ and $\delta = 2.0909$ are estimated, respectively.

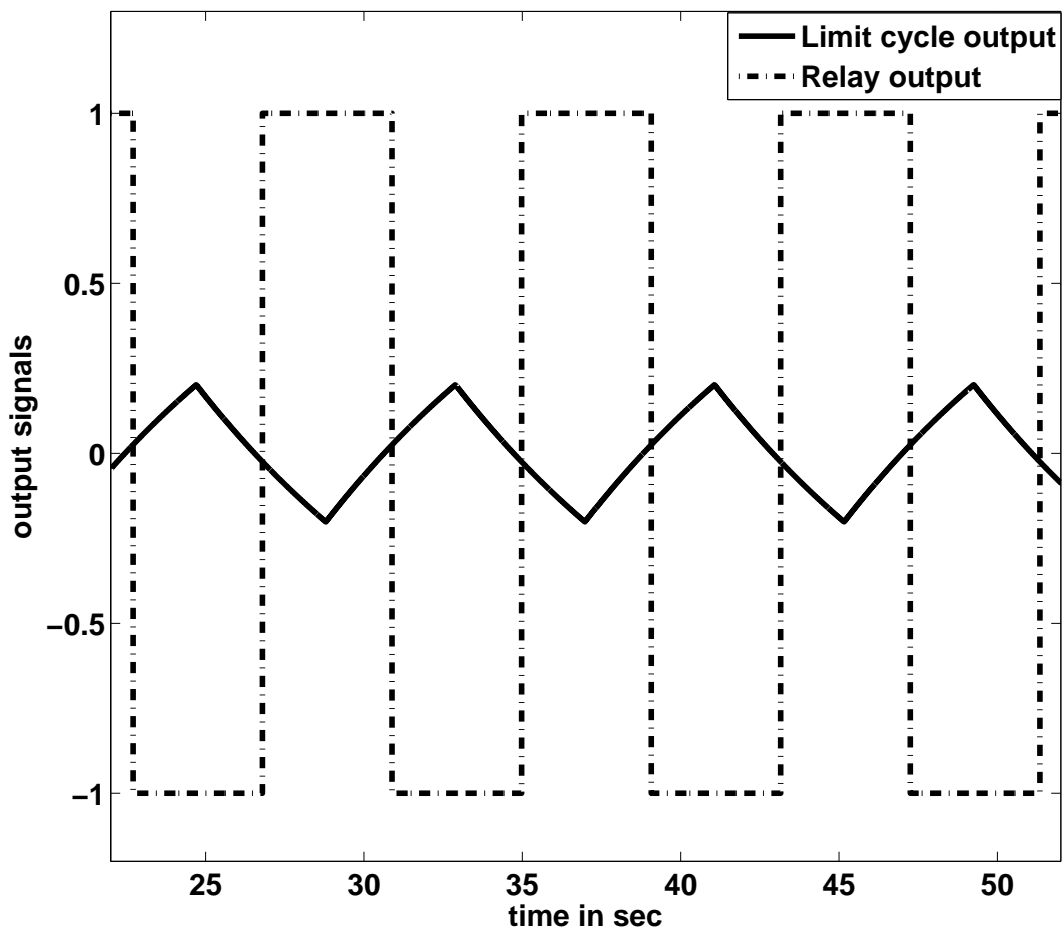


Figure 2.7: Relay and limit cycle outputs

During on-line identification test to obtain the sustained oscillations the initial controller parameters $K_P = 0.01$, $T_I = 0.5$ and $T_D = 0.125$ are chosen. Hence, the limit cycle and other parameters obtained during on-line test are $A_p = 0.2029$, $T_p = 4.0984$ and $K = 1.0$. These quantities are utilized in (2.23) and (2.24) to find out $\tau_1 = 8.0995$ and $\delta = 2.0915$, respectively. For the same process, Li et al. [18] used an ideal relay to estimate the process model parameters. To show the efficiency of proposed method under noisy environment, the process dynamics are identified during off-line mode of operation, in the presence of measurement noise with SNR of 20 dB. This noise effect is achieved using a white Gaussian noise of zero mean and 1.3526×10^{-4} variance. Using curve fitting technique the denoised signal is obtained. The noisy process output and denoised limit cycle output are as shown in Fig. 2.8.

The performance evaluation is carried out by calculating the frequency domain estimation error index (\tilde{E}) for each of the process models. This error is found by applying integral of absolute error criterion as

$$\tilde{E} = \int_0^{\omega_{cr}} \left| \frac{G_m(j\omega) - G(j\omega)}{G_m(j\omega)} \right| d\omega \quad (2.26)$$

where $G(j\omega)$ is actual process, $G_m(j\omega)$ is proposed model defined both in frequency domain and ω_{cr} the critical frequency of the process.

The identified process models and the model recommended by Li et al. [18] are given in Table 2.1 along with estimation error.

Table. 2.1: Comparison of process models for Example 1

Method	Process model	Error (\tilde{E})
Off-line	$\frac{1.0e^{-2.0909s}}{8.1167s+1}$	0.1381
Off-line with noise	$\frac{1.0e^{-1.9374s}}{8.1065s+1}$	0.1483
On-line	$\frac{1.0e^{-2.0915s}}{8.0995s+1}$	0.1393
Li et al. [18]	$\frac{0.988e^{-2.0s}}{8.02s+1}$	0.1414

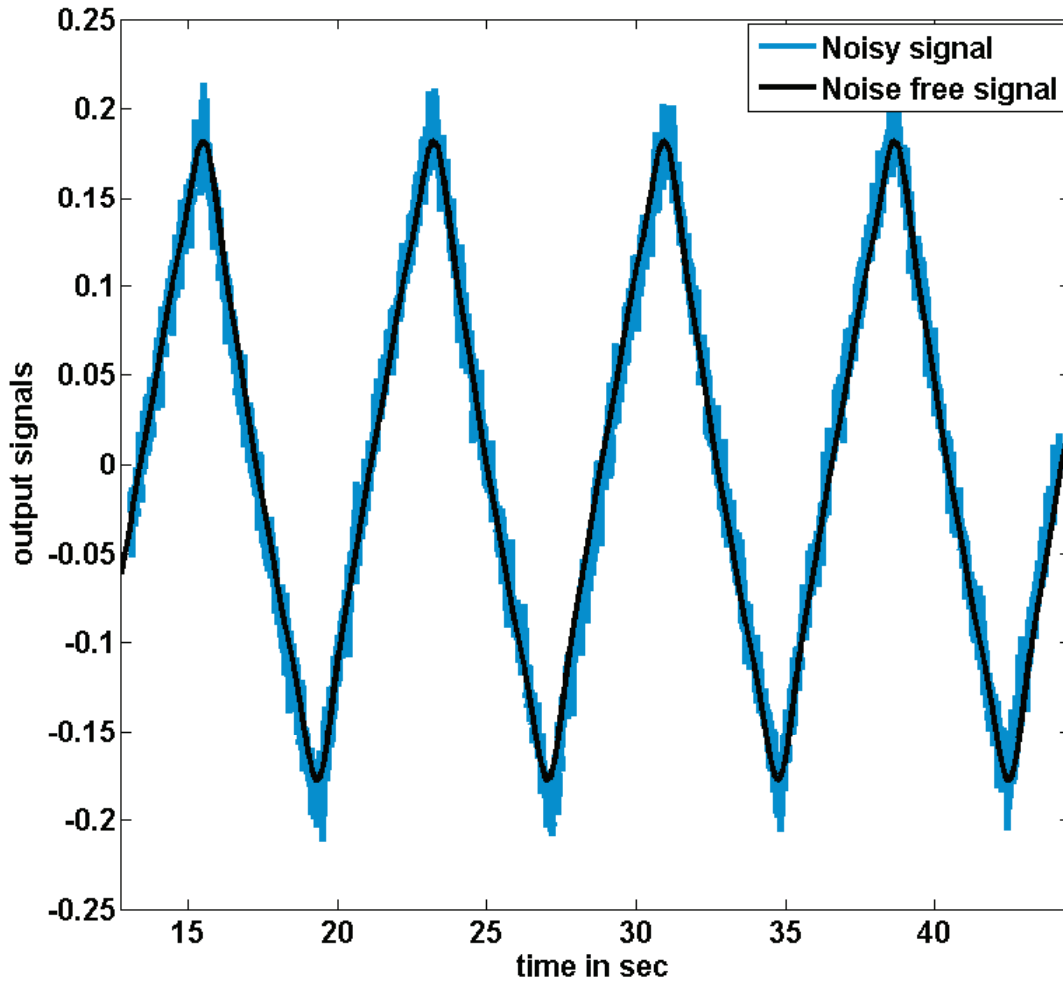


Figure 2.8: Noisy and denoised limit cycle outputs

2.4.2 SOPDT process model

The transfer function model of a stable or unstable SOPDT process is given by

$$G_m(s) = \frac{K e^{-\delta s}}{(\tau_1 s \pm 1)(\tau_2 s + 1)} \quad (2.27)$$

which in frequency domain becomes

$$G_m(j\omega) = \frac{K e^{-j\omega\delta}}{(j\omega\tau_1 \pm 1)(j\omega\tau_2 + 1)} \quad (2.28)$$

where τ_1 and τ_2 are the process time constants. Substituting (2.28) and (2.1) in the condition given by (2.2) for off-line method, following expression is obtained

$$\frac{4hKe^{-j\omega\delta} \left(\sqrt{A_p^2 - \varepsilon^2} - j\varepsilon \right)}{\pi A_p^2 (j\omega\tau_1 \pm 1)(j\omega\tau_2 + 1)} = -1 \quad (2.29)$$

Taking magnitude of the above equation, one obtains

$$\frac{4hK}{\pi A_p \sqrt{\left((\omega\tau_1)^2 + 1 \right) \left((\omega\tau_2)^2 + 1 \right)}} = 1 \quad (2.30)$$

Further simplifying the above expression for stable or unstable processes, we get

$$\omega^2 \left(\omega^2 (\tau_1 \tau_2)^2 + (\tau_1 \pm \tau_2)^2 \mp 2\tau_1 \tau_2 \right) = \left(\frac{4hK}{\pi A_p} \right)^2 - 1 \quad (2.31)$$

Above expression is rearranged to get

$$\tau_1 \pm \tau_2 = \sqrt{\frac{1}{\omega^2} \left(\left(\frac{4hK}{\pi A_p} \right)^2 - 1 \right) \pm 2\tau_1 \tau_2 - (\omega\tau_1 \tau_2)^2} \quad (2.32)$$

Hence, for stable processes

$$\tau_1 + \tau_2 = \sqrt{\frac{1}{\omega^2} \left(\left(\frac{4hK}{\pi A_p} \right)^2 - 1 \right) + 2\tau_1 \tau_2 - (\omega\tau_1 \tau_2)^2} \quad (2.33)$$

and for unstable processes

$$\tau_1 - \tau_2 = \sqrt{\frac{1}{\omega^2} \left(\left(\frac{4hK}{\pi A_p} \right)^2 - 1 \right) - 2\tau_1 \tau_2 - (\omega\tau_1 \tau_2)^2} \quad (2.34)$$

Now, substituting (2.28) and (2.1) in (2.2) and equating the phase angles, following expressions are obtained for stable and unstable processes, respectively

$$\tan^{-1}(\omega\tau_1) + \tan^{-1}(\omega\tau_2) = \pi - \omega\delta - \tan^{-1} \left(\frac{\varepsilon}{\sqrt{A_p^2 - \varepsilon^2}} \right) \quad (2.35)$$

$$\tan^{-1}(\omega\tau_1) - \tan^{-1}(\omega\tau_2) = \omega\delta + \tan^{-1} \left(\frac{\varepsilon}{\sqrt{A_p^2 - \varepsilon^2}} \right) \quad (2.36)$$

On further simplifying (2.35) we get

$$\frac{\omega(\tau_1 + \tau_2)}{1 - \omega^2 \tau_1 \tau_2} = \tan \left(\pi - \omega\delta - \tan^{-1} \left(\frac{\varepsilon}{\sqrt{A_p^2 - \varepsilon^2}} \right) \right) \quad (2.37)$$

Above expression is rearranged to get the following equation for stable processes

$$\tau_1 \tau_2 = \frac{1}{\omega^2} \left(1 - \frac{\omega (\tau_1 + \tau_2)}{\tan \left(\pi - \omega \delta - \tan^{-1} \left(\frac{\varepsilon}{\sqrt{A_p^2 - \varepsilon^2}} \right) \right)} \right) \quad (2.38)$$

Similarly, simplifying (2.36) we get

$$\frac{\omega (\tau_1 - \tau_2)}{1 + \omega^2 \tau_1 \tau_2} = \tan \left(\omega \delta + \tan^{-1} \left(\frac{\varepsilon}{\sqrt{A_p^2 - \varepsilon^2}} \right) \right) \quad (2.39)$$

The following expression is obtained for unstable process after rearranging the above equation

$$\tau_1 \tau_2 = \frac{1}{\omega^2} \left(\frac{\omega (\tau_1 - \tau_2)}{\tan \left(\omega \delta + \tan^{-1} \left(\frac{\varepsilon}{\sqrt{A_p^2 - \varepsilon^2}} \right) \right)} - 1 \right) \quad (2.40)$$

Using (2.33) and (2.38) and further solving, the following explicit expressions for stable SOPDT process are obtained

$$\tau_1 = \frac{2hK \sin \varphi_1}{\pi A_p \omega} + \frac{1}{\omega} \sqrt{\left(\frac{2hK \sin \varphi_1}{\pi A_p} \right)^2 - \frac{4hK \cos \varphi_1}{\pi A_p} - 1} \quad (2.41)$$

$$\tau_2 = \frac{2hK \sin \varphi_1}{\pi A_p \omega} - \frac{1}{\omega} \sqrt{\left(\frac{2hK \sin \varphi_1}{\pi A_p} \right)^2 - \frac{4hK \cos \varphi_1}{\pi A_p} - 1} \quad (2.42)$$

where

$$\varphi_1 = \delta \omega + \tan^{-1} \left(\frac{\varepsilon}{\sqrt{A_p^2 - \varepsilon^2}} \right) \quad (2.43)$$

Hence, the process model parameters τ_1 and τ_2 are estimated by solving (2.41) and (2.42) for stable processes.

Utilizing (2.34) and (2.40) and further solving, the following explicit expressions for unstable SOPDT process are obtained

$$\tau_1 = \frac{2hK \sin \varphi_1}{\pi A_p \omega} + \frac{1}{\omega} \sqrt{\left(\frac{2hK \sin \varphi_1}{\pi A_p} \right)^2 + \frac{4hK \cos \varphi_1}{\pi A_p} - 1} \quad (2.44)$$

$$\tau_2 = -\frac{2hK \sin \varphi_1}{\pi A_p \omega} + \frac{1}{\omega} \sqrt{\left(\frac{2hK \sin \varphi_1}{\pi A_p} \right)^2 + \frac{4hK \cos \varphi_1}{\pi A_p} - 1} \quad (2.45)$$

Now, Eqs. (2.44) and (2.45) are solved to find the process model parameters τ_1 and τ_2 for unstable processes during off-line identification.

Similarly, to obtain the expressions for on-line identification, Eqs. (2.28), (2.1) and (2.5) are substituted in (2.8) to get

$$\frac{Ke^{-j\omega\delta}(u+jv)}{(j\omega\tau_1 \pm 1)(j\omega\tau_2 + 1)} = -1 \quad (2.46)$$

where u and v are as mentioned in (2.21) and (2.22), respectively. Similar to off-line method as given above, the following expressions are obtained after taking the magnitude and phase angle of (2.46)

$$\tau_1 + \tau_2 = \sqrt{\frac{K^2(u^2 + v^2) - 1}{\omega} + 2\tau_1\tau_2 - (\omega\tau_1\tau_2)^2} \quad (2.47)$$

$$\tau_1\tau_2 = \frac{1}{\omega^2} \left[\frac{\omega(\tau_1 + \tau_2)}{\tan(\delta\omega - \tan^{-1}(\frac{v}{u}))} + 1 \right] \quad (2.48)$$

Eqs. (2.47) and (2.48) are simplified to derive the following explicit expressions

$$\tau_1 = \frac{K\sqrt{u^2 + v^2} \sin \varphi_2}{2\omega} + \frac{1}{\omega} \sqrt{\frac{K^2(u^2 + v^2) \sin^2 \varphi_2}{4} - K\sqrt{u^2 + v^2} \cos \varphi_2 - 1} \quad (2.49)$$

$$\tau_2 = \frac{K\sqrt{u^2 + v^2} \sin \varphi_2}{2\omega} - \frac{1}{\omega} \sqrt{\frac{K^2(u^2 + v^2) \sin^2 \varphi_2}{4} - K\sqrt{u^2 + v^2} \cos \varphi_2 - 1} \quad (2.50)$$

where

$$\varphi_2 = \delta\omega - \tan^{-1}\left(\frac{v}{u}\right) \quad (2.51)$$

Hence, the process model parameters τ_1 and τ_2 are estimated from (2.49) and (2.50) for stable SOPDT processes.

For unstable process models, the below mentioned expressions are found by taking the magnitude and phase angle of (2.46)

$$\tau_1 - \tau_2 = \sqrt{\frac{K^2(u^2 + v^2) - 1}{\omega} - 2\tau_1\tau_2 - (\omega\tau_1\tau_2)^2} \quad (2.52)$$

$$\tau_1\tau_2 = \frac{1}{\omega^2} \left[\frac{\omega(\tau_1 - \tau_2)}{\tan(\delta\omega - \tan^{-1}(\frac{v}{u}))} - 1 \right] \quad (2.53)$$

Eqs. (2.52) and (2.53) are further solved to get the following explicit expressions

$$\tau_1 = \frac{K\sqrt{u^2 + v^2} \sin \varphi_2}{2\omega} + \frac{1}{\omega} \sqrt{\frac{K^2(u^2 + v^2) \sin^2 \varphi_2}{4} + K\sqrt{u^2 + v^2} \cos \varphi_2 - 1} \quad (2.54)$$

$$\tau_2 = -\frac{K\sqrt{u^2 + v^2} \sin \varphi_2}{2\omega} + \frac{1}{\omega} \sqrt{\frac{K^2(u^2 + v^2) \sin^2 \varphi_2}{4} + K\sqrt{u^2 + v^2} \cos \varphi_2 - 1} \quad (2.55)$$

Now, to estimate the parameters τ_1 and τ_2 , Eqs. (2.54) and (2.55) are used for unstable processes during on-line mode of operation. The steady state gain K is estimated using the procedure mentioned in subsection 2.4.1.

To estimate the process time delay (δ) of SOPDT process model, Majhi [39] proposed a method which involves measurement of two parameters t_0 and t_1 where t_0 is the time instant at which relay switching takes place and t_1 is the time where second derivative output of limit cycle suffers discontinuity or sudden change so, $\delta = (t_1 - t_0)$. As the author used ideal relay where $t_0 = 0$ always, but in our method as relay with hysteresis is used where the relay switching takes place at t_0 which is non-zero. Hence, the method proposed by Majhi [39] is extended here to estimate the process time delay using relay with hysteresis.

Example 2

This example demonstrates estimation of stable SOPDT process model parameters for the following process [49]

$$G(s) = \frac{e^{-4s}}{(10s + 1)(2s + 1)}$$

During off-line identification the relay with parameters $h = 1$ and $\varepsilon = 0.02$, is applied to the above process to generate limit cycle and its second derivative output as shown in Fig. 2.9. The measured limit cycle parameters are $A_p = 0.353$, $T_p = 9.9722$ and $t_0 = 0.2263$ whereas $t_1 = 4.2263$ is measured from second derivative output of limit cycle. The process model parameters $K = 1.0$ and $\theta = 4.0$ are estimated from the procedure explained in subsections 2.4.1 and 2.4.2, respectively. Substituting these parameters along with limit cycle quantities in (2.41) and

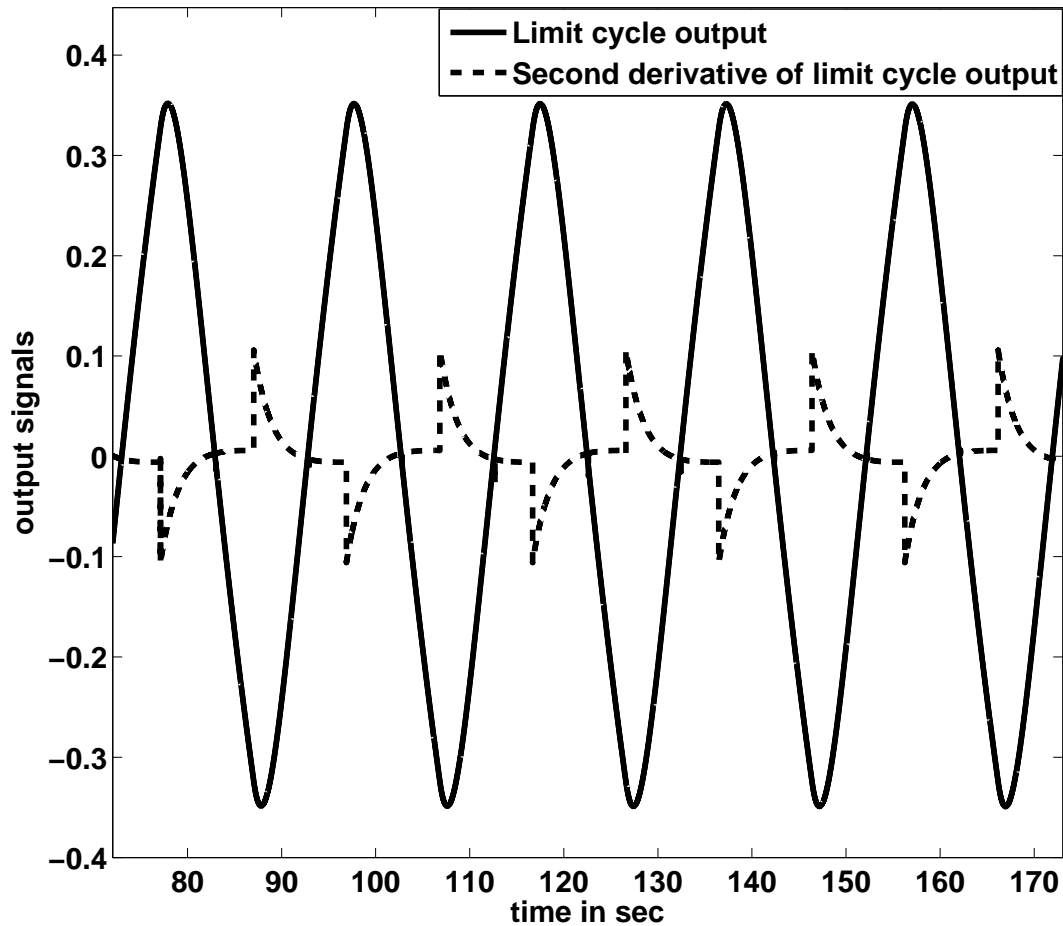


Figure 2.9: Limit cycle and its second derivative output

(2.42) and solved to estimate $\tau_1 = 8.9312$ and $\tau_2 = 2.1515$. Similarly, for on-line identification using the controller parameters $K_P = 0.01$, $T_I = 0.5$ and $T_D = 0.125$, the measurements made from limit cycle and its second derivative output are $A_p = 0.3599$, $T_p = 10.0602$, $t_0 = 0.2246$ and $t_1 = 4.2246$. The process model parameters $K = 1.0$ and $\theta = 4.0$ are obtained using the procedure explained above in this example. The values of K , θ and other limit cycle quantities are substituted in (2.49) and (2.50) to estimate $\tau_1 = 8.8556$ and $\tau_2 = 2.1712$. Fedele [49] proposed FOPDT model for this process using step input method. The identified process models during off-line and on-line mode of operation, in the form of transfer functions are given in Table 2.2 along with the model proposed by Fedele [49] and the corresponding estimation error for each process model. Even though the model suggested by Fedele [49] has less estimation error but

the author has not considered on-line identification test.

Table. 2.2: Comparison of process models for Example 2

Method	Process model	Error (\tilde{E})
Off-line	$\frac{1.0e^{-4.0s}}{(8.9312s+1)(2.1515s+1)}$	0.0206
On-line	$\frac{1.0e^{-4.0s}}{(8.8556s+1)(2.1712s+1)}$	0.0218
Fedele [49]	$\frac{1.0015e^{-5.6474s}}{10.4495s+1}$	0.0143

Example 3

Estimation of process model parameters of the following unstable SOPDT process [6] is explained in this example

$$G(s) = \frac{e^{-0.5s}}{(2s-1)(0.5s+1)}.$$

The off-line identification is carried out using the relay settings $h = 1$ and $\varepsilon = 0.2$ to generate limit cycle and its second derivative output with the parameters $A_p = 0.857$, $T_p = 6.5192$, $t_0 = 0.3646$ and $t_1 = 0.8646$. The limit cycle output is shown in Fig. 2.10. The parameters, $K = 1.0$ and $\delta = 0.50$ are obtained as explained in subsections 2.4.1 and 2.4.2, respectively. These parameters are utilized in (2.44) and (2.45) to find out the remaining process model parameters $\tau_1 = 2.0781$ and $\tau_2 = 0.6638$. Similarly, for on-line mode (using controller parameters $K_P = 0.001$, $T_I = 0.5$ and $T_D = 0.125$) the limit cycle parameters measured are $A_p = 0.8626$, $T_p = 6.6078$, $t_0 = 0.3632$ and $t_1 = 0.8632$. Using these quantities with $K = 1.0$ and $\delta = 0.50$ in (2.54) and (2.55) the model parameters are estimated as $\tau_1 = 2.0872$ and $\tau_2 = 0.6674$. For this process Vivek and Chidambaram [6] used Laplace transform technique and ideal relay to identify the process dynamics in terms of FOPDT model as given in Table 2.3 along with proposed models.

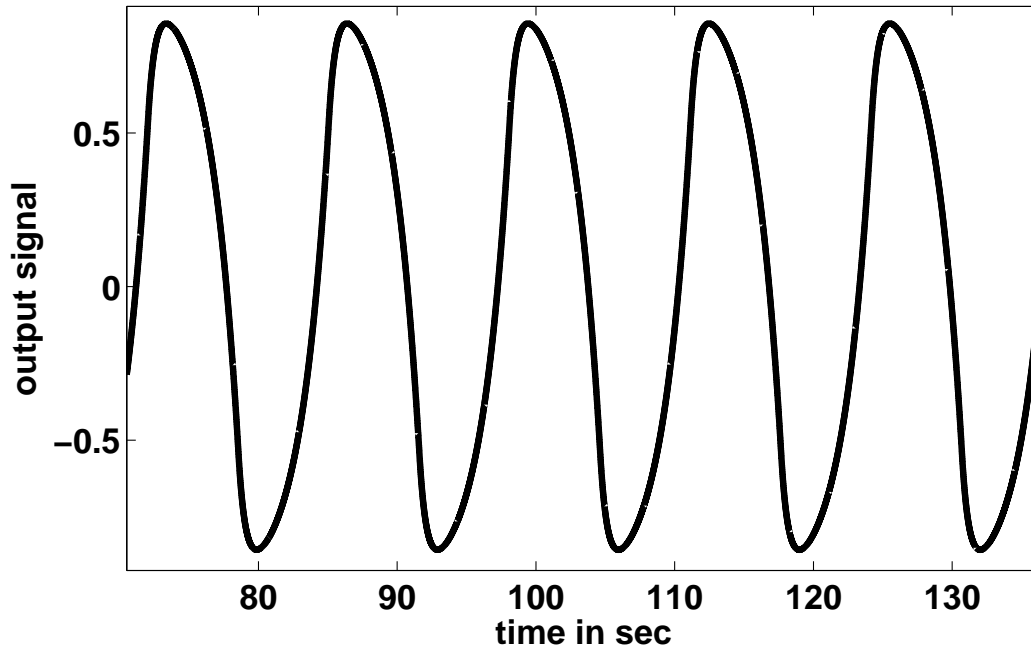


Figure 2.10: Limit cycle output

Table. 2.3: Comparison of process models for Example 3

Method	Process model	Error (\tilde{E})
Off-line	$\frac{1.0e^{-0.50s}}{(2.0781s-1)(0.6638s+1)}$	0.1171
On-line	$\frac{1.0e^{-0.50s}}{(2.0872s-1)(0.6674s+1)}$	0.1201
Vivek and Chidambaram [6]	$\frac{0.7534e^{-1.0412s}}{(2.1642s-1)}$	0.3838

2.4.3 Underdamped SOPDT process model

The stable SOPDT process model given in (2.27) can be represented with the following transfer function model for an underdamped SOPDT process

$$G_m(s) = \frac{Ke^{-\delta s}}{ms^2 + ns + 1} \quad (2.56)$$

where $m = \tau_1 \tau_2$ and $n = \tau_1 + \tau_2$ with the condition $n^2 < 4m$ for underdamped process. Rewriting (2.56) in the following form

$$G_m(s) = \frac{Ke^{-\delta s} \alpha_1 \beta_1}{(s - \alpha_1)(s - \beta_1)} \quad (2.57)$$

or

$$G_m(j\omega) = \frac{Ke^{-j\omega\delta} \alpha_1 \beta_1}{(j\omega - \alpha_1)(j\omega - \beta_1)} \quad (2.58)$$

where

$$\alpha_1 = \frac{-2}{n + j\sqrt{4m - n^2}}; \quad \beta_1 = \frac{-2}{n - j\sqrt{4m - n^2}} \quad (2.59)$$

For off-line mode, Eqs. (2.58) and (2.1) are substituted in (2.2) to get the following expression

$$\frac{4h \left(\sqrt{A_p^2 - \varepsilon^2} - j\varepsilon \right) Ke^{-j\omega\delta} \alpha_1 \beta_1}{\pi A_p^2 (j\omega - \alpha_1)(j\omega - \beta_1)} = -1 \quad (2.60)$$

The magnitudes are equated on both sides of (2.60) and simplified to obtain

$$\alpha_1 \beta_1 = \omega \pi A_p \sqrt{\frac{\omega^2 + \alpha_1^2 + \beta_1^2}{(4hK)^2 - (\pi A_p)^2}} \quad (2.61)$$

Similarly, equating the phase angles for (2.60) and the expression is shortened to

$$\alpha_1 + \beta_1 = \left(\frac{\alpha_1 \beta_1 - \omega^2}{\omega} \right) \tan \left(\pi + \omega\delta + \tan^{-1} \left(\frac{\varepsilon}{\sqrt{A_p^2 - \varepsilon^2}} \right) \right) \quad (2.62)$$

As α_1 and β_1 are in terms of the process model parameters m and n , Eqs. (2.61) and (2.62) are further simplified to obtain the following expressions

$$m = \frac{1}{\omega^2} \left[1 + \cos \left(\omega\delta + \tan^{-1} \left(\frac{\varepsilon}{\sqrt{A_p^2 - \varepsilon^2}} \right) \right) \right] \frac{4hK}{\pi A_p} \quad (2.63)$$

$$n = \sin \left(\omega\delta + \tan^{-1} \left(\frac{\varepsilon}{\sqrt{A_p^2 - \varepsilon^2}} \right) \right) \frac{4hK}{\omega \pi A_p} \quad (2.64)$$

Hence, the parameters m and n are calculated from (2.63) and (2.64), respectively for off-line identification test.

For on-line identification the corresponding equations are substituted in (2.8) to get

$$\frac{Ke^{-j\omega\delta}\alpha_1\beta_1}{(j\omega - \alpha_1)(j\omega - \beta_1)}(u + jv) = -1 \quad (2.65)$$

Like off-line method considering the magnitude and phase angle of the above equation to get

$$\alpha_1\beta_1 = \omega \sqrt{\frac{\omega^2 + \alpha_1^2 + \beta_1^2}{K^2(u^2 + v^2) - 1}} \quad (2.66)$$

$$\alpha_1 + \beta_1 = \left(\frac{\alpha_1\beta_1 - \omega^2}{\omega} \right) \tan \left(\pi + \omega\delta - \tan^{-1} \left(\frac{v}{u} \right) \right) \quad (2.67)$$

Eqs. (2.66) and (2.67) are resolved to obtain the following expressions

$$m = \frac{1}{\omega^2} \left[1 + K \sqrt{u^2 + v^2} \cos \left(\omega\delta - \tan^{-1} \left(\frac{v}{u} \right) \right) \right] \quad (2.68)$$

$$n = \left[\frac{K \sqrt{u^2 + v^2}}{\omega} \right] \sin \left(\omega\delta - \tan^{-1} \left(\frac{v}{u} \right) \right) \quad (2.69)$$

The parameters m and n are estimated from (2.68) and (2.69), respectively during on-line identification test. The remaining parameters K and δ are obtained as explained in subsections 2.4.1 and 2.4.2, respectively.

Example 4

In this example an underdamped SOPDT process [2] is considered as

$$G(s) = \frac{e^{-3s}}{s^2 + 0.4s + 1}.$$

For off-line identification the relay ($h = 1$ and $\varepsilon = 0.1$) input to the process generates limit cycle and its second derivative output with the parameters $A_p = 2.5716$, $T_p = 3.9601$, $t_0 = 0.0443$ and $t_1 = 3.0443$. Similar to Example 2, the process model parameters $K = 1.0$ and $\theta = 3.0$ are estimated. These parameters are substituted in (2.63) and (2.64) with limit cycle quantities to estimate $m = 0.9991$ and $n = 0.4127$, respectively. Similarly, for on-line identification (using controller parameters $K_p = 0.01$, $T_I = 0.5$ and $T_D = 0.125$) the measured limit cycle and its second derivative parameters are $A_p = 2.59$, $T_p = 4.001$, $t_0 = 0.0442$ and $t_1 = 3.0442$. So, $K = 1.0$ and $\theta = 3.0$ are estimated and these parameters are utilized with limit cycle quantities in (2.68) and (2.69) to estimate $m = 0.9975$ and $n = 0.4125$. The proposed models and the model sug-

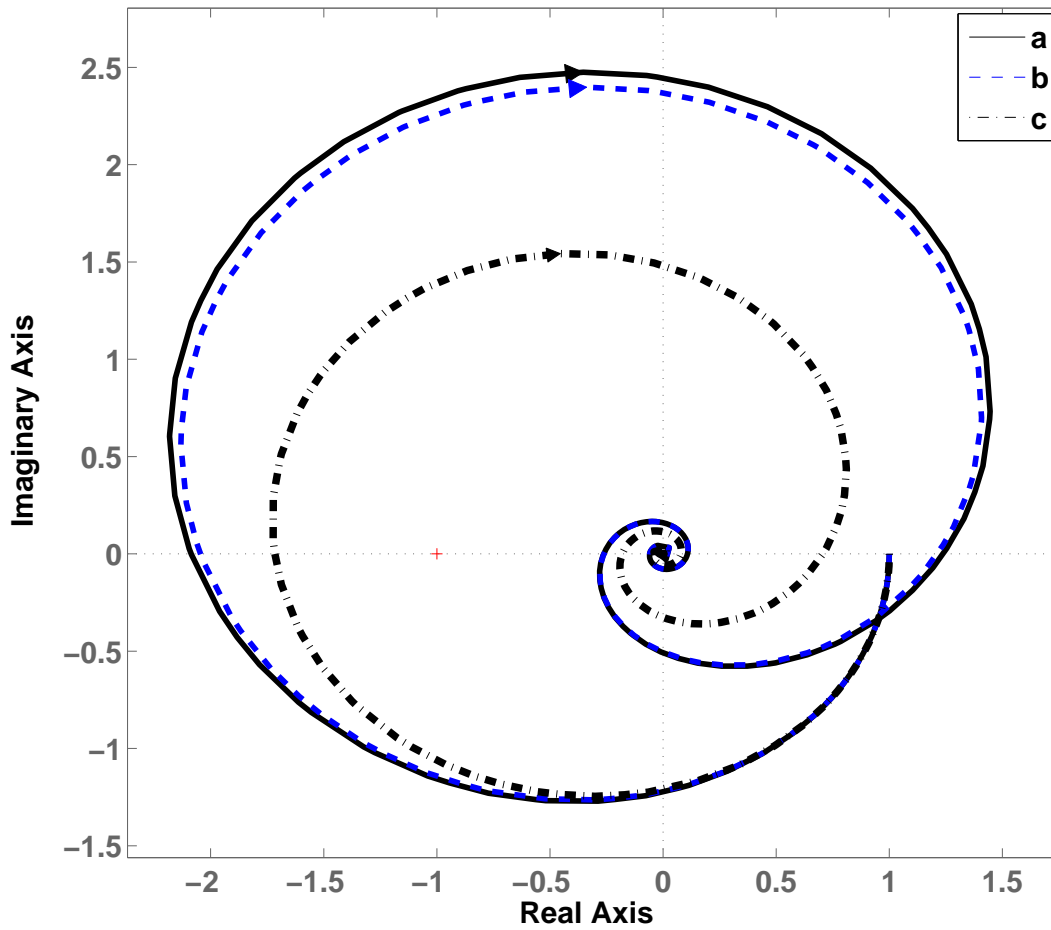


Figure 2.11: Nyquist plots for Example 4: (a) Actual process, (b) identified model (off-line) and (c) model proposed by Lavanya et al. [2]

gested by Lavanya et al. [2] using an ideal relay are given in Table 2.4 along with the respective estimation error. It can be observed that the proposed models have less estimation error than the model suggested by Lavanya et al. [2]. The results are also compared using Nyquist plots (for off-line method) as shown in Fig. 2.11. During off-line identification, a white Gaussian noise of variance 0.00329 is added to the process output to get a noisy signal with SNR of 30 dB. Repeating the above procedure, estimated process model parameters are $\delta = 2.9797$, $m = 1.0134$ and $n = 0.4158$. As the white Gaussian noise is characterized with high frequency, the process dynamics are also identified in the presence of low frequency noise with SNR of 30 dB, as $\delta = 3.0209$, $m = 0.9871$ and $n = 0.4012$. The low frequency noisy signal and the denoised

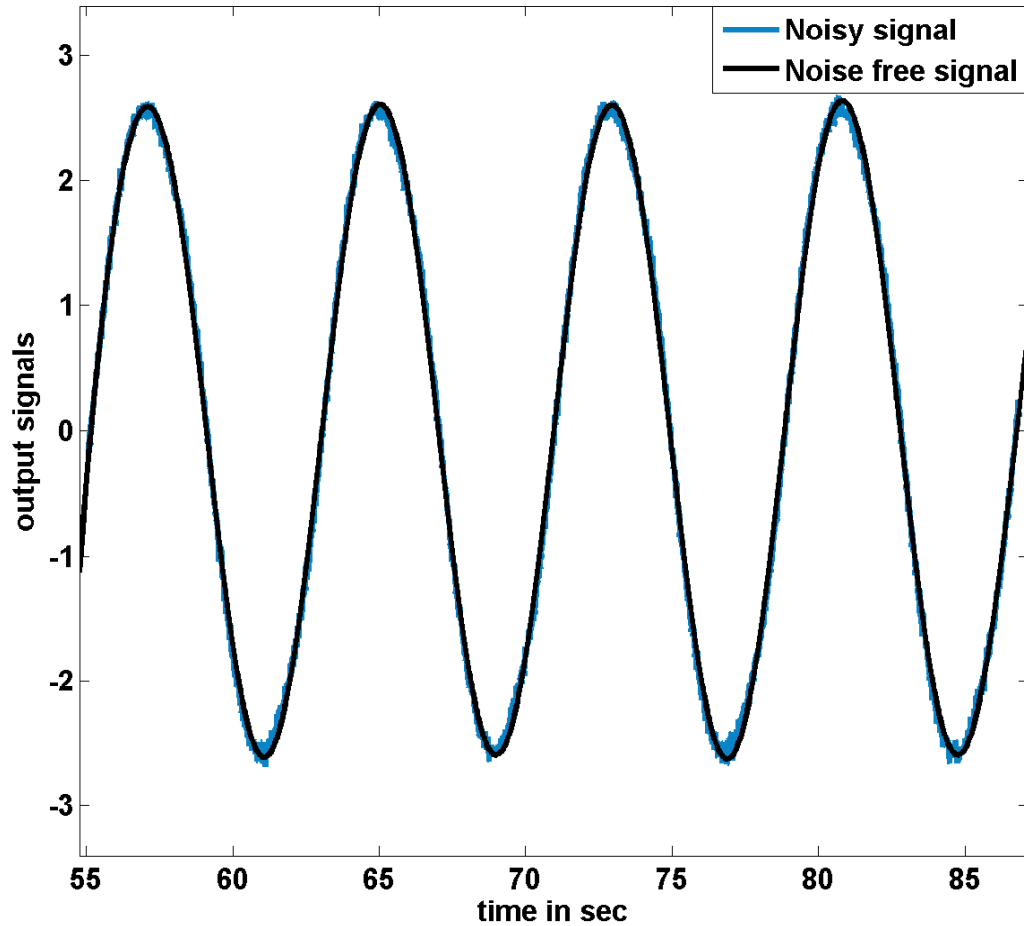


Figure 2.12: Low frequency noisy signal and denoised limit cycle outputs

limit cycle outputs are as shown in Fig. 2.12. For same SNR values the process model parameters estimated during on-line test are $m = 1.0039$, $n = 0.4173$ and $\delta = 2.9864$ (for high frequency noise) and $m = 1.0041$, $n = 0.4204$ and $\delta = 2.9721$ (for low frequency noise).

Table. 2.4: Comparison of process models for Example 4

Method	Process model	Error (\tilde{E})
Off-line	$\frac{1.0e^{-3.0s}}{(0.9991s^2+0.4127s+1)}$	0.0058
On-line	$\frac{1.0e^{-3.0s}}{(0.9975s^2+0.4125s+1)}$	0.0057
Lavanya et al. [2]	$\frac{1.0e^{-3.0s}}{(1.326s^2+0.68s+1)}$	0.1584

Example 5

One more underdamped SOPDT process [71] is considered in this example to study the robustness of the proposed method

$$G(s) = \frac{e^{-s}}{9s^2 + 2.4s + 1}.$$

The off-line and on-line relay tests are conducted with $h = 1$ and different values of ε to identify the process dynamics. The process model parameters K and δ are estimated from the procedure mentioned in subsections 2.4.1 and 2.4.2, respectively. The corresponding expressions for off-line and on-line method are solved using the known parameters to find out m and n . Chen [71] suggested two different FOPDT models for this process. The process models identified for different values of ε are given in Table 2.5 along with the models recommended by Chen [71]. The percentage (%) error of measured limit cycle quantities and estimated model parameters for different SNR values are given in Table 2.6.

Table. 2.5: Comparison of process models for Example 5

Method	ε	Process model	Error (\tilde{E})
Off-line	0.1	$\frac{1.0e^{-1.0s}}{(9.0991s^2 + 2.2857s + 1)}$	0.0128
	0.2	$\frac{1.0e^{-1.0s}}{(9.0991s^2 + 2.2793s + 1)}$	0.0135
	0.3	$\frac{1.0e^{-1.0s}}{(9.1157s^2 + 2.2716s + 1)}$	0.0144
On-line	0.1	$\frac{1.0e^{-1.0s}}{(9.0991s^2 + 2.2894s + 1)}$	0.0124
	0.2	$\frac{1.0e^{-1.0s}}{(9.0991s^2 + 2.2829s + 1)}$	0.0131
	0.3	$\frac{1.0e^{-1.0s}}{(9.1075s^2 + 2.2732s + 1)}$	0.0141
Chen [71]	–	$\frac{1.0e^{-3.35s}}{(3.96s + 1)}$	0.2948
	–	$\frac{1.0e^{-3.27s}}{(4.21s + 1)}$	0.3196

Table. 2.6: Effect of measurement noise on parameters in % error, for Example 5

	SNR (dB)	A_p	T_p	m	n	δ
Off-line	15	-1.3268	0.0172	1.5715	-0.4958	-4.19
	20	0.3478	0.0141	-0.1802	-0.0219	0.62
	25	0.1416	-0.0016	0.0011	0.1228	0.26
	30	-0.0772	-0.0016	0.0011	0.6405	0.62
On-line	15	-1.2114	-0.059	1.3848	-0.5519	-3.95
	20	-0.2872	-0.0047	0.0912	0.2146	-0.11
	25	-0.0125	-0.0047	-0.2715	0.5256	0.98
	30	-0.1249	-0.0124	0.0011	0.4029	0.26

2.4.4 Critically damped SOPDT process model

Let us consider the following transfer function model for critically damped SOPDT process

$$G_m(s) = \frac{Ke^{-\delta s}}{(\tau_1 s + 1)^2} \quad (2.70)$$

For off-line method, substituting (2.1) and frequency domain of (2.70) in (2.2) to achieve

$$\frac{4h \left(\sqrt{A_p^2 - \varepsilon^2} - j\varepsilon \right) Ke^{-j\omega\delta}}{\pi A_p^2 (j\omega\tau_1 + 1)^2} = -1 \quad (2.71)$$

The following expressions for the process model parameters τ_1 and K are obtained after considering the phase angle and magnitude of (2.71), respectively

$$\tau_1 = \frac{1}{\omega} \cot \left(\omega\delta + \tan^{-1} \left(\frac{\varepsilon}{\sqrt{A_p^2 - \varepsilon^2}} \right) / 2 \right) \quad (2.72)$$

$$K = \frac{\pi A_p \left[(\omega\tau_1)^2 + 1 \right]}{4h} \quad (2.73)$$

Hence, τ_1 and K are estimated from (2.72) and (2.73), respectively for off-line identification method.

For on-line identification the following expression is obtained by employing the required equations in (2.8)

$$\frac{Ke^{-j\omega\delta}(u+jv)}{(j\omega\tau_1+1)^2} = -1 \quad (2.74)$$

Considering the phase angle and magnitude of the above equation to derive

$$\tau_1 = \frac{1}{\omega} \cot\left(\omega\delta - \tan^{-1}\left(\frac{v}{u}\right)/2\right) \quad (2.75)$$

$$K = \frac{(\omega\tau_1)^2 + 1}{\sqrt{u^2 + v^2}} \quad (2.76)$$

Now, τ_1 and K are estimated from (2.75) and (2.76), respectively for on-line identification method and one more parameter δ is obtained from the method as mentioned in subsection 2.4.2.

Example 6

This example illustrates identification of critically damped SOPDT process dynamics for the following process [3]

$$G(s) = \frac{e^{-0.01s}}{(2s+1)^2}.$$

Application of off-line relay ($h = 1$ and $\varepsilon = 0.1$) feedback test generates the limit cycle and its second derivative output with the quantities $A_p = 0.1555$, $T_p = 2.3291$, $t_0 = 0.4889$ and $t_1 = 0.4989$. So, the time delay parameter, $\delta = 0.01$ is obtained. Substituting the required parameters in (2.72) and (2.73), the remaining process model parameters are estimated as $\tau_1 = 1.9938$ and $K = 1.0054$. Similarly, the parameters obtained during on-line test (using controller parameters $K_p = 0.01$, $T_I = 0.5$ and $T_D = 0.125$) are $A_p = 0.1558$, $T_p = 2.3279$, $t_0 = 0.4876$ and $t_1 = 0.4976$, so, $\delta = 0.01$. Utilizing these parameters in (2.75) and (2.76) the process model parameters are obtained as $\tau_1 = 1.9963$ and $K = 1.0085$. These identified process dynamics are represented in transfer function models in Table 2.7 along with the model proposed by Thyagarajan and Yu [3]. The results are also compared using Nyquist plots as shown in Fig. 2.13. The effect of measurement noise on limit cycle parameters and estimated process model parameters in

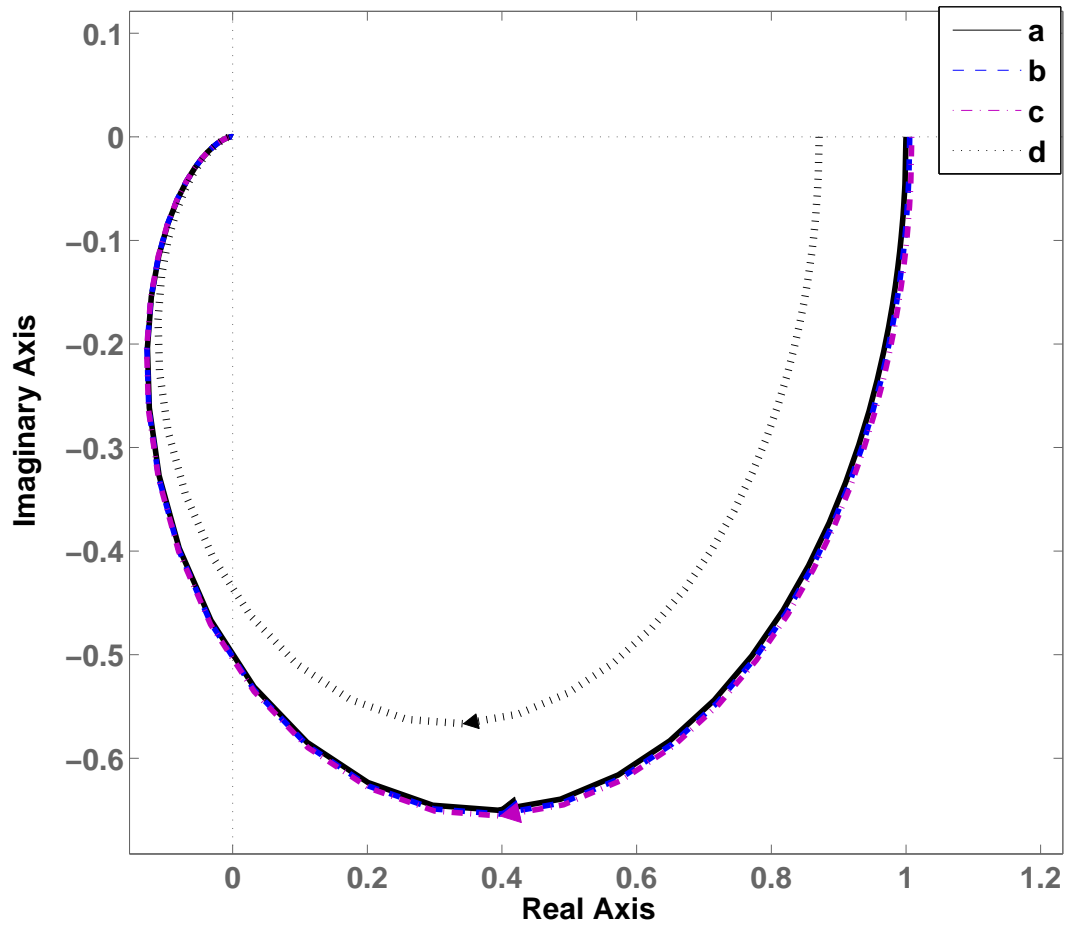


Figure 2.13: Nyquist plots for Example 6: (a) Actual process, (b) identified model (off-line), (c) identified model (on-line) and (d) model proposed by Thyagarajan & Yu [3]

percentage (%) error is given in Table 2.8 for on-line identification.

Table. 2.7: Comparison of process models for Example 6

Method	Process model	Error (\tilde{E})
Off-line	$\frac{1.0054e^{-0.01s}}{(1.9938s+1)^2}$	0.1109
On-line	$\frac{1.0085e^{-0.01s}}{(1.9963s+1)^2}$	0.1182
Thyagarajan & Yu [3]	$\frac{0.8709e^{-0.013s}}{(1.8978s+1)^2}$	0.4236

Table. 2.8: Effect of measurement noise on parameters in % error for Example 6

SNR (dB)	T_p	A_p	K	τ_1	δ
10	0.0301	-0.5135	-2.0129	-1.676	-3.0
15	0.0408	-0.3851	-1.2097	-0.8697	-1.0
20	0.0021	-0.0642	-0.2082	-0.1602	0
25	0.0064	-0.0642	-0.1784	-0.1502	-1.0

2.5 Generalized analytical expressions

In this section a generalized SOPDT process model is considered and the expressions are derived for on-line identification method, further these equations can be used to get the expressions for off-line method with some modifications. The generalized transfer function model of stable or unstable SOPDT process is given by

$$G_m(s) = \frac{Ke^{-\delta s}}{ms^2 + ns \pm 1} \quad (2.77)$$

or

$$G_m(j\omega) = \frac{Ke^{-j\omega\delta} \alpha_2 \beta_2}{(j\omega \mp \alpha_2)(j\omega - \beta_2)} \quad (2.78)$$

where

$$\alpha_2 = \frac{-2}{n + \sqrt{n^2 \mp 4m}}; \quad \beta_2 = \frac{\mp 2}{n - \sqrt{n^2 \mp 4m}} \quad (2.79)$$

The model given in (2.77) is realized in terms of SOPDT (stable or unstable), underdamped SOPDT, critically damped SOPDT, and FOPDT (stable or unstable) process models as described in the following subsections.

2.5.1 Expressions for SOPDT process model

The transfer function given in (2.77) can be realized as stable or unstable SOPDT process with the condition $n^2 > 4m$. For on-line identification, substituting (2.78), (2.1) and (2.5) into (2.8) and solved further to get

$$\frac{Ke^{-j\omega\delta}\alpha_2\beta_2}{(j\omega \mp \alpha_2)(j\omega - \beta_2)}(u + jv) = -1 \quad (2.80)$$

Substituting for α_2 and β_2 in the above equation and solved to obtain

$$\frac{Ke^{-j\omega\delta}}{m\omega^2 - j\omega n \mp 1} = \frac{u - jv}{u^2 + v^2} \quad (2.81)$$

Equating the magnitude and phase angle on both sides of (2.81), the following explicit expressions are obtained

$$m = \frac{1}{\omega^2} \left[1 + K\sqrt{u^2 + v^2} \cos \left(\omega\delta - \tan^{-1} \left(\frac{v}{u} \right) \right) \right] \quad (2.82)$$

for stable SOPDT process.

$$m = \frac{1}{\omega^2} \left[K\sqrt{u^2 + v^2} \cos \left(\omega\delta - \tan^{-1} \left(\frac{v}{u} \right) \right) - 1 \right] \quad (2.83)$$

for unstable SOPDT process.

$$n = \left[\frac{K\sqrt{u^2 + v^2}}{\omega} \right] \sin \left(\omega\delta - \tan^{-1} \left(\frac{v}{u} \right) \right) \quad (2.84)$$

for stable or unstable SOPDT processes.

Hence, the expressions given in (2.82) and (2.84) are used to estimate the process model parameters (m and n) for stable SOPDT process and (2.83) and (2.84) are utilized to obtain the parameters of unstable SOPDT process. The remaining parameters K and δ are obtained as explained in subsections 2.4.1 and 2.4.2, respectively.

The stable SOPDT process model given in (2.77) becomes an underdamped process for the condition $n^2 < 4m$ as described earlier in subsection 2.4.3 hence, α_2 and β_2 are replaced with α_1 and β_1 as mentioned in (2.59). It is observed that substituting these values of α_1 and β_1 in (2.80) for stable condition, the expressions obtained for m and n are as given in (2.82) and (2.84), respectively.

Now, a critically damped SOPDT process model is represented as

$$G_m(s) = \frac{Ke^{-\delta s}}{(\sqrt{m}s + 1)^2} \quad (2.85)$$

which is obtained by substituting $n = 2\sqrt{m}$ in (2.77) which is considered as stable process. Hence, this value of n , is put in (2.79) to get $\alpha_2 = \beta_2 = -1/\sqrt{m}$ which are utilized in (2.80) and reduced to

$$\frac{Ke^{-j\omega\delta}(u + jv)}{(j\omega\sqrt{m} + 1)^2} = -1 \quad (2.86)$$

Again, equating the magnitude and phase angle on both sides of the above equation we get

$$\sqrt{m} = \frac{1}{\omega} \left[\cot \left(\left(\omega\delta - \tan^{-1} \left(\frac{v}{u} \right) \right) / 2 \right) \right] \quad (2.87)$$

$$K = \frac{m\omega^2 + 1}{\sqrt{u^2 + v^2}} \quad (2.88)$$

Eqs. (2.87) and (2.88) are employed to estimate the process model parameters (\sqrt{m} and K) of critically damped SOPDT process. The process time delay (δ) is obtained from the method as described in subsection 2.4.2.

2.5.2 Expressions for FOPDT process model

The following stable or unstable FOPDT process model is obtained by making $m = 0$ in (2.77)

$$G_m(s) = \frac{Ke^{-\delta s}}{ns \pm 1} \quad (2.89)$$

Using $m = 0$ in (2.79), one can get $\alpha_2 = -1/n$ and $\beta_2 = \infty$ which are substituted in (2.80) and solved to obtain

$$\frac{Ke^{-j\omega\delta}(u + jv)}{(j\omega n \pm 1)} = -1 \quad (2.90)$$

Considering the magnitude and phase angle on both sides of the above equation the following explicit expressions are obtained

$$n = \frac{\sqrt{K^2(u^2 + v^2) - 1}}{\omega} \quad (2.91)$$

for stable or unstable process.

$$\delta = \frac{1}{\omega} \left[\pi + \tan^{-1} \left(\frac{v - u\omega n}{u + v\omega n} \right) \right] \quad (2.92)$$

for stable process.

$$\delta = \frac{1}{\omega} \left[\tan^{-1} \left(\frac{v + u\omega n}{u - v\omega n} \right) \right] \quad (2.93)$$

for unstable FOPDT process.

Hence, to estimate the FOPDT process model parameters (n and δ), Eqs. (2.91) and (2.92) are utilized for stable processes and Eqs. (2.91) and (2.93) for unstable processes. The steady state gain K is obtained by using the method as explained in subsection 2.4.1.

As mentioned earlier during off-line mode of operation, the relay test is conducted in the absence of controller. Hence, the expressions derived in subsections 2.5.1 and 2.5.2 can be modified with the following changes to identify the process dynamics during off-line mode

$$u = (4h\sqrt{A^2 - \varepsilon^2})/\pi A^2; \quad v = -4h\varepsilon/\pi A^2 \quad (2.94)$$

It can be observed that the expressions derived for FOPDT and SOPDT process models by considering the individual process in Section 2.4 and the expressions obtained for generalized process model in Section 2.5 are the same.

2.6 Summary

A simple DF technique is used to derive explicit expressions in terms of relay and limit cycle parameters to estimate the unknown process model parameters during off-line and on-line mode of operation. Relay with hysteresis is applied to get process information in the form of limit cycle. Different types of processes are considered and expressions are derived for individual process model to estimate the parameters. These process models are also generalized using a second order process model with time delay and accordingly expressions are derived. Examples

are considered in the form of transfer function models and parameters are estimated to show efficacy and robustness of the proposed method. Process dynamics are also identified in the presence of measurement noise.



CHAPTER 3

OFF-LINE AND ON-LINE IDENTIFICATION OF TITO PROCESSES

3.1 Introduction

Process identification plays an important role in automatic tuning of controllers in industries. In the literature a plenty of identification methods [3, 13, 35, 37, 39, 41, 48, 62, 72–75] are available for SISO processes using different types of relays and algorithms. Many of the industrial processes consist of multi-input-multi-output (MIMO) processes. The TITO (two-input-two-output) processes are one of the most commonly used categories of multivariable processes [24, 25]. As identification of TITO processes is generally a difficult task due to the interaction between the loops, it is desirable to identify TITO processes in terms of two SISO process models [76] for easier field implementation. Few methods are available for identification of multivariable processes. Wang et al. [23] proposed identification of TITO processes using decentralized relay feedback technique. Here the authors used biased relay and standard relay in the dominant loop and other loops, respectively. Choi et al. [26] proposed identification of multivariable processes (TITO) using sequential loop closing method. Padhy et al. [4] and Padhy and Majhi [27] proposed on-line identification of TITO processes using DF technique. Here the authors used ideal relay to acquire the process information. Li et al. [77] proposed identification of TITO processes applying step test.

In this chapter simple explicit expressions are derived using DF technique to identify the TITO process models during on-line and off-line mode of operation. Measurement noise is an impor-

tant issue in an identification problem. During the relay feedback experiments, amplitude of the limit cycle output is often corrupted with noise due to which the test may fail. To overcome the possible failure, a relay with hysteresis is considered in the proposed identification method. Simulation examples are included to illustrate usefulness of the proposed method.

3.2 Identification method

This section presents the procedure for on-line identification of TITO processes by relay based closed loop tests. The conventional on-line TITO system is shown in Fig. 3.1 which consists of the TITO process, two relays N_1 and N_2 , and PID controllers in the closed loops. The TITO process is represented by the following transfer function matrix

$$G(s) = \begin{bmatrix} G_{11}(s) & G_{12}(s) \\ G_{21}(s) & G_{22}(s) \end{bmatrix} \quad (3.1)$$

This TITO process is approximated by two SISO process models. The DF technique proposed in Chapter 2 is extended here to identify the TITO process in terms of the following model transfer function matrix

$$G_m(s) = \begin{bmatrix} G_{m1}(s) & 0 \\ 0 & G_{m2}(s) \end{bmatrix} \quad (3.2)$$

where $G_{m1}(s)$ and $G_{m2}(s)$ are the SISO transfer function models as given below

$$G_{mi}(s) = \frac{K_i e^{-\delta_i s}}{(1 + \tau_i s)^2} \quad \forall \quad i = 1, 2 \quad (3.3)$$

or in terms of frequency domain

$$G_{mi}(j\omega) = \frac{K_i e^{-j\omega\delta_i}}{(1 + j\omega\tau_i)^2} \quad (3.4)$$

where K_i , τ_i and δ_i are the steady state gain, the time constant and the time delay of the process model, respectively. These process model parameters (K_i , τ_i and δ_i) are unknown and that are to be estimated.

It can be observed in Fig. 3.1 that the relays (N_1 and N_2) are in parallel with the controllers G_{c1} and G_{c2} . Equivalent representation of Fig. 3.1 is redrawn in Fig. 3.2. It can be seen from Fig.

3.2 that the controllers are in the inner feedback paths and help in stabilizing the process during identification. In describing function analysis, the relays with hysteresis are approximated by gains of

$$N_i = \frac{4h_i \left(\sqrt{A_{pi}^2 - \varepsilon_i^2} - j\varepsilon_i \right)}{\pi A_{pi}^2} \quad \forall \quad i = 1, 2 \quad (3.5)$$

where h_i is the amplitude of relay, ε_i the hysteresis width of relay and A_{pi} the peak amplitude of limit cycle for corresponding loops 1 and 2. The relay parameters (h_1 , h_2 , ε_1 and ε_2) are user defined and the peak amplitude of limit cycle (A_{p1} and A_{p2}) is measured from the corresponding limit cycle output. Let $G_c(s)$ be the PID controller matrix given by

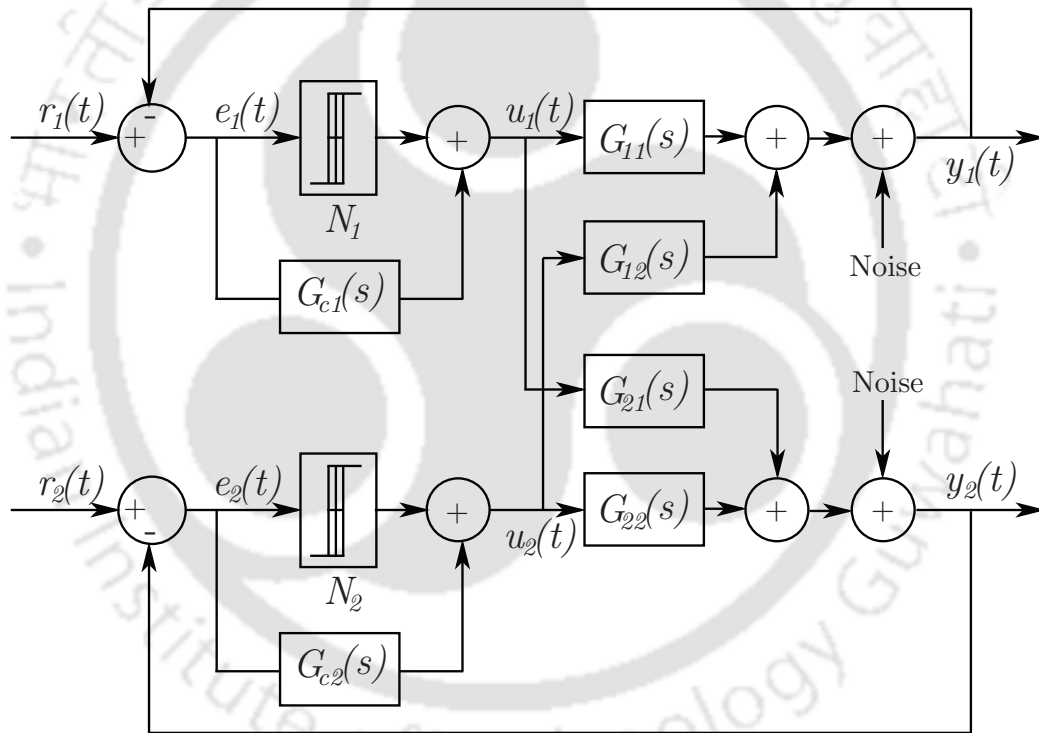


Figure 3.1: Conventional TITO system with relay and controller

$$G_c(s) = \begin{bmatrix} G_{c1}(s) & 0 \\ 0 & G_{c2}(s) \end{bmatrix} \quad (3.6)$$

where

$$G_{ci}(s) = K_{Pi} \left(1 + \frac{1}{T_{iS}} + \frac{T_{Di}S}{\alpha_i T_{Di}S + 1} \right) \quad (3.7)$$

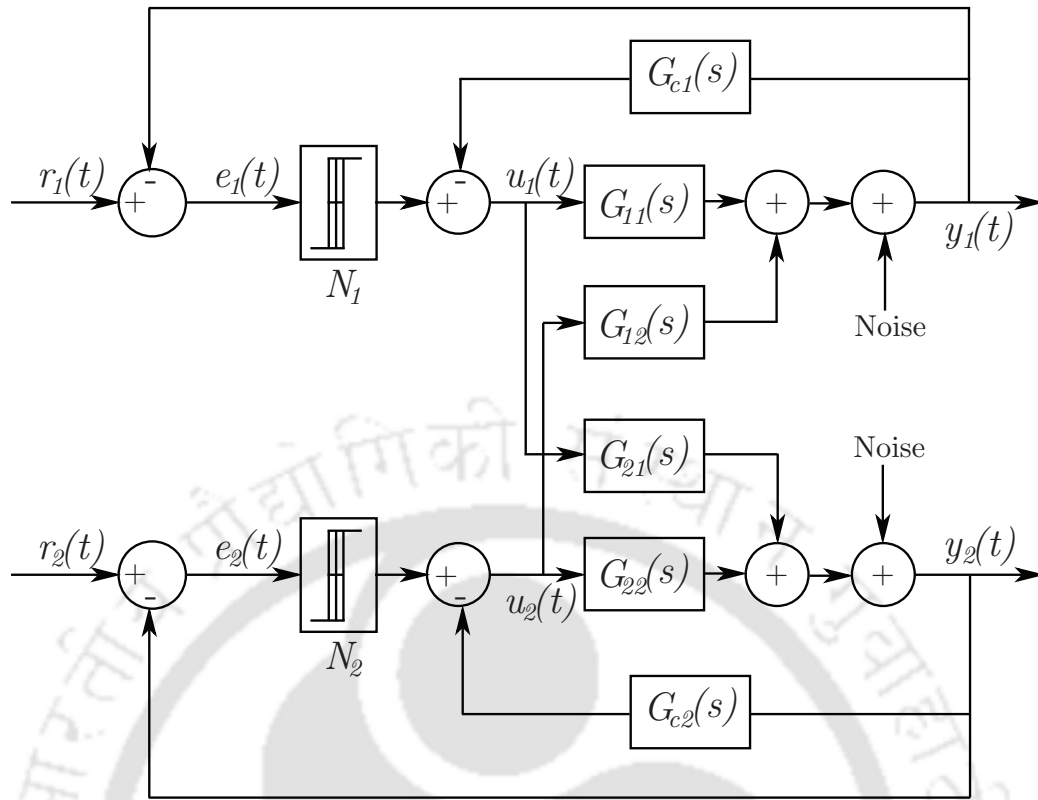


Figure 3.2: Equivalent representation of Fig. 3.1

In the above expression α_i is the derivative filter constant of the i^{th} loop. Since this derivative filter constant is very small, it is neglected for ease in analysis in the following derivations. Hence, the above expression can be written as

$$G_{ci}(s) = K_{Pi} \left(1 + \frac{1}{T_{Ii}s} + T_{Di}s \right) \quad (3.8)$$

or

$$G_{ci}(j\omega) = K_{Pi} \left(1 + \frac{1}{j\omega T_{Ii}} + j\omega T_{Di} \right) \quad (3.9)$$

The controller parameters (K_{Pi} , T_{Ii} and T_{Di}) are pre-specified to obtain the sustained oscillations.

Let the describing function matrix be

$$N = \begin{bmatrix} N_1 & 0 \\ 0 & N_2 \end{bmatrix} \quad (3.10)$$

where N_1 and N_2 are the gains of the relays with hysteresis for loops 1 and 2, respectively. The estimation of process model parameters is described in the following section.

3.3 Estimation of process model parameters

The peak amplitude A_{pi} and half time period T_{pi} of the limit cycle outputs are measured assuming that both the loops under limit cycle condition have the same frequencies. The auto-tuning test results in stable limit cycle outputs for any non-zero h_1 and h_2 subject to the condition

$$N_i \bar{G}_{mi}(j\omega) = -I \quad (3.11)$$

where

$$\bar{G}_{mi}(j\omega) = \frac{G_{mi}(j\omega)}{I + G_{mi}(j\omega)G_{ci}(j\omega)} \quad (3.12)$$

and I is an identity matrix of the order of $G_{mi}(j\omega)$. Then, (3.11) becomes

$$G_{mi}(j\omega)(N_i + G_{ci}(j\omega)) = -I \quad (3.13)$$

Substituting for N_i , $G_{mi}(j\omega)$ and $G_{ci}(j\omega)$ from (3.5), (3.4) and (3.9), respectively in the above equation and resolving we obtain

$$\frac{K_i e^{-j\omega\delta_i} (u + jv)}{(1 + j\omega\tau_i)^2} = -1 \quad (3.14)$$

where

$$u = \frac{4h_i}{\pi A_{pi}^2} (\sqrt{A_{pi}^2 - \epsilon_i^2}) + K_{pi} \quad (3.15)$$

and

$$v = \omega K_{pi} T_{Di} - \frac{K_{pi}}{\omega T_{Li}} - \frac{4h_i \epsilon_i}{\pi A_{pi}^2} \quad (3.16)$$

Equating the magnitudes of both sides of (3.14) and further simplifying we get

$$\omega\tau_i = \sqrt{K_i \sqrt{u^2 + v^2} - 1} \quad (3.17)$$

which is represented in terms of the process model parameter τ_i as

$$\tau_i = \frac{\sqrt{K_i \sqrt{u^2 + v^2} - 1}}{\omega} \quad (3.18)$$

Similarly, equating the phase angles of both sides of (3.14) and solving

$$\omega\delta_i = \pi + \tan^{-1}\left(\frac{v}{u}\right) - 2\tan^{-1}(\omega\tau_i) \quad (3.19)$$

or in terms of δ_i ,

$$\delta_i = \frac{\pi + \tan^{-1}\left(\frac{v}{u}\right) - 2\tan^{-1}(\omega\tau_i)}{\omega} \quad (3.20)$$

Thus, using the explicit expressions (3.18) and (3.20), the process model parameters τ_i and δ_i are estimated, respectively.

Since, using DF method only two parameters can be estimated hence, the steady state gain K_i of the process is obtained from the method proposed by Padhy et al. [4].

The expressions derived for on-line identification are modified to get the equations for estimation of process model parameters during off-line mode of operation with the following changes in u and v

$$u = (4h_i\sqrt{A_{pi}^2 - \varepsilon_i^2})/\pi A_{pi}^2; \quad v = -4h_i\varepsilon_i/\pi A_{pi}^2 \quad (3.21)$$

Hence, substituting for u and v in (3.18) and (3.20) the following expressions are obtained

$$\tau_i = \frac{1}{\omega} \left[\sqrt{\frac{4h_i K_i}{\pi A_{pi}} - 1} \right] \quad (3.22)$$

$$\delta_i = \frac{1}{\omega} \left[\pi - 2\tan^{-1}(\omega\tau_i) - \tan^{-1}\left(\frac{\varepsilon_i}{\sqrt{A_{pi}^2 - \varepsilon_i^2}}\right) \right] \quad (3.23)$$

Now, Eqs. (3.22) and (3.23) are used to estimate the process model parameters (τ_i and δ_i) during off-line mode of operation.

3.4 Simulation results

Two examples are considered in this section to illustrate usefulness of the proposed identification method. For on-line identification the initial PID controller parameters are set to $K_{P_i} = 0.1$, $T_{I_i} = 1$ and $T_{D_i} = 0.25$, for $i = 1, 2$. These values are decided from a number of simulation results. To test the proposed method in the face of measurement noise, a white Gaussian noise of zero mean and certain variance is added at the outputs of loops 1 and 2 simultaneously to create noisy oscillations. Fourier series based curve fitting technique [1,39] is used to recover the noise free limit cycle output. The process is decoupled completely by using the decoupler obtained by Wang et al.'s method [78] assuming that the full matrix transfer function model of the process is known.

Example 1

Let us consider the following transfer matrix of a TITO process [4, 79]

$$G(s) = \frac{1}{den(s)} \begin{bmatrix} 1 & \frac{-2.4}{1+0.5s} \\ \frac{0.5}{1+0.1s} & 1 \end{bmatrix}$$

where $den(s) = (1 + 0.1s)(1 + 0.2s)^2$.

For on-line identification, relay ($h_1 = h_2 = 1$ and $\epsilon_1 = \epsilon_2 = 0.1$) inputs are simultaneously applied to both the loops 1 and 2 to obtain the limit cycles. The limit cycle generated from loop 1 is as shown in Fig. 3.3, similar output is generated from loop 2. The parameters measured from these limit cycles are $A_{p1} = 0.2903$, $T_{p1} = 0.3272$ for loop 1 similarly, for loop2 $A_{p2} = 0.2576$, $T_{p2} = 0.3273$.

The steady state gains $K_1 = 2.2$ and $K_2 = 2.2$ are obtained from the method proposed by Padhy et al. [4]. Using the corresponding values in (3.18) and (3.20), the process model parameters τ_1 , τ_2 , δ_1 and δ_2 are estimated. Similarly, the process dynamics are identified in the presence of measurement noise of 20 dB SNR. Using curve fitting technique [1,39] the denoised limit cycle is obtained, Fig. 3.4 shows the noisy and denoised limit cycle outputs from loop 1. Hence, the identified process models are given below

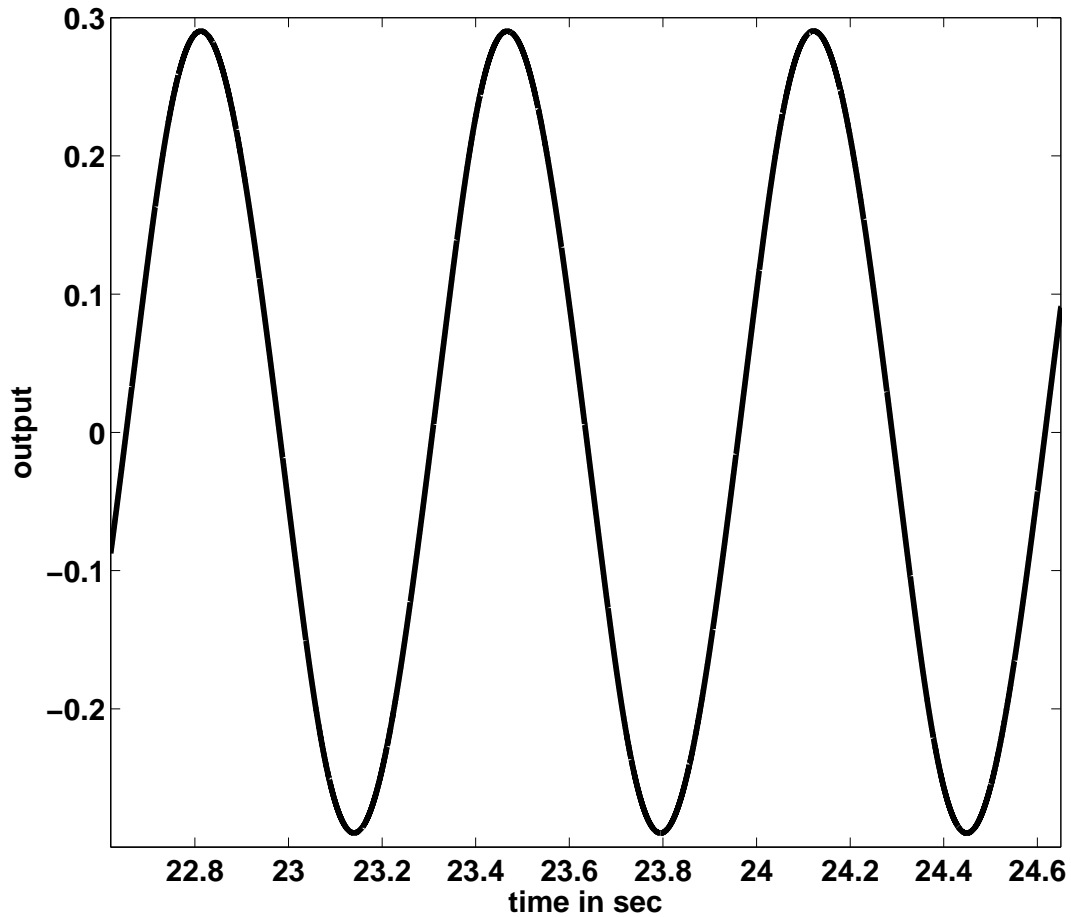


Figure 3.3: Limit cycle output from loop 1

$$G_m(s)_{without\ noise} = \begin{bmatrix} \frac{2.2e^{-0.0374s}}{(1+0.3072s)^2} & 0 \\ 0 & \frac{2.2e^{-0.0279s}}{(1+0.3277s)^2} \end{bmatrix}$$

$$G_m(s)_{with\ noise} = \begin{bmatrix} \frac{2.2e^{-0.036s}}{(1+0.3064s)^2} & 0 \\ 0 & \frac{2.2e^{-0.0254s}}{(1+0.3316s)^2} \end{bmatrix}$$

During off-line mode of operation the following process model is obtained by repeating the above procedure and using (3.22) and (3.23)

$$G_m(s) = \begin{bmatrix} \frac{2.2e^{-0.036s}}{(1+0.3051s)^2} & 0 \\ 0 & \frac{2.2e^{-0.0269s}}{(1+0.3263s)^2} \end{bmatrix}$$

The process model suggested by Padhy et al. [4] using an ideal relay is

$$G_m(s) = \begin{bmatrix} \frac{2.2e^{-0.0412s}}{(1+0.3163s)^2} & 0 \\ 0 & \frac{2.2e^{-0.0404s}}{(1+0.3226s)^2} \end{bmatrix}$$

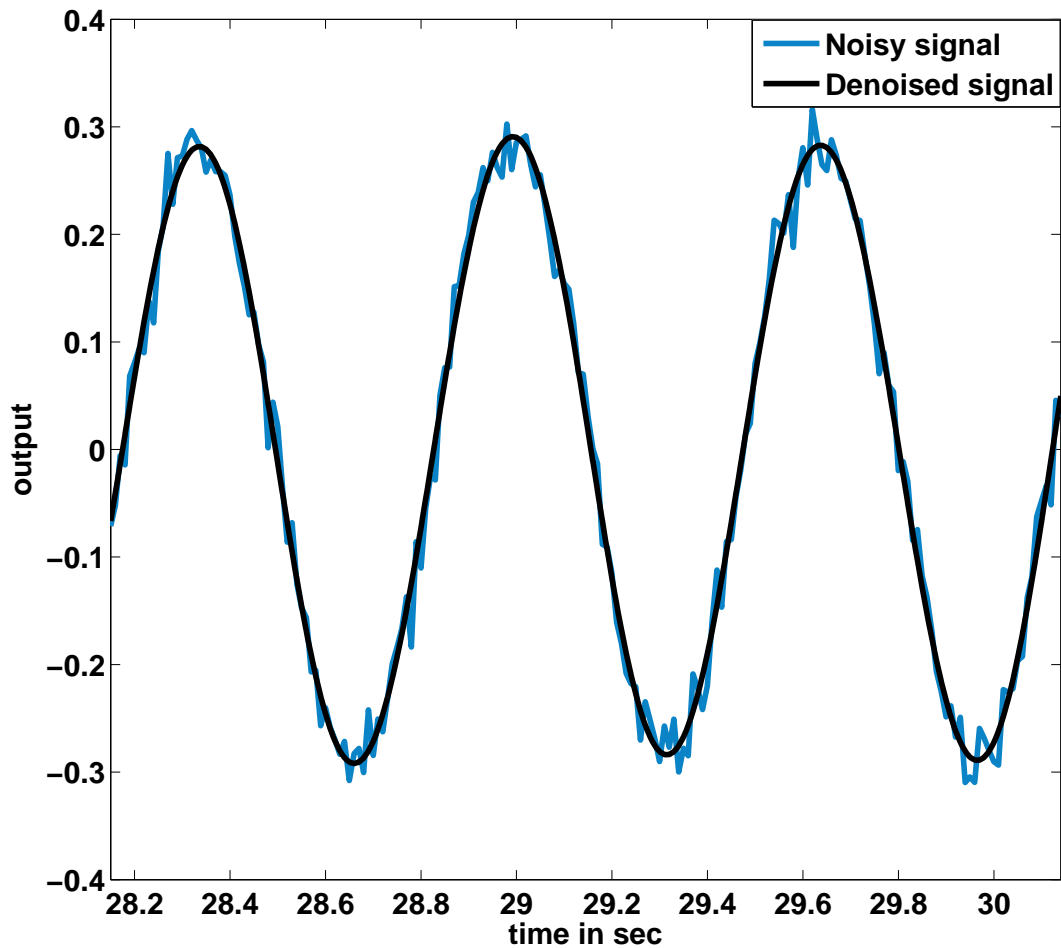


Figure 3.4: Noisy and denoised limit cycle outputs from loop 1

The decoupled model obtained by using Wang et al.'s [78] method is

$$G_m(s) = \begin{bmatrix} \frac{250s^2+3000s+11000}{s^5+32s^4+385s^3+2150s^2+5500s+5000} & 0 \\ 0 & \frac{250s^2+3000s+11000}{s^5+32s^4+385s^3+2150s^2+5500s+5000} \end{bmatrix}$$

The Nyquist plots of first and second equivalent diagonal elements of the above process models are shown in Figs. 3.5 and 3.6, respectively and it can be observed that the plots are close to each other. The error analysis (using H_∞ norm) of the proposed models, the decoupled model and the model suggested by Padhy et al. [4] is given in Table 3.1.

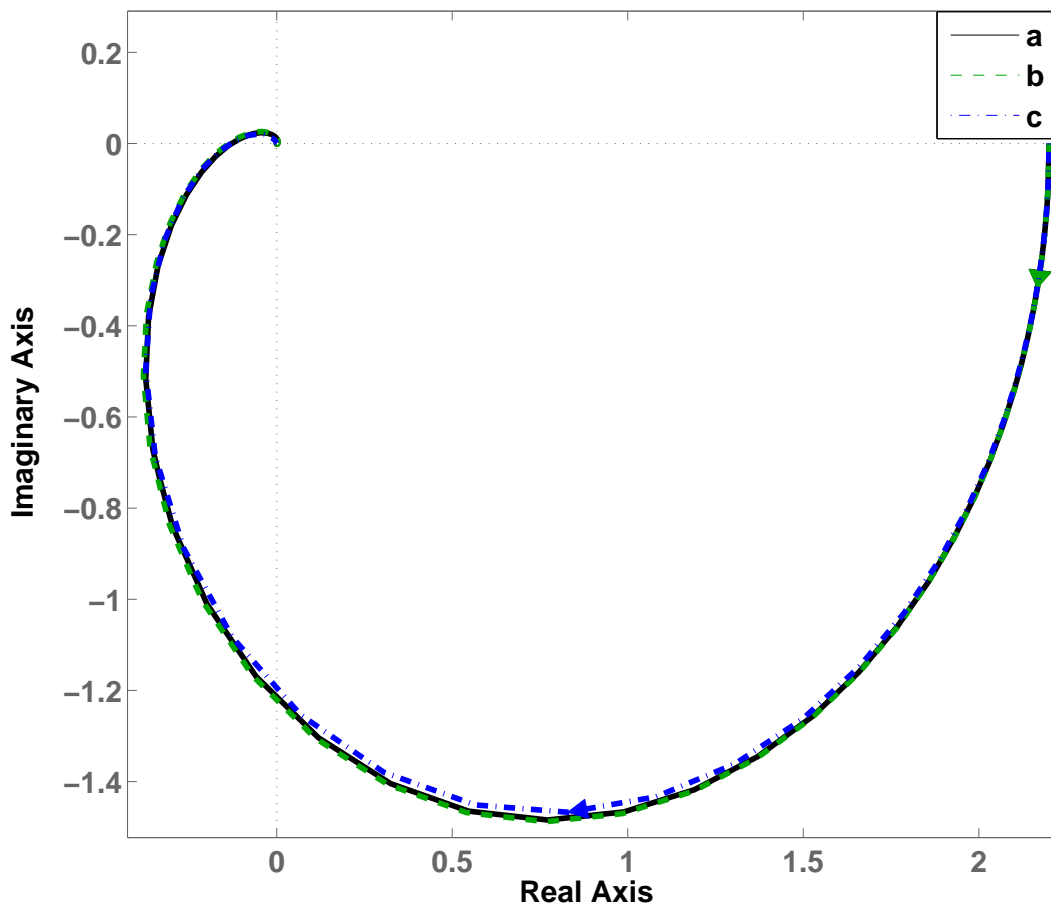


Figure 3.5: Nyquist plots: (a) proposed model, (b) proposed by Padhy et al. [4] and (c) decoupled model

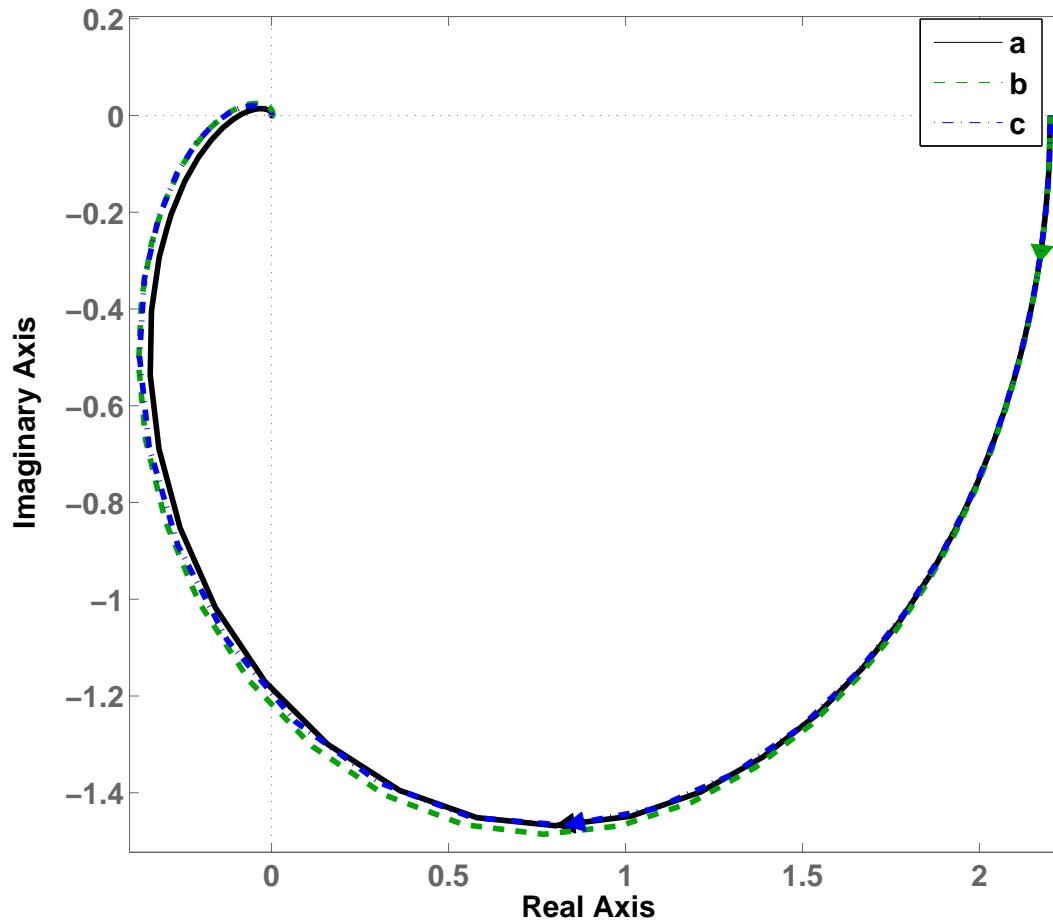


Figure 3.6: Nyquist plots: (a) proposed model, (b) proposed by Padhy et al. [4] and (c) decoupled model

Table. 3.1: Error analysis using H_∞ norm

Proposed method	H_∞ norm
On-line without noise	0.1886
On-line with noise	0.1886
Off-line without noise	0.1886
Padhy et al. [4]	0.1886
Decoupled by Wang et al. [78]	0.1475

Example 2

The following TITO process [27, 79] is considered in this example

$$G(s) = \frac{1}{den(s)} \begin{bmatrix} (1.5s + 1) & 0.2(0.75s + 1) \\ 0.6(0.75s + 1) & 0.8(1.2s + 1) \end{bmatrix}$$

where $den(s) = (1 + s)(1 + 2s)^2(1 + 0.5s)$.

Here also the limit cycles are generated by applying relay inputs simultaneously to loops 1 and 2 on-line. The relay settings used are $h_1 = h_2 = 1$ and $\varepsilon_1 = \varepsilon_2 = 0.1$ and the limit cycle quantities measured from loop 1 are $A_{p1} = 0.2652$, $T_{p1} = 2.7381$ and from loop2 $A_{p2} = 0.2566$, $T_{p2} = 2.7382$. Similar to Example 1 the steady state gains $K_1 = 0.849$ and $K_2 = 0.678$ are obtained. Eqs. (3.18) and (3.20) are solved utilizing the required values to calculate the process model parameters τ_1 , τ_2 , δ_1 and δ_2 . The process model parameters are also estimated in the presence of measurement noise of 20 dB SNR. The noisy and denoised limit cycle outputs from loop 1 are as shown in Fig. 3.7. Hence, the proposed process models are

$$G_m(s)_{without\ noise} = \begin{bmatrix} \frac{0.849e^{-0.5517s}}{(1+1.5526s)^2} & 0 \\ 0 & \frac{0.678e^{-0.6408s}}{(1+1.3621s)^2} \end{bmatrix}$$

$$G_m(s)_{with\ noise} = \begin{bmatrix} \frac{0.849e^{-0.4592s}}{(1+1.618s)^2} & 0 \\ 0 & \frac{0.678e^{-0.5447s}}{(1+1.4092s)^2} \end{bmatrix}$$

Similarly, the process model identified during off-line test is

$$G_m(s) = \begin{bmatrix} \frac{0.849e^{-0.5519s}}{(1+1.5544s)^2} & 0 \\ 0 & \frac{0.678e^{-0.6411s}}{(1+1.3635s)^2} \end{bmatrix}$$

The process model suggested by Padhy and Majhi [27] using an ideal relay is

$$G_m(s) = \begin{bmatrix} \frac{0.849e^{-0.4370s}}{(1+1.6698s)^2} & 0 \\ 0 & \frac{0.678e^{-0.4272s}}{(1+1.5343s)^2} \end{bmatrix}$$

The decoupled model obtained by using Wang et al.'s [78] method is

$$G_m(s) = \begin{bmatrix} \frac{17.1562s^2 + 24.75s + 8.5}{24s^5 + 116s^4 + 206s^3 + 171s^2 + 67s + 10} & 0 \\ 0 & \frac{5.49s^2 + 7.92s + 2.72}{12s^5 + 56s^4 + 95s^3 + 75s^2 + 28s + 4} \end{bmatrix}$$

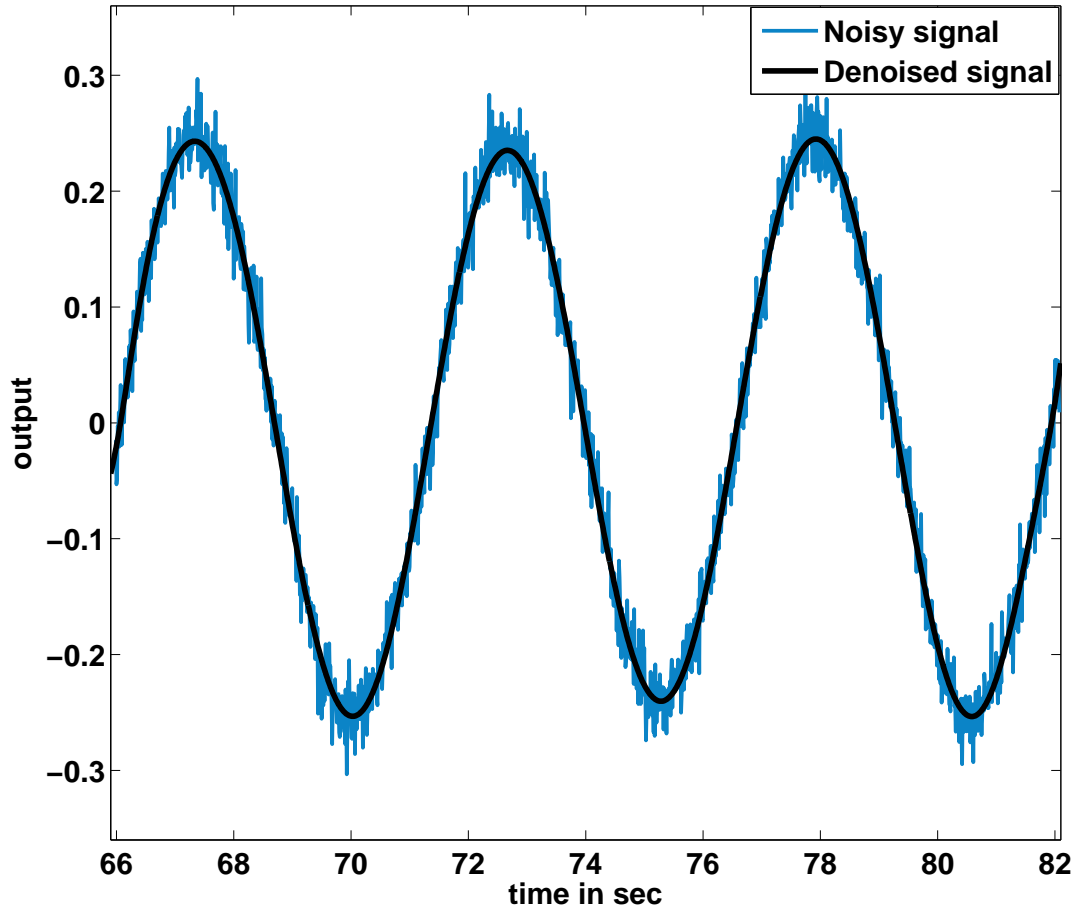


Figure 3.7: Noisy and denoised limit cycle outputs from loop 1

The estimated process model parameters are compared with parameters suggested by Padhy and Majhi [27] and the error analysis is given in Table 3.2.

Table. 3.2: Error analysis for estimated parameters for Example 2

Proposed method	τ_1	τ_2	δ_1	δ_2
On-line without noise	0.0702	0.1122	0.2625	0.5
On-line with noise	0.0310	0.0815	0.0508	0.2750
Off-line without noise	0.0691	0.1113	0.2629	0.5007

3.5 Summary

In this chapter an on-line and off-line identification of TITO processes using describing function of relay with hysteresis is presented. A relay with hysteresis is applied simultaneously to both the loops to extract the process information through limit cycle output. Two well-known examples are considered to show the usefulness of the proposed identification method even in the presence of measurement noise. Simulation results are verified with the help of Nyquist plots. Further, based on the identified models the PID controller parameters can be updated on demand when the PID tuning rules are available in terms of the model parameters.



CHAPTER 4

RELAY WITH HYSTERESIS AND STATE SPACE BASED IDENTIFICATION

4.1 Introduction

Identification of accurate process dynamics plays significant role in design of model based controllers. As it is seen in Chapter 2 that process identification can be done by using DF method which gives approximate process model parameters. In the literature many authors [12–16, 80] used DF technique to estimate unknown process model parameters of various processes. In DF technique, approximations are made on the gain of a relay which acts as a static nonlinear device. Hence estimated process model parameters are approximate and maximum two parameters can be estimated. To overcome these limitations researchers started working towards development of exact methods so that accurate process model parameters are obtained. Kaya and Atherton [72] proposed identification of stable and unstable FOPDT and SOPDT process dynamics based on exact asymmetrical limit cycle analysis. Srinivasan and Chidambaram [41] used Laplace transform approach and modified asymmetrical relay feedback method to get improved FOPDT model parameters. Their method requires selection of an extra parameter γ (displacement in the relay amplitude) for accurate estimation of process gain and ultimate frequency. Wang et al. [35] developed exact expressions for time periods and amplitudes of the limit cycle using relay with hysteresis for a FOPDT process model. Initially the authors used biased relay to get oscillatory waveforms to identify the process dynamics. But using biased relay caused larger disturbances than unbiased relay, later the authors used unbiased relay to obtain

improved results. Chang et al. [17] developed analytical expressions for identification of first order, second order and higher order processes using Z-transform method. Atherton and Majhi [62] proposed on-line identification of stable and unstable FOPDT and SOPDT processes, using asymmetrical relay feedback test. Panda and Yu [81] developed process model equations in time domain to estimate the unknown parameters of overdamped, critically damped and underdamped process models. Panda et al. [48] proposed algorithms for estimation of integrating and time delay process model parameters using single relay feedback test. Majhi [39] developed analytical expressions for parametric identification of first order, second order and higher order processes using ideal relay. The author used Fourier series based curve fitting technique to obtain clean limit cycle from noisy process output. In the literature many authors used ideal relay or asymmetrical relay for identification of process dynamics, with or without noise. But the effect of measurement noise can be reduced using relay with hysteresis [10]. Generally, hysteresis width is set to twice the standard deviation of noise [7]. So, in proposed method a new control structure which comprises of relay with hysteresis, the process and a denoising block, is used to increase the robustness of process dynamics identification under noisy environment. The approaches proposed in [39] are extended in this work to develop mathematical expressions for estimation of unknown process model parameters using relay with hysteresis.

Process identification algorithms are also proposed based on relay with hysteresis [5, 16, 35, 47, 82]. Our proposed method has the following advantages as compared with other algorithms: a) derivations of more number of exact equations, b) measurement of more number of limit cycle parameters for symmetrical relay feedback tests, c) on-line elimination of measurement noise with the help of a new control strategy and d) generalized expressions to estimate the unknown parameters of a class of process models.

In this chapter, identification of stable or unstable first order, second order overdamped, underdamped, critically damped and integrating process dynamics is presented. Relay with hysteresis is used to induce a limit cycle output and using this information, unknown process model parameters are estimated. State space based generalized analytical expressions are derived to achieve accurate results. Expressions are derived for off-line identification of SISO process dynamics.

In real time systems, measurement noise is an important issue during identification of process dynamics. A relay with hysteresis reduces the effect of measurement noise, in addition a denoising block is proposed to recover the original limit cycle. Simulation results are included to validate the effectiveness of the proposed method.

4.2 Identification method

In this section a new control structure as shown in Fig. 4.1 is proposed to identify the unknown process dynamics and to mitigate the effects of measurement noise. This structure consists of a relay with hysteresis in series with the unknown process and a denoising block. The functioning of this denoising block is explained in subsection 4.2.1. In Fig. 4.1 application of relay input to the process generates limit cycle output. This limit cycle output consists of process information in the form of various parameters. These limit cycle quantities and relay parameters are substituted in the expressions derived for corresponding process models to identify the process dynamics.

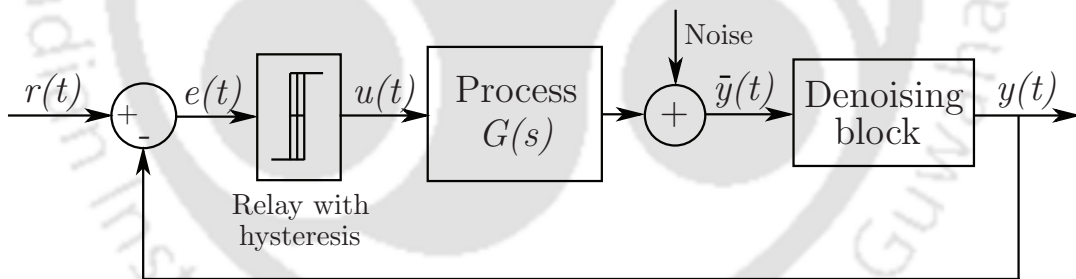


Figure 4.1: Proposed relay feedback identification scheme

The generalized transfer function model of a stable or unstable SOPDT process is given as

$$G_m(s) = \frac{Ke^{-\delta s}}{(\tau_1 s \pm 1)(\tau_2 s + 1)} \quad (4.1)$$

where τ_1 and τ_2 are the time constants, K the steady state gain and δ the time delay of the process. It is assumed that τ_1 is larger than τ_2 and K is positive. The above expression is rewritten in terms of f_1 and f_2 as

$$\frac{y(s)}{u(s)e^{-\delta s}} = \frac{\pm K f_1 f_2}{(s - f_1)(s - f_2)} \quad (4.2)$$

where $f_1 = \mp \frac{1}{\tau_1}$ and $f_2 = -\frac{1}{\tau_2}$. The process model considered in (4.1) is realized in terms of FOPDT, SOPDT including overdamped, underdamped, critically damped, integrating and unstable process models.

4.2.1 Measurement noise and denoising

In process industries generally, the process output is corrupted with measurement noise. Hence, a noise free output can be obtained with the help of an integrator at the process output or by using an off-line method such as curve fitting technique. But addition of an integrator at the process output changes the order of actual process leading to inaccurate measurements. The design of an integrator is dependent on process frequency which will not be known due to unknown process dynamics. These issues motivate us to propose the on-line denoising block as shown in Fig. 4.2 which consists of a derivative block (D_1) followed by a closed loop sequence of an integrator and one more derivative block (D_2). The expression for D_1 and D_2 is written as

$$D_1 = D_2 = \frac{T_D s}{\alpha T_D s + 1} \quad (4.3)$$

where T_D is the derivative time constant and α the derivative filter coefficient. Normally, α is very small ($\ll 1$). Generally, information signal and the measurement noise are considered as uncorrelated while carrying out their additive addition.

$$\bar{y}(t) = \mathbf{c}\mathbf{x}(t) + \text{rand}(\text{size}(\mathbf{x}(t))) \quad (4.4)$$

When the differentiation of contaminated signal is carried out, the rate of change of signal and measurement noise is yielded. Further, to recover the actual response, the output of D_1 is passed through a closed loop control having an integrator and a differentiator D_2 as shown in Fig. 4.2.

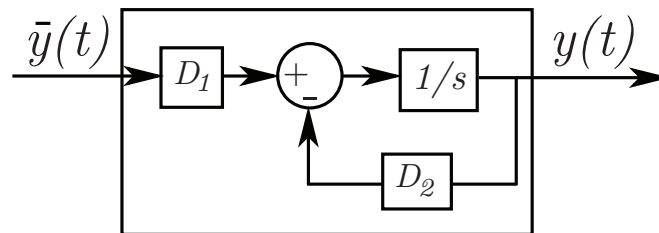


Figure 4.2: Denoising block

The function of D_2 is to find out the variation of signal and noise content followed by filtering and forward to adder where difference between the actual variation of noisy signal from D_1 and D_2 is obtained. Further, those variations are finally mitigated by an integrator which also helps in removing the higher order harmonics present at the derivative (D_1) output, assuming zero initial conditions. Hence, the process of denoising is carried out to obtain a noise free limit cycle output $y(t)$. Lee et al. [83] proposed an identification method to suppress significant effects of higher order harmonic terms of process output using integrals of relay feedback responses. Lee et al. [70] used high pass filter to remove slow drifts and a low pass filter to eliminate the high frequency noise from the noisy process output. Then, Kim et al. [84] used an integrator at the process output to obtain chattering-free response. Their method can not be implemented for identification of lower order processes, since the integrator which is connected at the process output, will change the order of the actual process dynamics and also yields inaccurate ultimate period. Our proposed denoising block is advantageous in retaining the order of the unknown process during identification.

Remark: As the output of derivative D_1 is in terms of the rate of change of the noisy limit cycle with reference to time. This rate of change is bounded with unknown amplitude. The absolute value of this bound could be enormously high or maintained at an acceptable level by varying the sampling time. With reference to real time applications this sampling time can be defined by the user corresponding to a tolerable derivative output. However, in the proposed structure, a sampling time of 0.01s yields satisfactory results in noise removal, while increasing the upper bound of the derivative output which may not be acceptable in the context of practical applications. This limitation can be overcome by an addition of a derivative gain which should be less than unity (up to two digits of precision).

4.3 Derivation of analytical expressions

The limit cycle output ($y(t)$), its second derivative output for SOPDT process and the delayed relay output are shown in Fig. 4.3. The parameters indicated in Fig. 4.3, h and ε are relay parameters as amplitude and hysteresis width, respectively A_p , T_p and t_p are limit cycle parameters as peak amplitude, half period and peak time, respectively t_0 is the time instant at hysteresis value where actual relay switching takes place and t_1 is the time where the second derivative output of limit cycle shows abrupt change and $\delta = t_1 - t_0$. In case of FOPDT processes, t_1 is measured from first derivative output of limit cycle.

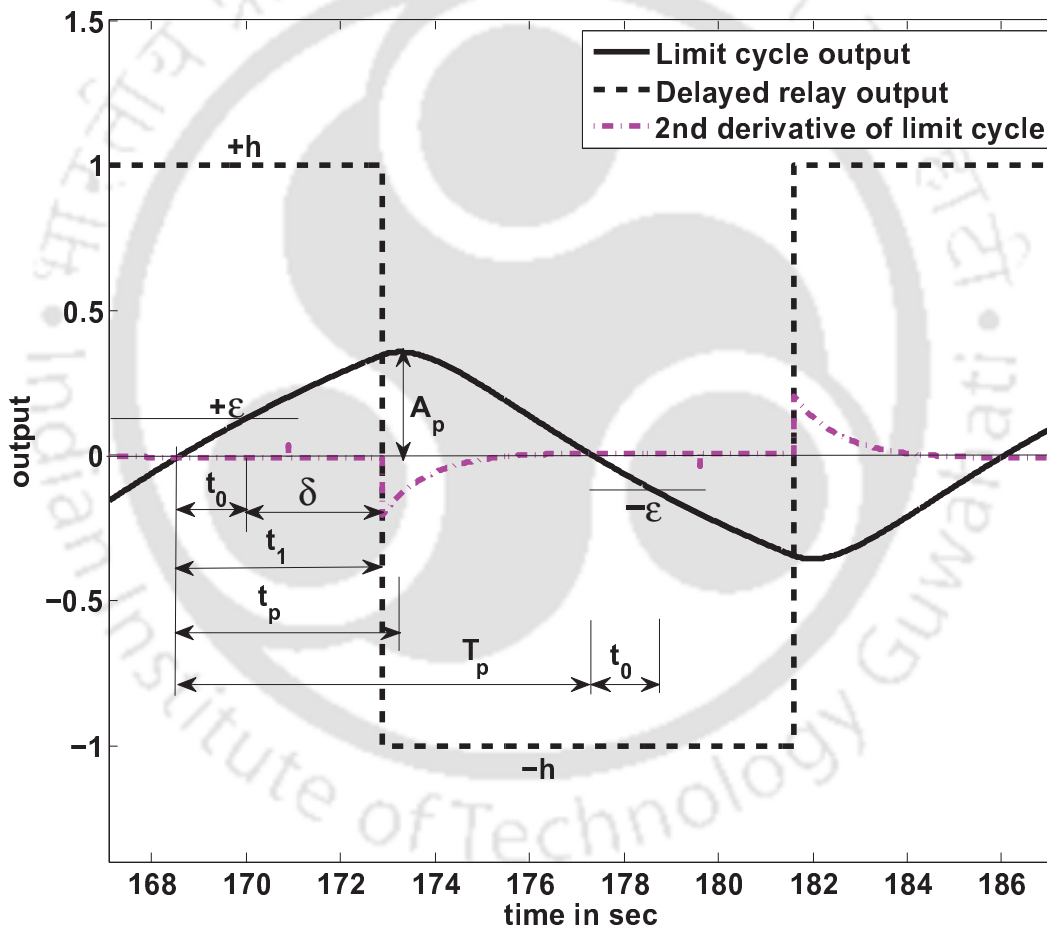


Figure 4.3: Limit cycle output and its second derivative for SOPDT process

The mathematical derivations are carried out using state space technique. The standard form of state space equations of a system when the process contains a time delay, δ are given by

$$\dot{\mathbf{x}}(t) = \mathbf{A}\mathbf{x}(t) + \mathbf{b}u(t - \delta) \quad (4.5)$$

$$y(t) = \mathbf{c}\mathbf{x}(t) \quad (4.6)$$

where \mathbf{A} is a 2×2 square matrix, \mathbf{b} is 2×1 column vector, \mathbf{c} is 1×2 row vector. Transforming (4.2) from transfer function to the following state space representation

$$\dot{\mathbf{x}}(t) = \begin{bmatrix} f_1 & 0 \\ 0 & f_2 \end{bmatrix} \begin{bmatrix} x_1(t) \\ x_2(t) \end{bmatrix} + \begin{bmatrix} a \\ -a \end{bmatrix} u(t - \delta) \quad (4.7)$$

$$y(t) = \begin{bmatrix} 1 & 1 \end{bmatrix} \mathbf{x}(t) \quad (4.8)$$

(Detailed derivation of Eqs. (4.7) and (4.8) is given in Appendix A.2)

Comparing (4.7) and (4.8) with the state space Eqs. (4.5) and (4.6), respectively the matrices \mathbf{A} , \mathbf{b} and \mathbf{c} are given as

$$\mathbf{A} = \begin{bmatrix} f_1 & 0 \\ 0 & f_2 \end{bmatrix}; \mathbf{b} = \begin{bmatrix} a \\ -a \end{bmatrix}; \mathbf{c} = \begin{bmatrix} 1 & 1 \end{bmatrix} \quad (4.9)$$

where f_1 and f_2 are the eigenvalues of \mathbf{A} and

$$a = \frac{\pm K f_1 f_2}{(f_1 - f_2)} \quad (4.10)$$

Assume that there exists a symmetrical limit cycle with half period T_p as shown in Fig. 4.3 which is obtained with the initial condition $\mathbf{x}(t_0)$. It can be observed from Fig. 4.3 that even though relay switching from $+h$ to $-h$, takes place at time t_0 , the delayed relay output provides two piecewise constant input signals to the process for positive or negative limit cycle output. Hence, the solution of (4.5) for time ranges $t_0 \leq t \leq t_1$ and $t_1 \leq t \leq (T_p + t_0)$ becomes, respectively as

$$\mathbf{x}(t) = \mathbf{e}^{\mathbf{A}(t-t_0)} \mathbf{x}(t_0) + \mathbf{A}^{-1}(\mathbf{e}^{\mathbf{A}(t-t_0)} - \mathbf{I})\mathbf{b}h \quad (4.11)$$

$$\mathbf{x}(t) = \mathbf{e}^{\mathbf{A}(t-t_1)} \mathbf{x}(t_1) - \mathbf{A}^{-1}(\mathbf{e}^{\mathbf{A}(t-t_1)} - \mathbf{I})\mathbf{b}h \quad (4.12)$$

where \mathbf{I} is 2×2 identity matrix. Due to equal half cycles the limit cycle is symmetrical hence, it follows that $\mathbf{x}(T_p + t_0) = -\mathbf{x}(t_0)$. Substituting $t = T_p + t_0$ in (4.12), the following expressions

are obtained

$$\mathbf{x}(T_p + t_0) = \mathbf{e}^{\mathbf{A}(T_p + t_0 - t_1)} \mathbf{x}(t_1) - \mathbf{A}^{-1}(\mathbf{e}^{\mathbf{A}(T_p + t_0 - t_1)} - \mathbf{I})\mathbf{b}h \quad (4.13)$$

$$\mathbf{x}(T_p + t_0) = \mathbf{e}^{\mathbf{A}(T_p - (t_1 - t_0))} \mathbf{x}(t_1) - \mathbf{A}^{-1}(\mathbf{e}^{\mathbf{A}(T_p - (t_1 - t_0))} - \mathbf{I})\mathbf{b}h \quad (4.14)$$

As $\delta = (t_1 - t_0)$, above equation reduces to

$$\mathbf{x}(T_p + t_0) = \mathbf{e}^{\mathbf{A}(T_p - \delta)} \mathbf{x}(t_1) - \mathbf{A}^{-1}(\mathbf{e}^{\mathbf{A}(T_p - \delta)} - \mathbf{I})\mathbf{b}h \quad (4.15)$$

Putting $t = t_1$ in (4.11) one obtains

$$\mathbf{x}(t_1) = \mathbf{e}^{\mathbf{A}(t_1 - t_0)} \mathbf{x}(t_0) + \mathbf{A}^{-1}(\mathbf{e}^{\mathbf{A}(t_1 - t_0)} - \mathbf{I})\mathbf{b}h \quad (4.16)$$

or

$$\mathbf{x}(t_1) = \mathbf{e}^{\mathbf{A}\delta} \mathbf{x}(t_0) + \mathbf{A}^{-1}(\mathbf{e}^{\mathbf{A}\delta} - \mathbf{I})\mathbf{b}h \quad (4.17)$$

Substituting the above equation in (4.15) the following expression is obtained

$$\mathbf{x}(T_p + t_0) = \mathbf{e}^{\mathbf{A}T_p} \mathbf{x}(t_0) + \mathbf{A}^{-1}(\mathbf{e}^{\mathbf{A}T_p} - 2\mathbf{e}^{\mathbf{A}(T_p - \delta)} + \mathbf{I})\mathbf{b}h \quad (4.18)$$

But $\mathbf{x}(T_p + t_0) = -\mathbf{x}(t_0)$ hence, above equation reduces to the initial condition given by

$$\mathbf{x}(t_0) = (\mathbf{I} + \mathbf{e}^{\mathbf{A}T_p})^{-1} \mathbf{A}^{-1}(2\mathbf{e}^{\mathbf{A}(T_p - \delta)} - \mathbf{e}^{\mathbf{A}T_p} - \mathbf{I})\mathbf{b}h \quad (4.19)$$

These Eqs. (4.11), (4.12), (4.17) and (4.19) are used to get the expressions for relay and limit cycle parameters as described in the following subsections.

4.3.1 Expression for ε

The condition for sustained oscillations using relay with hysteresis is

$$y(t_0) = \mathbf{c}\mathbf{x}(t_0) = \varepsilon \quad (4.20)$$

Simplifying the initial condition given in (4.19), the following expression is obtained

$$\mathbf{x}(t_0) = \begin{bmatrix} \frac{ah(2e^{f_1(T_p - \delta)} - e^{f_1 T_p} - 1)}{f_1(1 + e^{f_1 T_p})} \\ \frac{-ah(2e^{f_2(T_p - \delta)} - e^{f_2 T_p} - 1)}{f_2(1 + e^{f_2 T_p})} \end{bmatrix} \quad (4.21)$$

Substituting (4.21) and $\mathbf{c} = \begin{bmatrix} 1 & 1 \end{bmatrix}$ in (4.20) and resolving we get

$$\varepsilon = ah \left(\frac{2e^{f_1(T_p-\delta)} - e^{f_1 T_p} - 1}{f_1(1 + e^{f_1 T_p})} - \frac{2e^{f_2(T_p-\delta)} - e^{f_2 T_p} - 1}{f_2(1 + e^{f_2 T_p})} \right) \quad (4.22)$$

Using (4.10) in the above expression and further simplifying one obtains

$$\varepsilon = \frac{\pm Kh}{(f_1 - f_2)} \left(f_2 \left(\frac{2e^{-f_1 \delta}}{1 + e^{-f_1 T_p}} - 1 \right) - f_1 \left(\frac{2e^{-f_2 \delta}}{1 + e^{-f_2 T_p}} - 1 \right) \right) \quad (4.23)$$

4.3.2 Expression for t_p

The expression for t_p is achieved using (4.12) as follows. Substituting $t = t_p$ in (4.12) gives the following expression

$$\mathbf{x}(t_p) = \mathbf{e}^{\mathbf{A}(t_p-t_1)} \mathbf{x}(t_1) - \mathbf{A}^{-1}(\mathbf{e}^{\mathbf{A}(t_p-t_1)} - \mathbf{I}) \mathbf{b}h \quad (4.24)$$

Now, $\mathbf{x}(t_1)$ from (4.17) is solved to get

$$\mathbf{x}(t_1) = \begin{bmatrix} \frac{ah e^{f_1 \delta} (2e^{f_1(T_p-\delta)} - e^{f_1 T_p} - 1)}{f_1(1 + e^{f_1 T_p})} + \frac{ah(e^{f_1 \delta} - 1)}{f_1} \\ -\frac{ah e^{f_2 \delta} (2e^{f_2(T_p-\delta)} - e^{f_2 T_p} - 1)}{f_2(1 + e^{f_2 T_p})} - \frac{ah(e^{f_2 \delta} - 1)}{f_2} \end{bmatrix} \quad (4.25)$$

On further simplification one obtains $\mathbf{x}(t_1)$ as

$$\mathbf{x}(t_1) = \begin{bmatrix} \frac{ah}{f_1} \left(\frac{e^{f_1 T_p} - 1}{e^{f_1 T_p} + 1} \right) \\ -\frac{ah}{f_2} \left(\frac{e^{f_2 T_p} - 1}{e^{f_2 T_p} + 1} \right) \end{bmatrix} \quad (4.26)$$

Substituting (4.26) in (4.24) and resolving yields the expression for $\mathbf{x}(t_p)$ as mentioned below

$$\mathbf{x}(t_p) = \begin{bmatrix} \frac{ah e^{f_1(t_p-t_1)} (e^{f_1 T_p} - 1)}{f_1(1 + e^{f_1 T_p})} - \frac{ah(e^{f_1(t_p-t_1)} - 1)}{f_1} \\ -\frac{ah e^{f_2(t_p-t_1)} (e^{f_2 T_p} - 1)}{f_2(1 + e^{f_2 T_p})} + \frac{ah(e^{f_2(t_p-t_1)} - 1)}{f_2} \end{bmatrix} \quad (4.27)$$

which is reduced to

$$\mathbf{x}(t_p) = \begin{bmatrix} \frac{ah}{f_1} \left(\frac{-2e^{f_1(t_p-t_1)}}{1 + e^{f_1 T_p}} + 1 \right) \\ \frac{ah}{f_2} \left(\frac{2e^{f_2(t_p-t_1)}}{1 + e^{f_2 T_p}} - 1 \right) \end{bmatrix} \quad (4.28)$$

Since the first derivative of peak amplitude is zero, which is represented as

$$\dot{y}(t_p) = \mathbf{c}\mathbf{x}(t_p) = 0 \quad (4.29)$$

or

$$\mathbf{cAx}(t_p) - \mathbf{cb}h = 0 \quad (4.30)$$

Since $\mathbf{cb} = 0$, above equation reduces to

$$\mathbf{cAx}(t_p) = 0 \quad (4.31)$$

Substituting for \mathbf{c} , \mathbf{A} from (4.9) and $\mathbf{x}(t_p)$ from (4.28) in the above expression and solving gives the following expressions

$$e^{(t_p-t_1)(f_1-f_2)} = \frac{1 + e^{f_1 T_p}}{1 + e^{f_2 T_p}} \quad (4.32)$$

or

$$t_p = t_1 + \frac{1}{(f_1 - f_2)} \ln \left(\frac{1 + e^{f_1 T_p}}{1 + e^{f_2 T_p}} \right) \quad (4.33)$$

4.3.3 Expression for A_p

The expression for A_p is obtained by substituting for \mathbf{c} and $\mathbf{x}(t_p)$ in the following expression

$$y(t_p) = A_p = \mathbf{cx}(t_p) \quad (4.34)$$

$$A_p = \frac{ah}{f_1} \left(\frac{-2e^{f_1(t_p-t_1)}}{1 + e^{f_1 T_p}} + 1 \right) + \frac{ah}{f_2} \left(\frac{2e^{f_2(t_p-t_1)}}{1 + e^{f_2 T_p}} - 1 \right) \quad (4.35)$$

Using (4.33) the following expressions are obtained

$$e^{f_1(t_p-t_1)} = \left(\frac{1 + e^{f_1 T_p}}{1 + e^{f_2 T_p}} \right)^{\frac{f_1}{f_1-f_2}} \quad (4.36)$$

$$e^{f_2(t_p-t_1)} = \left(\frac{1 + e^{f_1 T_p}}{1 + e^{f_2 T_p}} \right)^{\frac{f_2}{f_1-f_2}} \quad (4.37)$$

Now using (4.10), (4.36) and (4.37) in (4.35) and further simplifying one obtains the expression for A_p as given below

$$A_p = \pm Kh \left(2 \left(1 + e^{f_1 T_p} \right)^{\frac{f_2}{f_1-f_2}} \left(1 + e^{f_2 T_p} \right)^{\frac{-f_1}{f_1-f_2}} - 1 \right) \quad (4.38)$$

These derivations for ε , t_p and A_p are used to get the expressions for stable or unstable SOPDT process model parameters as given in Section 4.4.

4.3.4 Estimation of δ

Initially, Majhi [39] proposed a method to find the process time delay δ from the measurements of t_0 and t_1 . There the author used ideal relay in which case $t_0 = 0$ always, but in our proposed method since relay with hysteresis is used hence, $y(t) = \varepsilon$ at $t = t_0$ which is non-zero. From the graph shown in Fig. 4.3 it can be observed that $t_1 = t_0 + \delta$, due to non-monotonic characteristic of the limit cycle output. Hence, the method proposed by Majhi [39] is extended here to estimate the process time delay δ . For FOPDT processes t_1 is measured from first derivative output of $y(t)$ similarly, for SOPDT processes it is measured from second derivative output of $y(t)$.

4.4 Process identification

4.4.1 SOPDT process model

In this subsection expressions are derived to estimate the unknown process model parameters of stable or unstable SOPDT process model as given in (4.1). Expressing (4.23), (4.33) and (4.38) in terms of τ_1 and τ_2 as

$$\varepsilon = \pm Kh \left(\frac{-\tau_1}{\tau_1 \mp \tau_2} \left(\frac{2e^{\frac{\pm\delta}{\tau_1}}}{1 + e^{\frac{\pm T_p}{\tau_1}}} - 1 \right) \pm \frac{\tau_2}{\tau_1 \mp \tau_2} \left(\frac{2e^{\frac{\delta}{\tau_2}}}{1 + e^{\frac{T_p}{\tau_2}}} - 1 \right) \right) \quad (4.39)$$

$$t_p = t_1 + \frac{\tau_1 \tau_2}{\tau_1 \mp \tau_2} \ln \left(\frac{1 + e^{\frac{\mp T_p}{\tau_1}}}{1 + e^{\frac{-T_p}{\tau_2}}} \right) \quad (4.40)$$

$$A_p = \pm Kh \left(2 \left(1 + e^{\frac{\mp T_p}{\tau_1}} \right)^{\frac{-\tau_1}{\tau_1 \mp \tau_2}} \left(1 + e^{\frac{-T_p}{\tau_2}} \right)^{\frac{\pm\tau_2}{\tau_1 \mp \tau_2}} - 1 \right) \quad (4.41)$$

Rearranging (4.39), (4.40) and (4.41) in the following form of equations for stable or over-damped process model

$$(\tau_1 - \tau_2) - \frac{Kh}{\varepsilon} \left(\tau_1 \left(1 - \frac{2e^{\frac{\delta}{\tau_1}}}{1 + e^{\frac{T_p}{\tau_1}}} \right) + \tau_2 \left(\frac{2e^{\frac{\delta}{\tau_2}}}{1 + e^{\frac{T_p}{\tau_2}}} - 1 \right) \right) = 0 \quad (4.42)$$

$$(\tau_1 - \tau_2) - \frac{\tau_1 \tau_2}{(t_p - t_1)} \ln \left(\frac{1 + e^{-\frac{T_p}{\tau_1}}}{1 + e^{-\frac{T_p}{\tau_2}}} \right) = 0 \quad (4.43)$$

$$Kh \left(2 \left(1 + e^{-\frac{T_p}{\tau_1}} \right)^{\frac{-\tau_1}{\tau_1 - \tau_2}} \left(1 + e^{-\frac{T_p}{\tau_2}} \right)^{\frac{\tau_2}{\tau_1 - \tau_2}} - 1 \right) - A_p = 0 \quad (4.44)$$

Similarly for unstable processes

$$(\tau_1 + \tau_2) - \frac{Kh}{\varepsilon} \left(\tau_1 \left(\frac{2e^{\frac{\delta}{\tau_1}}}{1 + e^{-\frac{T_p}{\tau_1}}} - 1 \right) + \tau_2 \left(\frac{2e^{\frac{\delta}{\tau_2}}}{1 + e^{-\frac{T_p}{\tau_2}}} - 1 \right) \right) = 0 \quad (4.45)$$

$$(\tau_1 + \tau_2) - \frac{\tau_1 \tau_2}{(t_p - t_1)} \ln \left(\frac{1 + e^{\frac{T_p}{\tau_1}}}{1 + e^{-\frac{T_p}{\tau_2}}} \right) = 0 \quad (4.46)$$

$$Kh \left(1 - 2 \left(1 + e^{\frac{T_p}{\tau_1}} \right)^{\frac{-\tau_1}{\tau_1 + \tau_2}} \left(1 + e^{-\frac{T_p}{\tau_2}} \right)^{\frac{-\tau_2}{\tau_1 + \tau_2}} \right) - A_p = 0 \quad (4.47)$$

Therefore substituting for ε , δ , h , T_p , A_p , t_p and t_1 and solving simultaneously the set of Eqs. (4.42), (4.43) and (4.44) the stable SOPDT process model parameters K , τ_1 and τ_2 are estimated. Similarly, to estimate the parameters of unstable process model, Eqs. (4.45), (4.46) and (4.47) are solved simultaneously. The simultaneous solution of these nonlinear expressions is carried out by using the MATLAB function *fsolve* assuming suitable initial values. The details of using *fsolve* function is given in Appendix A.4.

Example 1

Let us consider a stable SOPDT process [12, 42, 82]

$$G(s) = \frac{e^{-2s}}{(10s + 1)(s + 1)}$$

A single relay with the settings $h = 1$ and $\varepsilon = 0.2$ is applied to the above process to generate the limit cycle output. The measurements made on the limit cycle and its second derivative output are $t_p = 4.6436$, $t_1 = 4.2536$, $t_0 = 2.2536$, $T_p = 8.7198$ and $A_p = 0.3566$. From t_1 and t_0 , the process time delay is estimated as $\delta = 2.0$. Now, using the relay parameters, limit cycle quantities and δ in (4.42), (4.43) and (4.44) and solving these expressions simultaneously, the estimated process model parameters are $K = 0.9923$, $\tau_1 = 9.8997$ and $\tau_2 = 1.0105$. The performance evaluation is carried out by calculating the estimation error (\tilde{E}) index as described

in Chapter 2. The proposed model is compared with the models identified by Shen et al. [12], Liu et al. [82] and Vivek and Chidambaram [42] with estimation error (\tilde{E}) in Table 4.1. To show the usefulness of the proposed method, relay test is conducted under noisy environment where a white Gaussian noise of zero mean and certain variance for different values of SNR, is injected at the process output. As mentioned earlier, the denoised block shown in Fig. 4.1 is used to recover the noise free limit cycle output. And process model parameters are again estimated from the measurements of denoised limit cycle quantities. The noisy and denoised limit cycle outputs for 10 dB SNR are as shown in Fig. 4.4. The percentage errors of parameters, measured and estimated in the presence of measurement noise which varies from 10 dB to 30 dB SNR, are given in Table 4.2.

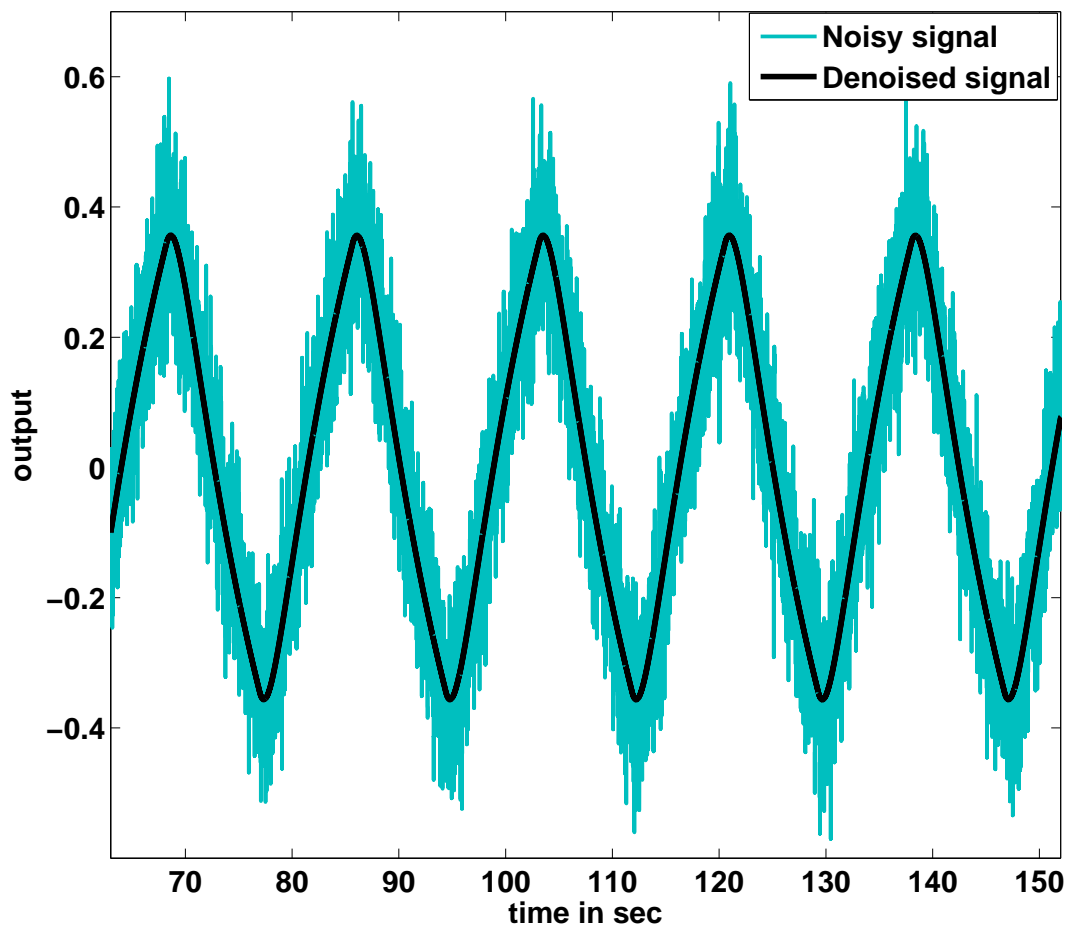


Figure 4.4: Noisy and denoised signals

Table. 4.1: Comparison of process models for Example 1

Method	Process model	Error (\tilde{E})
Proposed	$\frac{0.9923e^{-2.0s}}{(9.8997s+1)(1.0105s+1)}$	0.0006
Shen et al. [12]	$\frac{0.998e^{-2.0s}}{(9.14s+1)(1.044s+1)}$	0.0369
Liu et al. [82]	$\frac{1.0122e^{-2.0037s}}{(10.1178s+1)(0.992s+1)}$	0.0028
Vivek and Chidambaram [42]	$\frac{1.03e^{-2.84s}}{(11.98s+1)}$	0.0378

Table. 4.2: Effect of measurement noise on parameters in % error, for Example 1

SNR (dB)	A_p	T_p	t_1	t_0	t_p	K	τ_1	τ_2	δ
10	0.028	0.001	-0.004	-0.008	-0.019	-0.40	-0.574	0.680	0
20	0.028	0.006	-0.018	-0.035	-0.015	-0.570	-0.793	0.950	0
30	0.028	0.004	0.007	0.008	-0.032	0.020	0.005	0.050	0.005

It can be observed from Table 4.1 that the presented technique yields process models with less estimation error as compared with other methods. Table 4.2 indicates that the measured limit cycle parameters and estimated model parameters are within 1% error for different SNR values.

Example 2

In this example the following unstable SOPDT process [5, 6] is taken

$$G(s) = \frac{e^{-0.5s}}{(2s-1)(0.5s+1)}.$$

Applying the above procedure with relay settings $h = 1$ and $\varepsilon = 0.1$, the limit cycle parameters obtained are $t_p = 1.551$, $t_1 = 0.691$, $t_0 = 0.191$, $T_p = 4.0325$ and $A_p = 0.6394$ hence, $\delta = 0.50$. Using these parameters in (4.45), (4.46) and (4.47) and solving them simultaneously the following process model parameters are estimated $K = 1.0069$, $\tau_1 = 2.0152$ and $\tau_2 = 0.5057$.

The FOPDT model suggested by Liu and Gao [5] using relay with hysteresis is given in Table

4.3 along with the model proposed by Vivek and Chidambaram [6] with the corresponding estimation error values. These results are compared using Nyquist plots as shown in Fig. 4.5 and it can be observed that the proposed method gives good results.

In the presence of measurement noise of 1% standard deviation, Vivek and Chidambaram [6] suggested FOPDT model with the parameters $K = 0.5332$, $\tau = 1.3524$ and $\delta = 0.8807$, our proposed method gives the model parameters as $K = 0.9947$, $\tau_1 = 1.9872$, $\tau_2 = 0.4980$ and $\delta = 0.4981$. Hence, application of single relay feedback testing and proposed expressions helps in achieving improved results for unstable SOPDT processes.

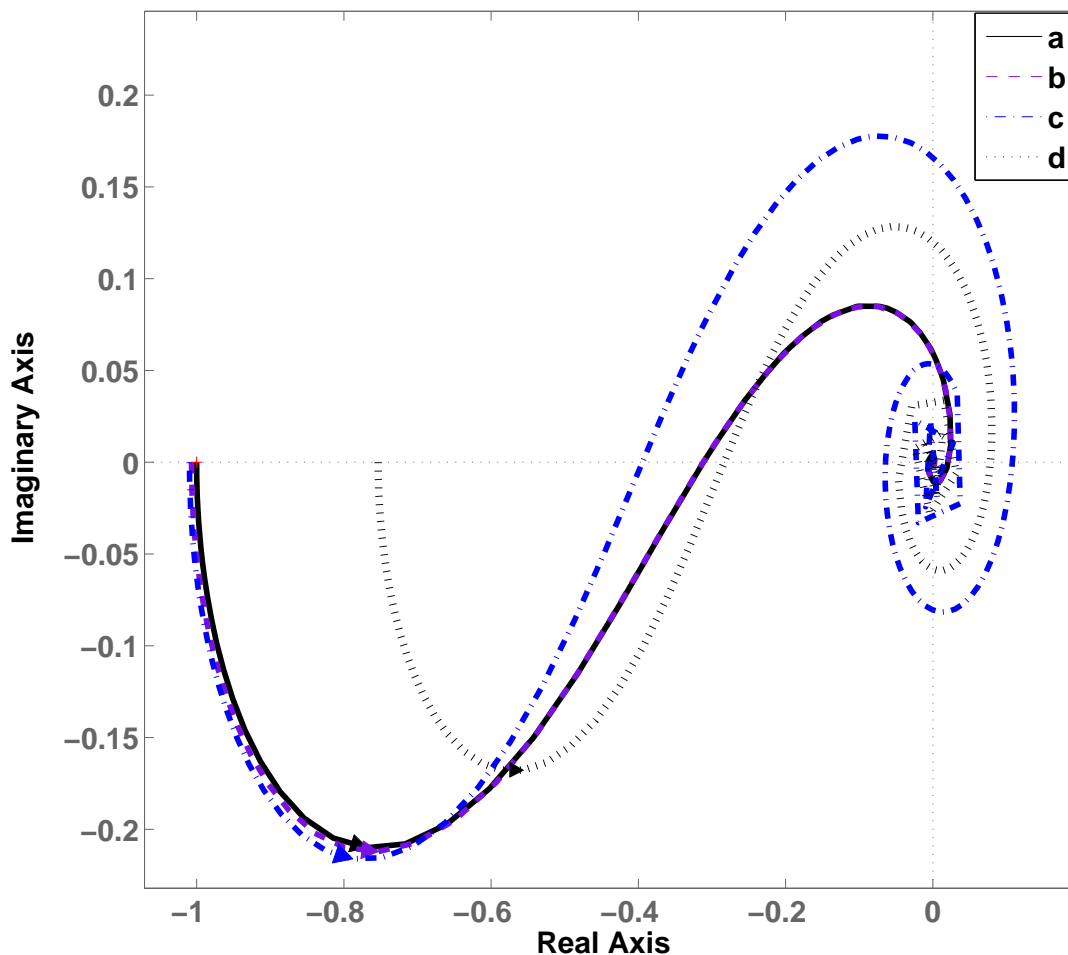


Figure 4.5: Nyquist plots for Example 2: (a) Actual process, (b) proposed model, (c) model proposed by Liu and Gao [5] and (d) model proposed by Vivek and Chidambaram [6]

Table. 4.3: Comparison of process models for Example 2

Method	Process model	Error (\tilde{E})
Proposed	$\frac{1.0069e^{-0.50s}}{(2.0152s-1)(0.5057s+1)}$	0.002
Liu and Gao [5]	$\frac{1.0097e^{-1.36s}}{(2.74s-1)}$	0.2159
Vivek and Chidambaram [6]	$\frac{0.7534e^{-1.0412s}}{(2.1642s-1)}$	0.3838

4.4.2 FOPDT process model

A stable or unstable FOPDT process model is obtained by putting $\tau_2 = 0$ in (4.1) as

$$G_m(s) = \frac{Ke^{-\delta s}}{\tau_1 s \pm 1} \quad (4.48)$$

Hence, the SOPDT process model expressions obtained in subsection 4.4.1 are framed to achieve the equations for estimation of FOPDT process model parameters K and τ_1 . Substituting $\tau_2 = 0$ in the expressions (4.39) and (4.41) and further simplifying we get

$$\varepsilon = \pm Kh \left(1 - \frac{2e^{\frac{\pm\delta}{\tau_1}}}{1 + e^{\frac{\pm T_p}{\tau_1}}} \right) \quad (4.49)$$

$$A_p = \pm Kh \left(\frac{2}{1 + e^{\frac{\pm T_p}{\tau_1}}} - 1 \right) \quad (4.50)$$

Rearranging Eqs. (4.49) and (4.50) for stable processes as

$$Kh \left(1 - \frac{2e^{\frac{\delta}{\tau_1}}}{1 + e^{\frac{T_p}{\tau_1}}} \right) - \varepsilon = 0 \quad (4.51)$$

$$Kh \tanh \left(\frac{0.5T_p}{\tau_1} \right) - A_p = 0 \quad (4.52)$$

Substituting for ε , δ , h , T_p and A_p and solving simultaneously (4.51) and (4.52) the stable FOPDT process model parameters (K and τ_1) are estimated.

Representing Eqs. (4.49) and (4.50) for unstable processes as

$$Kh \left(\frac{2e^{\frac{-\delta}{\tau_1}}}{1 + e^{\frac{-T_p}{\tau_1}}} - 1 \right) - \varepsilon = 0 \quad (4.53)$$

$$Kh \tanh \left(\frac{0.5T_p}{\tau_1} \right) - A_p = 0 \quad (4.54)$$

Now, substituting the required quantities in (4.53) and (4.54) and solving simultaneously the unstable FOPDT process model parameters (K and τ_1) are estimated. The process time delay δ is obtained from the measurements of t_1 and t_0 as explained in subsection 4.3.4.

Example 3

Consider the following stable FOPDT process [5, 41, 42]

$$G(s) = \frac{e^{-2s}}{10s + 1}.$$

A single relay with parameters $h = 1$ and $\varepsilon = 0.1$ is applied to the above process to generate the limit cycle output. So $\delta = 2.0$ is obtained from the measurements of $t_1 = 3.0536$ and $t_0 = 1.0536$. Substituting $T_p = 5.3897$, $A_p = 0.2631$ and $\delta = 2.0$ in (4.51) and (4.52) and solving simultaneously the model parameters are estimated as $K = 0.9994$ and $\tau_1 = 9.9957$. Table 4.4 shows the comparison of these results along with estimation error (\tilde{E}) for the proposed model and the models identified by Vivek and Chidambaram [42], Srinivasan and Chidambaram [41] using asymmetrical relay and Liu and Gao [5] using unbiased relay with hysteresis.

To identify the process dynamics in the presence of measurement noise, a white Gaussian noise of variance 0.0023 which gives SNR of 10 dB, is added at the process output. The noisy output signal and the denoised signal are as shown in Fig. 4.6. Using the denoised limit cycle quantities in corresponding expressions as mentioned above in this example, the process model parameters are estimated as $K = 0.9986$, $\tau_1 = 9.9923$ and $\delta = 2.0$. For measurement noise of 0.5% S.D., Srinivasan and Chidambaram [41] suggested the model parameters as $K = 0.9336$, $\tau_1 = 9.3638$ and $\delta = 2.03$, whereas our proposed method yields $K = 1.0017$, $\tau_1 = 10.0206$ and $\delta = 1.9994$. This example shows that the proposed method gives more accurate process model parameters even under noisy environment.

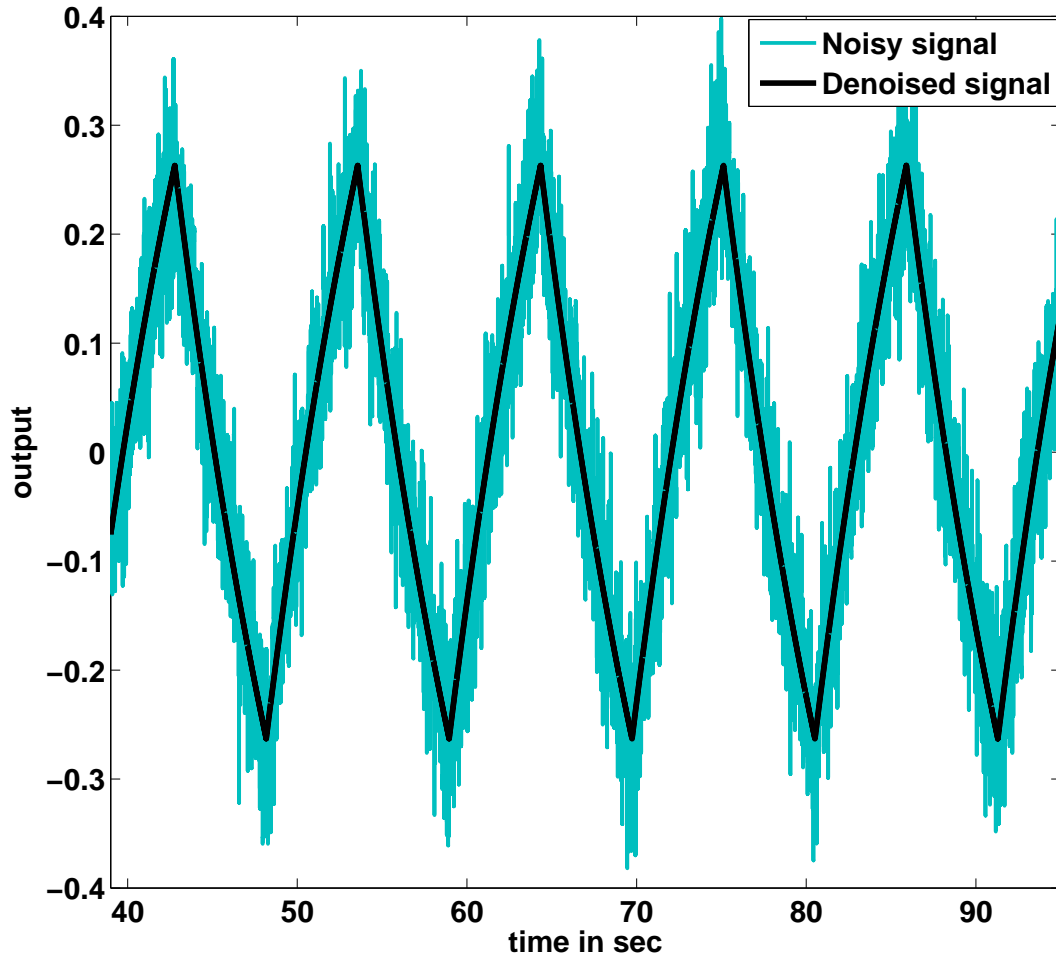


Figure 4.6: Noisy and denoised signals

Table. 4.4: Comparison of process models for Example 3

Method	Process model	Error (\tilde{E})
Proposed	$\frac{0.9994e^{-2.0s}}{9.9957s+1}$	0.0002
Srinivasan and Chidambaram [41]	$\frac{1.03e^{-2.3s}}{10.3s+1}$	0.1132
Liu and Gao [5]	$\frac{1.0048e^{-2.0024s}}{10.049s+1}$	0.0019
Vivek and Chidambaram [42]	$\frac{0.9467e^{-2.0s}}{9.5028s+1}$	0.0156

Example 4

Here, the following unstable FOPDT process [5, 13, 47] is taken for process dynamics identification

$$G(s) = \frac{e^{-0.4s}}{s-1}.$$

Using single relay feedback test with relay parameters $h = 1$ and $\varepsilon = 0.1$, the limit cycle parameters obtained are $t_1 = 0.4953$, $t_0 = 0.0953$, $T_p = 1.5198$ and $A_p = 0.641$. Hence $\delta = 0.40$ is obtained, substituting for δ , T_p and A_p in (4.53) and (4.54) and solving simultaneously, $K = 1.0$ and $\tau_1 = 1.0$ are obtained. Further the results are compared with the models identified by Marchetti et al. [13] and Liu and Gao [5, 47] in Table 4.5 along with estimation error. For noisy environment, the percentage errors of measured parameters and estimated model parameters are tabulated in Table 4.6 for SNR values varying from 10 dB to 30 dB.

Table 4.5: Comparison of process models for Example 4

Method	Process model	Error (\tilde{E})
Proposed	$\frac{1.0e^{-0.40s}}{1.0s-1}$	0
Marchetti et al. [13]	$\frac{0.928e^{-0.392s}}{0.757s-1}$	0.3716
Liu and Gao [47]	$\frac{1.0001e^{-0.40s}}{0.9954s-1}$	0.0106
Liu and Gao [5]	$\frac{0.99e^{-0.4022s}}{0.9891s-1}$	0.0265

Table 4.6: Effect of measurement noise on parameters in % error, for Example 4

SNR (dB)	A_p	T_p	t_1	t_0	K	τ_1	δ
10	-0.187	0.032	0.061	0.314	-0.180	0.050	0
20	0.093	0.052	-0.061	-0.209	-0.060	-0.160	-0.025
30	0.031	0.065	-0.040	0	-0.150	-0.190	-0.050

4.4.3 Underdamped SOPDT process model

Considering (4.1) in the standard stable SOPDT transfer function form as

$$G_m(s) = \frac{Kq e^{-\delta s}}{ms^2 + ns + q} \quad (4.55)$$

where $m = \tau_1 \tau_2$, $n = \tau_1 + \tau_2$ and assuming $q = 1$ without loss of generality. Hence, the above transfer function is reduced to the following underdamped process model

$$G_m(s) = \frac{K e^{-\delta s}}{ms^2 + ns + 1} \quad (4.56)$$

or

$$\frac{y(s)}{u(s)e^{-\delta s}} = \frac{K}{ms^2 + ns + 1} \quad (4.57)$$

Here it is to be noted that for underdamped processes $n^2 < 4m$ with reference to (4.56). Expressing (4.57) in terms of f_1 and f_2 as follows

$$\frac{y(s)}{u(s)e^{-\delta s}} = \frac{K f_1 f_2}{(s - f_1)(s - f_2)} \quad (4.58)$$

where $f_1 = \gamma_1 + j\gamma_2$ and $f_2 = \gamma_1 - j\gamma_2$

where

$$\gamma_1 = \frac{-n}{2m} \quad (4.59)$$

and

$$\gamma_2 = \frac{\sqrt{4m - n^2}}{2m} \quad (4.60)$$

Solving (4.59) and (4.60) for m and n , the following expressions are obtained

$$m = \frac{1}{\gamma_1^2 + \gamma_2^2} \quad (4.61)$$

$$n = \frac{-2\gamma_1}{\gamma_1^2 + \gamma_2^2} \quad (4.62)$$

Since $m = \tau_1 \tau_2$ and $n = \tau_1 + \tau_2$, so, τ_1 and τ_2 in terms of γ_1 and γ_2 become

$$\tau_1 = \frac{-\gamma_1 + j\gamma_2}{\gamma_1^2 + \gamma_2^2} \quad (4.63)$$

$$\tau_2 = \frac{-\gamma_1 - j\gamma_2}{\gamma_1^2 + \gamma_2^2} \quad (4.64)$$

Using τ_1 and τ_2 in SOPDT expressions (4.42), (4.43) and (4.44) and solving these equations, following expressions are obtained.

$$\left(Kh \left(\frac{2e^{\gamma_1(T_p - \delta)}}{1 + 2e^{\gamma_1 T_p} \cos(\gamma_2 T_p) + e^{2\gamma_1 T_p}} \left(\frac{\gamma_1}{\gamma_2} \sin(\gamma_2(T_p - \delta)) - \cos(\gamma_2(T_p - \delta)) \right) - e^{\gamma_1 T_p} \left(\frac{\gamma_1}{\gamma_2} \sin(\gamma_2 \delta) + \cos(\gamma_2 \delta) \right) \right) + 1 \right) - \varepsilon = 0 \quad (4.65)$$

$$\gamma_2 - \frac{1}{(t_p - t_1)} \tan^{-1} \left(\frac{e^{\gamma_1 T_p} \sin(\gamma_2 T_p)}{1 + e^{\gamma_1 T_p} \cos(\gamma_2 T_p)} \right) = 0 \quad (4.66)$$

$$\gamma_1 - \frac{1}{(t_p - t_1)} \ln \left(\frac{\sqrt{1 + 2e^{\gamma_1 T_p} \cos(\gamma_2 T_p) + e^{2\gamma_1 T_p}}}{2} \left(\frac{A_p}{Kh} + 1 \right) \right) = 0 \quad (4.67)$$

Now, γ_1 , γ_2 and K are obtained by solving (4.65), (4.66) and (4.67) simultaneously. Substituting γ_1 and γ_2 in (4.61) and (4.62) and solving them, m and n are estimated. Process time delay δ is obtained from the measurements of t_1 and t_0 .

Example 5

This example considers an underdamped process [2] as

$$G(s) = \frac{e^{-0.01s}}{s^2 + 0.6s + 1}.$$

Relay ($h = 1$ and $\varepsilon = 0.25$) feedback testing generates the limit cycle with quantities $t_p = 0.8471$, $t_1 = 0.2571$, $t_0 = 0.2471$, $T_p = 1.8098$ and $A_p = 0.5575$, hence $\delta = 0.01$. Expressions (4.65), (4.66) and (4.67) are solved simultaneously using the relay and limit cycle parameters to obtain $\gamma_1 = -0.2995$, $\gamma_2 = 0.9557$ and $K = 0.9954$. Now, using γ_1 and γ_2 in (4.61) and (4.62) and solving these two equations the model parameters $m = 0.9969$ and $n = 0.5972$ are obtained. The process model parameters obtained by Lavanya et al. [2] are $K = 1.0$, $\delta = 0.01$, $m = 0.8953$ and $n = 0.922$. The estimation error for our proposed model is $\tilde{E} = 0.0108$, where as Lavanya et al.'s [2] model has 0.8069. Considering the effect of measurement noise in the range of 10 dB to 30 dB SNR, the % error of measured and estimated parameters are presented in Table 4.7.

Table. 4.7: Effect of measurement noise on parameters in % error, for Example 5

SNR (dB)	A_p	T_p	t_1	t_0	t_p	K	m	n	δ
10	0.017	0	0.038	0.040	0	1.060	0.70	1.0	0
20	0.017	0	0.038	0.040	0	1.060	0.70	1.0	0
30	0	0.005	0.038	0.040	0	0.810	0.530	0.80	0

4.4.4 Critically damped SOPDT process model

The expressions obtained for underdamped SOPDT process model in subsection 4.4.3 are utilized here to derive the equations for identification of critically damped SOPDT process model. The following transfer function for critically damped SOPDT process model is obtained by substituting $m = \tau_1^2$ and $n = 2\tau_1$ in (4.56).

$$G_m(s) = \frac{Ke^{-\delta s}}{(\tau_1 s + 1)^2} \quad (4.68)$$

Using the corresponding values of m and n in (4.59) and (4.60) gives $\gamma_1 = -1/\tau_1$ and $\gamma_2 = 0$, respectively. Hence, using $\gamma_2 = 0$ in (4.65) to (4.67), we obtain the expressions in terms of τ_1 , K and δ as follows.

Eq. (4.66) is reduced to

$$\tan(\gamma_2(t_p - t_1)) = \frac{\sin(\gamma_2 T_p)}{e^{-\gamma_1 T_p} + \cos(\gamma_2 T_p)} \quad (4.69)$$

which is again modified as

$$t_p - t_1 = \frac{e^{\gamma_1 T_p}}{1 + e^{\gamma_1 T_p}} \left(\frac{\sin(\gamma_2 T_p)}{\gamma_2} \right) \quad (4.70)$$

Using L'Hôpital's rule above equation is further simplified to obtain the following expressions

$$t_p - t_1 = \frac{T_p}{1 + e^{-\gamma_1 T_p}} \quad (4.71)$$

$$-\gamma_1 T_p = \ln \left(\frac{T_p}{t_p - t_1} - 1 \right) \quad (4.72)$$

Replacing $\gamma_1 = -1/\tau_1$ in the above equation we get

$$\tau_1 = \frac{T_p}{\ln \left(\frac{T_p}{t_p - t_1} - 1 \right)} \quad (4.73)$$

Now, Eq. (4.67) is solved to get

$$A_p = Kh \left(\frac{2e^{\gamma_1(t_p - t_1)}}{\sqrt{1 + 2e^{\gamma_1 T_p} + e^{2\gamma_1 T_p}}} - 1 \right) \quad (4.74)$$

or

$$A_p = Kh \left(\frac{2e^{\gamma_1(t_p - t_1)} - e^{\gamma_1 T_p} - 1}{1 + e^{\gamma_1 T_p}} \right) \quad (4.75)$$

Substituting for γ_1 in the above expression and simplified to

$$K = \frac{A_p \left(1 + e^{T_p/\tau_1} \right)}{h \left(2e^{(T_p + t_1 - t_p)/\tau_1} - e^{T_p/\tau_1} - 1 \right)} \quad (4.76)$$

Similarly, the expression for ε is obtained from (4.65) as

$$\varepsilon = Kh \left[\frac{2e^{\gamma_1(T_p - \delta)}}{1 + 2e^{\gamma_1 T_p} + e^{2\gamma_1 T_p}} \left(\frac{\gamma_1 \sin(\gamma_2(T_p - \delta))}{\gamma_2} - 1 - e^{\gamma_1 T_p} \left(\frac{\gamma_1 \sin(\gamma_2 \delta)}{\gamma_2} + 1 \right) \right) + 1 \right] \quad (4.77)$$

Putting the corresponding values of γ_1 and γ_2 the above equation is further simplified

$$Kh \left[\frac{2e^{\delta/\tau_1} \left(e^{T_p/\tau_1} (\delta - T_p - \tau_1) - \tau_1 + \delta \right)}{\tau_1 (1 + e^{T_p/\tau_1})^2} + 1 \right] - \varepsilon = 0 \quad (4.78)$$

Hence, the unknown process model parameters τ_1 and K are estimated from explicit expressions (4.73) and (4.76), respectively similarly δ is obtained from (4.78) using MATLAB function *fzero*.

Example 6

This examples considers the following SOPDT critically damped process [3]

$$G(s) = \frac{e^{-0.01s}}{(2s+1)^2}.$$

Using relay with parameters $h = 1$ and $\varepsilon = 0.1$, the measured limit cycle parameters are $A_p = 0.1555$, $T_p = 2.3291$, $t_1 = 0.4989$ and $t_p = 1.0529$. These parameters are substituted in the explicit expressions (4.73) and (4.76) to estimate the unknown process model parameters $\tau_1 = 2.0$ and $K = 0.9999$, respectively and using these parameters in (4.78), $\delta = 0.010$ is obtained. Similarly, the process model is identified in the presence of measurement noise of 10 dB SNR. The proposed models are given in Table 4.8 along with the model suggested by Thyagarajan and Yu [3].

Table. 4.8: Comparison of process models for Example 6

Method	Process model	Error (\tilde{E})
Proposed without noise	$\frac{0.9999e^{-0.010s}}{(2.0s+1)^2}$	0.0009
Proposed with noise	$\frac{0.9999e^{-0.0099s}}{(2.0s+1)^2}$	0.0051
Thyagarajan and Yu [3]	$\frac{0.8709e^{-0.013s}}{(1.8978s+1)^2}$	0.4236

4.4.5 Integrating SOPDT process model

Now, let us consider (4.55) as an overdamped (stable) process and assume $Kq = \bar{K}$ to represent in the following form

$$G_m(s) = \frac{\bar{K}e^{-\delta s}}{ms^2 + ns + q} \quad (4.79)$$

which is converted to the following integrating SOPDT process model by making $m = \tau_1$, $n = 1$ and $q = 0$

$$G_m(s) = \frac{\bar{K}e^{-\delta s}}{s(\tau_1 s + 1)} \quad (4.80)$$

Assuming $f_1 \rightarrow 0$, $f_2 = -1/\tau_1$ and $K = \bar{K}$ in the expressions obtained in subsections 4.3.1 - 4.3.3 for stable process model, the following equations are derived to estimate the unknown process model parameters \bar{K} , τ_1 and δ . Utilizing (4.32) in (4.23) and solving gives the following expression

$$\varepsilon = \frac{\bar{K}h}{(f_1 - f_2)} \left[f_2 \left(\frac{2f_1 T_p - 2f_1 \delta - f_1 T_p}{1 + e^{f_1 T_p}} \right) - f_1 \left(\frac{2e^{f_2(T_p - \delta - t_p + t_1)} - 2}{1 + e^{f_1 T_p}} \right) \right] \quad (4.81)$$

Further simplification leads to

$$\varepsilon = \frac{\bar{K}h}{f_2} \left(0.5f_2 T_p - f_2 \delta - e^{f_2(T_p - t_p + t_0)} + 1 \right) \quad (4.82)$$

Replacing f_2 by $(-1/\tau_1)$ in the above equation and rearranging we get

$$\bar{K}h \left(0.5T_p - \delta + \tau_1 e^{\frac{(t_p - t_0 - T_p)}{\tau_1}} - \tau_1 \right) - \varepsilon = 0 \quad (4.83)$$

To obtain the expression for \bar{K} , (4.32) is utilized in (4.38) and further simplified to get

$$A_p = \bar{K}h \left(\frac{2e^{f_1(t_p - t_1)}}{1 + e^{f_1 T_p}} - 1 \right) \quad (4.84)$$

The corresponding value of f_1 is substituted in the above equation and solved to

$$A_p = \bar{K}h(0.5T_p - t_p + t_1) \quad (4.85)$$

or

$$\bar{K} = \frac{A_p}{h(0.5T_p - t_p + t_1)} \quad (4.86)$$

Now, using $f_1 \rightarrow 0$ in (4.32) gives

$$e^{-f_2(t_p - t_1)} = \frac{2 + f_1 T_p}{1 + e^{f_2 T_p}} \quad (4.87)$$

which is further reduced to

$$\left(1 + e^{f_2 T_p} \right) e^{-f_2(t_p - t_1)} = 2 \quad (4.88)$$

or

$$2e^{f_2(t_p - t_1)} - e^{f_2 T_p} - 1 = 0 \quad (4.89)$$

Representing the above equation in terms of τ_1 as

$$2e^{\frac{(t_1-t_p)}{\tau_1}} - e^{\frac{-T_p}{\tau_1}} - 1 = 0 \quad (4.90)$$

Hence, substituting the parameters of relay and limit cycle in expression (4.86), \bar{K} is estimated, similarly other parameters τ_1 and δ are obtained from simultaneous solution of Eqs. (4.83) and (4.90).

Example 7

Let us consider a second order integrating process with time delay [48]

$$G(s) = \frac{e^{-0.2s}}{s(s+1)}.$$

A relay with parameters $h = 1$ and $\varepsilon = 0.2$ is applied to the above process to generate limit cycle. The measured limit cycle and it's second derivative parameters $A_p = 0.5895$, $T_p = 2.3898$, $t_1 = 0.4612$, $t_0 = 0.2612$ and $t_p = 1.0666$ along with relay parameters are substituted in expression (4.86) to estimate $\bar{K} = 1.0$. Similarly, the remaining parameters $\tau_1 = 0.9999$ and $\delta = 0.20$ are obtained from solving (4.83) and (4.90) simultaneously. To show the validity of the proposed method, the process dynamics are also identified in the presence of measurement noise of 20 dB SNR. The proposed models in the absence of measurement noise and with noise are given in Table 4.9 along with the model proposed by Panda et al. [48] without noise effect. From Table 4.9, it can be observed that the proposed method can be successfully used to identify the process models under noisy environment also.

Table. 4.9: Comparison of process models for Example 7

Method	Process model	Error (\tilde{E})
Proposed model without noise	$\frac{1.0e^{-0.20s}}{s(0.9999s+1)}$	0.0001
Proposed model with noise	$\frac{1.001e^{-0.1996s}}{s(1.0013s+1)}$	0.0008
By Panda et al. [48]	$\frac{1.0e^{-0.20s}}{s(0.9998s+1)}$	0.0003

Above simulation results show that the proposed identification scheme gives better results even

in the presence of measurement noise as compared to other methods. From the procedure explained in Section 4.5, the proposed algorithm can be used in real time applications to identify the process dynamics.

4.5 Implementation of proposed method in real plants

The procedure to implement the proposed method for identification of the process dynamics of real plants is detailed in this section. A simple dc motor can be assumed as a real process whose dynamics is characterized by the ratio of motor speed to input voltage. Referring to Fig. 4.1, a relay with hysteresis induces a limit cycle output when connected in series feedback to the plant or process. Relay with an operational characteristics, acts as an electrically operated switch. In the literature [9], it has been reported that a solid state relay can be implemented in order to achieve an accurate plant dynamics as compared to conventional electro-mechanical relay. A relay can be implemented either by using a FPAA (Field Programmable Analog Array) [85] or op-amps (Operational Amplifiers) by setting the sampling time, relay amplitude and hysteresis values in the range of milliseconds, volts and millivolts, respectively. These relay parameters are user defined and can be modified in order to control the amplitude of limit cycle output. The relay is connected in such a way that it would bring a periodic and oscillatory behavior in the plant output characteristics. The denoising block consisting of derivative blocks and an integrator can be implemented using a set of op-amps or FPAA. Therefore, a denoised limit cycle can be yielded with reduced noise effect and also the multiple switching at relay output gets mitigated. A recovered limit cycle and the relay output can be observed on oscilloscope connected at the plant output and relay output terminals, respectively. The limit cycle and other parameters as shown in Fig. 4.3 can be measured by making simple observation. Using these parameters in the corresponding expressions derived, the process can be modeled. The summing point and comparator at the forward and feedback paths, respectively can be designed using op-amps. The flowchart as shown in Fig. 4.7 facilitates in understanding the above explained procedure in a simple way.

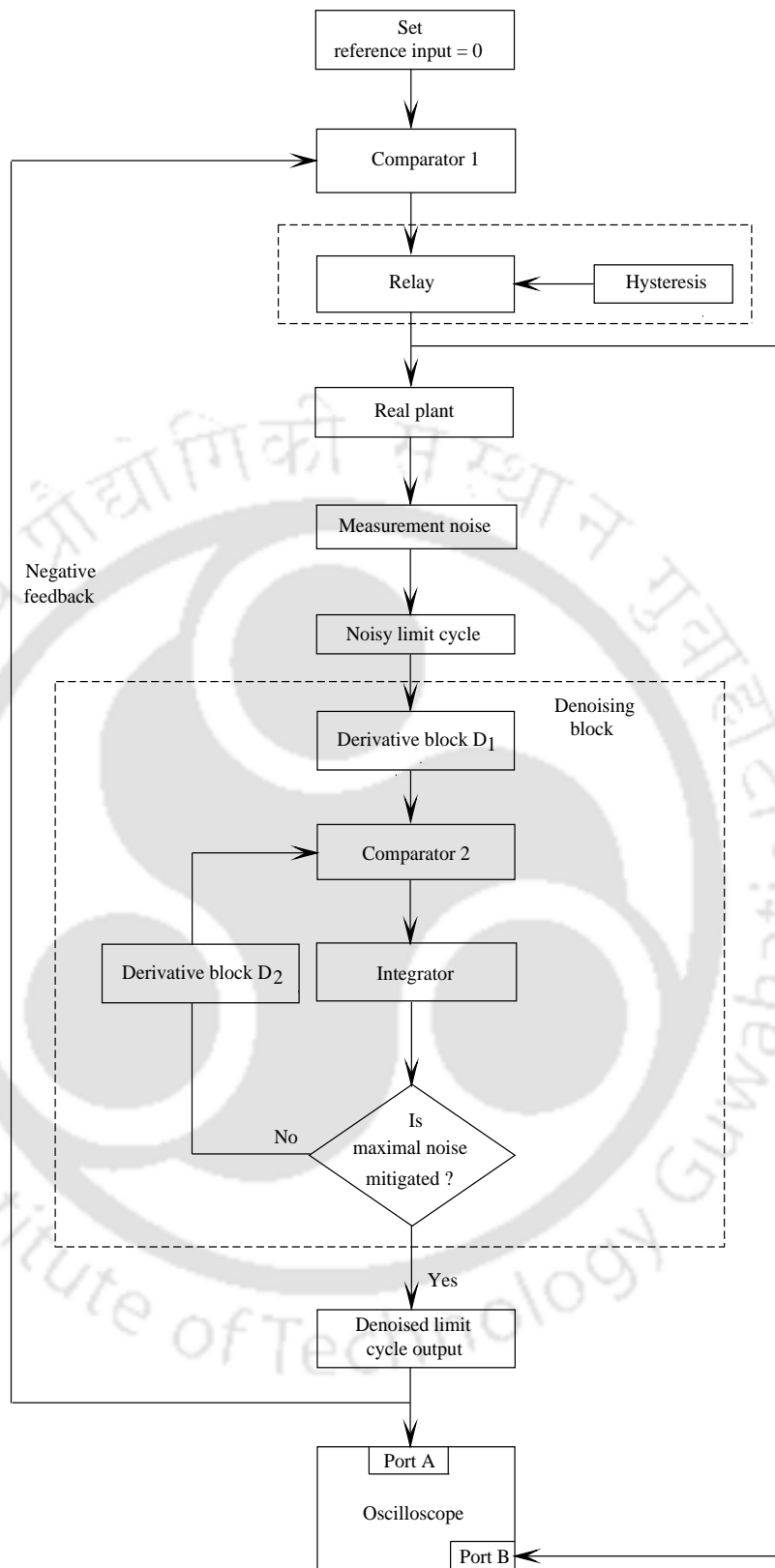


Figure 4.7: Flowchart for implementation procedure

4.6 Summary

Methods are proposed for identification of accurate process dynamics of stable and unstable first order, second order overdamped, underdamped, critically damped and integrating processes with time delay. Generalized SOPDT process model is considered and expressions are derived to estimate the unknown model parameters. State space method is used to develop the expressions so that accurate model parameters are estimated. To estimate the process model parameters in the face of measurement noise, the process output is corrupted with noise and for denoising, a simple but effective closed loop denoising block is introduced in proposed relay feedback control structure. To show the efficiency of the proposed method, well known examples are considered and simulation tests are carried out under noisy environment.



CHAPTER 5

IDENTIFICATION OF PROCESSES WITH NON-MINIMUM PHASE CHARACTERISTICS

5.1 Introduction

Some complex chemical processes exhibit non-minimum phase (NMP) characteristics and these processes may provide erroneous information if the identification is not accurate. In the literature, initially identification methods are developed using describing function (DF) technique [10–12, 18]. In this DF method the nonlinear device relay is approximated by a gain hence, the process model parameters estimated are not exact. In process identification accuracy of the estimated parameters is important to design controller for satisfactory performance of the process. Hence, many authors developed exact methods [3, 35, 37, 39, 42, 43, 47, 49] generally for all pole processes with time delay. A process with time delay or with RHP zero can be considered as NMP process. These NMP characteristics can be observed in some complex chemical systems [62], Zhang et al. [63] described ship's path control system in restricted waters as NMP system. The drum-boiler dynamics [86] represent one of the real time examples for NMP process. To mention few more examples are a valve control system, a telescope azimuth angle control system [9] and water level in boiler drum [48, 87]. Few methods are available for identification of NMP process dynamics. Panda et al. [48] addressed about the transient response of the process with a zero in the numerator. Padhy and Majhi [88] derived state space based analytical expressions for identification of time delay and NMP process dynamics using ideal relay. But the authors have not considered the effects of measurement noise in the pro-

cess output. Ramakrishnan and Chidambaram [68] suggested algorithms for identification of SOPDT process dynamics employing an asymmetrical relay test and Laplace transform technique. Here, the authors have considered a second order NMP process without time delay as one of the case studies. Many a times in process industries the output is distorted with measurement noise leading to chattering in the process output. So, the estimated process model parameters will not be accurate which in turn affect the design of controller and performance of the process operation. In proposed method a noise free limit cycle is obtained with the help of a modified denoising block and relay with hysteresis in the closed loop. Hence, presented technique works well in real time scenarios. In the literature identification methods are available for particular type of process, few authors have considered more than one type of processes but without noise. The method suggested in this chapter can be applied to more than one type of process model in the presence of measurement noise.

In this chapter time domain based generalized analytical expressions are derived to estimate exact process model parameters of a class of stable NMP processes with time delay using a single relay with hysteresis in closed loop. Analytical expressions are derived for off-line identification of SISO NMP processes with time delay. The process models are considered for FOPDT, SOPDT overdamped, underdamped, critically damped and integrating processes. Relay as an input to the process generates sustained oscillations or limit cycles whose parameters are utilized in the expressions to identify the unknown process model dynamics. In practice measurement noise is an important issue which can corrupt the process output causing multiple switching and finally leads to erroneous process identification. Relay with hysteresis reduces the effect of noise and further mitigation of noise is achieved with the help of a denoising block so that a clean process output is obtained. Processes modeled in the form of transfer functions are considered to test the presented technique. Results are analyzed and compared with recent methods available in the literature to demonstrate the effectiveness and validity of the suggested method, which also holds true for process output with chattering caused due to measurement noise.

5.1.1 Contributions compared to the reference [1]

This subsection highlights the contributions of this chapter as compared to [1]. Using ideal relay, Majhi [1] derived set of expressions applying state space method for estimation of process model parameters of NMP processes with time delay consisting of single or multiple poles and applied Fourier series based curve fitting technique to mitigate the effects of measurement noise from limit cycle output. Majhi's [1] method can be used to estimate maximum three parameters at a time among four unknowns of the transfer function model. Liu and Gao [67] considered the process model suggested by Majhi [1] and proposed algorithms to estimate all four parameters of the transfer function model. But the process model considered by Majhi [1] and Liu and Gao [67] has repeated poles and this model cannot be generalized to process models like underdamped and integrating. The methods proposed in [1, 67] motivated to further generalize a second order NMP process model with time delay to FOPDT and SOPDT NMP process models with repeated and non-repeated poles. Using our proposed method four unknown parameters are estimated at a time.

5.2 Identification method

The closed loop identification scheme as shown in Fig. 5.1 consists of a relay with hysteresis, the NMP process and a denoising block. This denoising block consists of a single derivative and an integrator in the closed loop. Here also the derivative block generates first derivative output in terms of the rate of change of noisy limit cycle $\bar{y}(t)$ with reference to time and the integrator removes higher order harmonics present in the derivative output, assuming zero initial conditions. Hence, a clean limit cycle output $y(t)$ is generated. During process identification, with relay input the system generates sustained oscillations hence, the reference input $r(t)$ is made zero. The user defined relay parameters and the measured limit cycle parameters are substituted in the corresponding analytical expressions to estimate the unknown process model parameters of NMP processes.

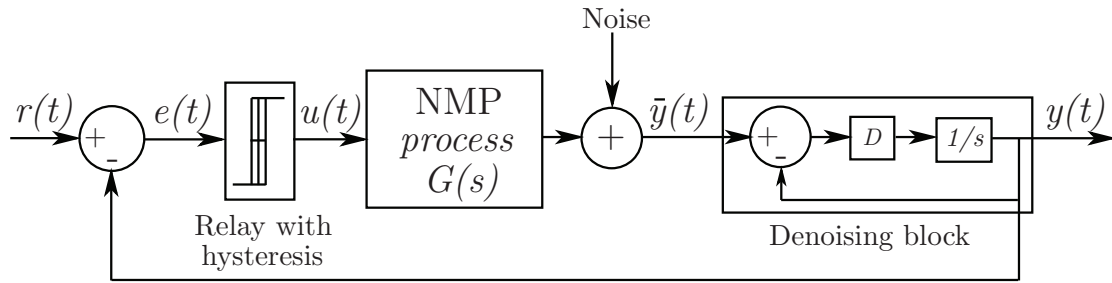


Figure 5.1: Relay feedback block diagram with denoising block

The generalized transfer function model of a stable NMP process with time delay is given as

$$G_m(s) = \frac{Kq(-zs + 1)e^{-\delta s}}{ms^2 + ns + q} \quad (5.1)$$

which consists of the unknown parameters to be estimated as K (steady state gain), δ (process time delay), z (the zero on the right half of the s -plane), m , n (process parameters) and q is assumed to be 1 here without loss of generality for deriving expressions but for an integrating process model it is taken as zero. The transfer function mentioned in (5.1) can be realized in different types of NMP process models like FOPDT, SOPDT overdamped, underdamped, critically damped and integrating. The relay input causes the process to generate limit cycles, which are in the form of sustained oscillations and carry the process information. Also the delayed relay output provides two constant piecewise linear inputs to the process for the time ranges $t_0 \leq t \leq t_1$ and $t_1 \leq t \leq (T_p + t_0)$, where T_p is the half period of limit cycle, t_0 is the time at which the relay switches from $+h$ to $-h$ (h is relay height or amplitude), t_1 is the time at which the second derivative output of limit cycle experiences instant change, in case of FOPDT processes, t_1 is measured from first derivative output of limit cycle.

5.3 Analytical expressions for parametric estimation

In this section the state space method used in Chapter 4 is applied to derive the analytical expressions which are used to estimate the unknown process model parameters with the help of relay and limit cycle information. Hence, the detailed derivations shown in Section 4.3 and subsections 4.3.1 - 4.3.3 are not repeated here but for convenience few equations are rewritten

as follows.

The standard form of state space equations for processes with time delay are given by

$$\dot{\mathbf{x}}(t) = \mathbf{A}\mathbf{x}(t) + \mathbf{b}u(t - \delta) \quad (5.2)$$

$$y(t) = \mathbf{c}\mathbf{x}(t) \quad (5.3)$$

where \mathbf{A} is a 2×2 square matrix, \mathbf{b} is 2×1 column vector, \mathbf{c} is 1×2 row vector. The expressions derived for $\mathbf{x}(t_0)$, $\mathbf{x}(t_1)$ and $\mathbf{x}(t_p)$ are rewritten as

$$\mathbf{x}(t_0) = (\mathbf{I} + \mathbf{e}^{\mathbf{A}T_p})^{-1} \mathbf{A}^{-1} (2\mathbf{e}^{\mathbf{A}(T_p - \delta)} - \mathbf{e}^{\mathbf{A}T_p} - \mathbf{I}) \mathbf{b}h \quad (5.4)$$

$$\mathbf{x}(t_1) = \mathbf{e}^{\mathbf{A}(t_1 - t_0)} \mathbf{x}(t_0) + \mathbf{A}^{-1} (\mathbf{e}^{\mathbf{A}(t_1 - t_0)} - \mathbf{I}) \mathbf{b}h \quad (5.5)$$

$$\mathbf{x}(t_p) = \mathbf{e}^{\mathbf{A}(t_p - t_1)} \mathbf{x}(t_1) - \mathbf{A}^{-1} (\mathbf{e}^{\mathbf{A}(t_p - t_1)} - \mathbf{I}) \mathbf{b}h \quad (5.6)$$

Now, the NMP process model given in (5.1) is represented as

$$G_m(s) = \frac{K f_1 f_2 (s + f_0) e^{-\delta s}}{f_0 (s - f_1) (s - f_2)} \quad (5.7)$$

where

$$f_0 = -1/z \quad (5.8)$$

$$f_1 = \frac{-2q}{n + \sqrt{n^2 - 4mq}} \quad (5.9)$$

$$f_2 = \frac{-2q}{n - \sqrt{n^2 - 4mq}} \quad (5.10)$$

Transforming the transfer function given in (5.7) to state space form as

$$\dot{\mathbf{x}}(t) = \begin{bmatrix} f_1 & 0 \\ 0 & f_2 \end{bmatrix} \begin{bmatrix} x_1(t) \\ x_2(t) \end{bmatrix} + \begin{bmatrix} a_1 \\ -a_2 \end{bmatrix} u(t - \delta) \quad (5.11)$$

$$y(t) = \begin{bmatrix} 1 & 1 \end{bmatrix} \begin{bmatrix} x_1(t) \\ x_2(t) \end{bmatrix} \quad (5.12)$$

(Detailed derivation of Eqs. (5.11) and (5.12) from (5.7) is given in Appendix A.3.)

Comparing (5.11) and (5.12) with (5.2) and (5.3), respectively the matrices \mathbf{A} , \mathbf{b} and \mathbf{c} are given

as

$$\mathbf{A} = \begin{bmatrix} f_1 & 0 \\ 0 & f_2 \end{bmatrix}; \mathbf{b} = \begin{bmatrix} a_1 \\ -a_2 \end{bmatrix}; \mathbf{c} = \begin{bmatrix} 1 & 1 \end{bmatrix} \quad (5.13)$$

where f_1 and f_2 are the eigenvalues of \mathbf{A} and

$$a_1 = \frac{Kf_1f_2(f_0+f_1)}{f_0(f_1-f_2)} \quad \text{and} \quad a_2 = \frac{Kf_1f_2(f_0+f_2)}{f_0(f_1-f_2)}$$

Now, Eqs. (5.4), (5.5) and (5.6) are simplified, respectively to

$$\mathbf{x}(t_0) = \begin{bmatrix} \frac{a_1h(2e^{f_1(T_p-\delta)} - e^{f_1T_p-1})}{f_1(1+e^{f_1T_p})} \\ \frac{-a_2h(2e^{f_2(T_p-\delta)} - e^{f_2T_p-1})}{f_2(1+e^{f_2T_p})} \end{bmatrix} \quad (5.14)$$

$$\mathbf{x}(t_1) = \begin{bmatrix} \frac{a_1h}{f_1} \left(\frac{e^{f_1T_p-1}}{1+e^{f_1T_p}} \right) \\ \frac{-a_2h}{f_2} \left(\frac{e^{f_2T_p-1}}{1+e^{f_2T_p}} \right) \end{bmatrix} \quad (5.15)$$

$$\mathbf{x}(t_p) = \begin{bmatrix} \frac{a_1h}{f_1} \left(\frac{-2e^{f_1(t_p-t_1)}}{1+e^{f_1T_p}} + 1 \right) \\ \frac{a_2h}{f_2} \left(\frac{2e^{f_2(t_p-t_1)}}{1+e^{f_2T_p}} - 1 \right) \end{bmatrix} \quad (5.16)$$

These expressions (5.14), (5.15) and (5.16) are further utilized to obtain the equations for relay parameter ε (hysteresis width at which relay switching takes place), limit cycle parameters t_p (peak time), A_p (peak amplitude) and A_d (amplitude at discontinuity in limit cycle output) as follows.

The necessary condition to generate sustained oscillations is given by

$$y(t_0) = \mathbf{c}\mathbf{x}(t_0) = \varepsilon \quad (5.17)$$

Substituting for \mathbf{c} and $\mathbf{x}(t_0)$ in (5.17) and resolved to get

$$\varepsilon - \frac{Kh}{f_1-f_2} \left[f_2 \left(2 \frac{(f_0+f_1)e^{f_1(T_p-\delta)}}{f_0(1+e^{f_1T_p})} - 1 \right) - f_1 \left(2 \frac{(f_0+f_2)e^{f_2(T_p-\delta)}}{f_0(1+e^{f_2T_p})} - 1 \right) \right] = 0 \quad (5.18)$$

To get the expression for t_p , the first derivative of peak amplitude is represented as

$$\dot{y}(t_p) = \mathbf{c}\dot{\mathbf{x}}(t_p) = 0 \quad (5.19)$$

Expansion of the above equation leads to

$$\mathbf{c}\mathbf{A}\mathbf{x}(t_p) - \mathbf{c}\mathbf{b}h = 0 \quad (5.20)$$

Substituting (5.16) and other corresponding expressions in (5.20) and simplified to obtain

$$t_p - t_1 - \frac{1}{(f_1 - f_2)} \ln \left[\frac{(f_0 + f_2)(1 + e^{f_1 T_p})}{(f_0 + f_1)(1 + e^{f_2 T_p})} \right] = 0 \quad (5.21)$$

The expression for peak amplitude (A_p) is obtained as follows

$$A_p = y(t_p) = \mathbf{c}\mathbf{x}(t_p) \quad (5.22)$$

Equations for \mathbf{c} and $\mathbf{x}(t_p)$ are utilized in (5.22) and reduced to

$$A_p - Kh \left[2 \left(\frac{f_0 + f_1}{f_0 (1 + e^{f_1 T_p})} \right)^{\frac{-f_2}{f_1 - f_2}} \left(\frac{f_0 + f_2}{f_0 (1 + e^{f_2 T_p})} \right)^{\frac{f_1}{f_1 - f_2}} - 1 \right] = 0 \quad (5.23)$$

In the given process model apart from time delay δ as there are four unknown parameters so, one more new expression is derived as follows.

The half limit cycle output of SOPDT NMP process is as shown in Fig. 5.2. Let A_d be the amplitude at time t_1 or discontinuity in limit cycle output therefore,

$$y(t_1) = A_d = \mathbf{c}\mathbf{x}(t_1) \quad (5.24)$$

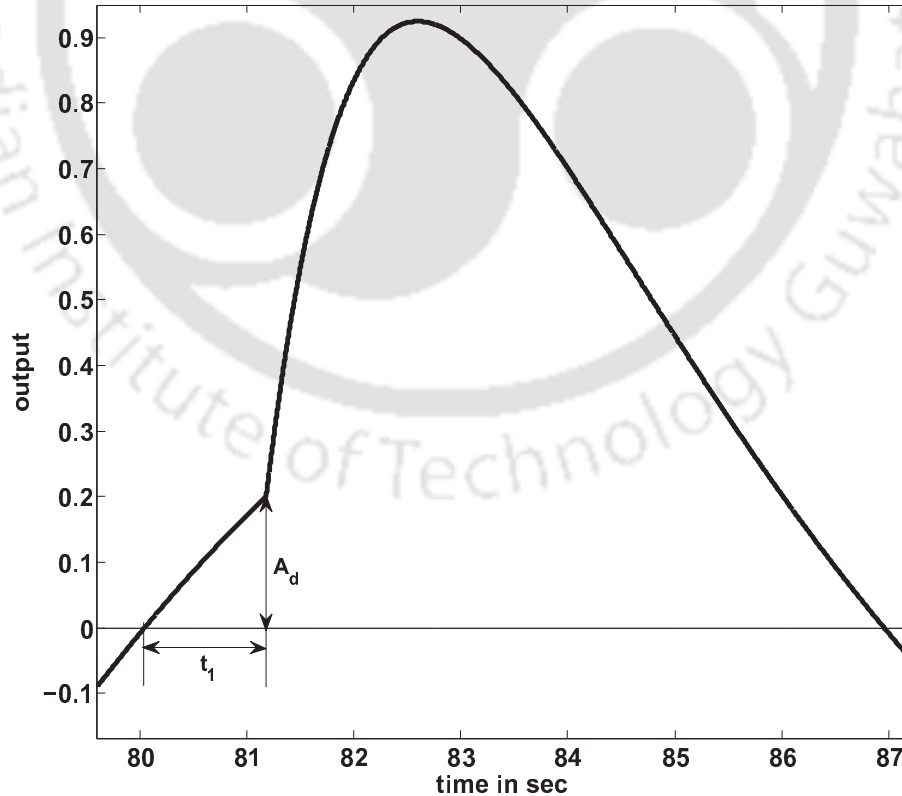


Figure 5.2: Half limit cycle output

Substituting for \mathbf{c} and $\mathbf{x}(t_1)$ in (5.24) the following expression is derived

$$A_d = \frac{a_1 h}{f_1} \left(\frac{e^{f_1 T_p} - 1}{1 + e^{f_1 T_p}} \right) - \frac{a_2 h}{f_2} \left(\frac{e^{f_2 T_p} - 1}{1 + e^{f_2 T_p}} \right) \quad (5.25)$$

Utilizing the corresponding values for a_1 and a_2 in the above equation and further simplifying we get

$$A_d - \frac{Kh}{f_1 - f_2} \left[f_2 \frac{(f_0 + f_1)(e^{f_1 T_p} - 1)}{f_0(1 + e^{f_1 T_p})} - f_1 \frac{(f_0 + f_2)(e^{f_2 T_p} - 1)}{f_0(1 + e^{f_2 T_p})} \right] = 0 \quad (5.26)$$

Hence, the expressions (5.18), (5.21), (5.23) and (5.26) are further explored to derive the corresponding equations for different types of process models as mentioned in the following section.

5.4 Process identification

5.4.1 FOPDT NMP process model

The following FOPDT NMP process model is obtained with $m = 0$ and $q = 1$ in (5.1)

$$G_m(s) = \frac{K(-zs + 1)e^{-\delta s}}{ns + 1}. \quad (5.27)$$

Hence, for this model $f_0 = -1/z$, $f_1 = -1/n$ and $f_2 \rightarrow -\infty$ which are substituted in (5.18), (5.21), (5.23) and (5.26) and solved, respectively to get

$$2 \left(\frac{z}{n} + 1 \right) + \left(\frac{\varepsilon}{Kh} - 1 \right) \left(e^{(T_p - \delta)/n} + e^{-\delta/n} \right) = 0 \quad (5.28)$$

$$t_p - t_1 = 0 \quad (5.29)$$

$$\frac{A_p}{Kh} - \frac{2(1 + z/n)}{1 + e^{-T_p/n}} + 1 = 0 \quad (5.30)$$

$$\frac{A_d}{Kh} \left(1 + e^{-T_p/n} \right) + e^{-T_p/n} \left(\frac{2z}{n} + 1 \right) - 1 = 0 \quad (5.31)$$

The above Eqs. (5.28) - (5.31) are solved simultaneously to estimate the unknown process model parameters K , δ , z and n . These nonlinear expressions are solved simultaneously by using the MATLAB function *fsolve* assuming suitable initial values. The details of using *fsolve* function is given in Appendix A.4.

Example 1

Let us consider a FOPDT NMP process with the following transfer function

$$G(s) = \frac{(-s+1)e^{-s}}{2s+1}.$$

Applying single relay ($h = 1$ and $\varepsilon = 0.3$) input to the above process generates limit cycle as shown in Fig. 5.3. The limit cycle and its first derivative output parameters measured are $t_p = 1.7133$, $t_1 = 1.7133$, $t_0 = 0.7133$, $T_p = 3.6054$, $A_p = 1.5754$ and $A_d = 0.5754$. These quantities are substituted in (5.28) - (5.31) and solved simultaneously to estimate the exact process model parameters as $K = 1.0$, $\delta = 1.0$, $z = 1.0$ and $n = 2.0$.

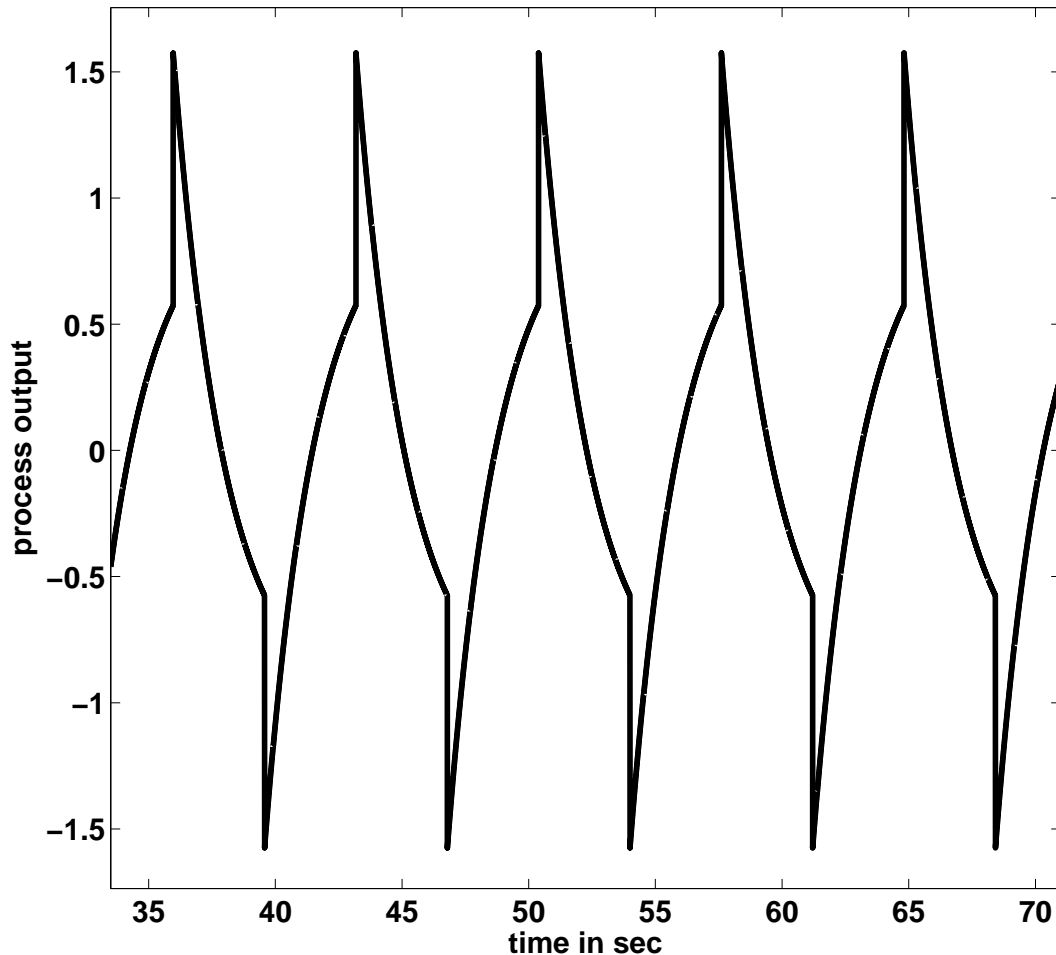


Figure 5.3: Process output

5.4.2 Overdamped SOPDT NMP process model

Let us consider the model given in (5.1) as an overdamped SOPDT process model with $q = 1$ as mentioned below

$$G_m(s) = \frac{K(-zs + 1)e^{-\delta s}}{ms^2 + ns + 1} \quad (5.32)$$

Eqs. (5.9) and (5.10) are simplified for the process model parameters m and n as

$$m = \frac{1}{f_1 f_2} \quad (5.33)$$

$$n = \frac{-(f_1 + f_2)}{f_1 f_2} \quad (5.34)$$

Eqs. (5.18), (5.21), (5.23) and (5.26) are solved simultaneously to calculate the parameters in terms of K , f_0 , f_1 and f_2 . Hence, apart from K the process model parameter z is obtained from f_0 and m and n are obtained from (5.33) and (5.34), respectively.

Example 2

This example considers an overdamped SOPDT NMP process [88]

$$G(s) = \frac{(-s + 1)e^{-s}}{10s^2 + 7s + 1}$$

The relay test is carried out with the parameters $h = 1$ and $\varepsilon = 0.35$, without noise to obtain the limit cycle and its second derivative output parameters as $t_p = 4.6683$, $t_1 = 3.4565$, $t_0 = 2.4565$, $T_p = 9.0675$, $A_p = 0.6194$ and $A_d = 0.4604$, so $\delta = 1.0$ is obtained. Substituting these parameters in expressions (5.18), (5.21), (5.23) and (5.26) and solved simultaneously to find the parameters $K = 1.0002$, $f_0 = -1.0$, $f_1 = -0.5001$ and $f_2 = -0.1999$. Hence, $z = 1.0$, $m = 10.0030$ and $n = 7.0021$ are obtained from f_0 , f_1 and f_2 using the procedure as explained in subsection 5.4.2. Similarly, a relay test is carried out in the presence of measurement noise of 20 dB SNR, the noisy and denoised limit cycles are as shown in Fig. 5.4. The measurements made on the denoised limit cycle and its second derivative output are $t_p = 4.6686$, $t_1 = 3.4557$, $t_0 = 2.4559$, $T_p = 9.0673$, $A_p = 0.6194$ and $A_d = 0.4604$. Applying the the procedure as mentioned above in this example the process model is identified. For this process, Padhy and Majhi [88] used an ideal relay to estimate the process model parameters without considering noise effect. The

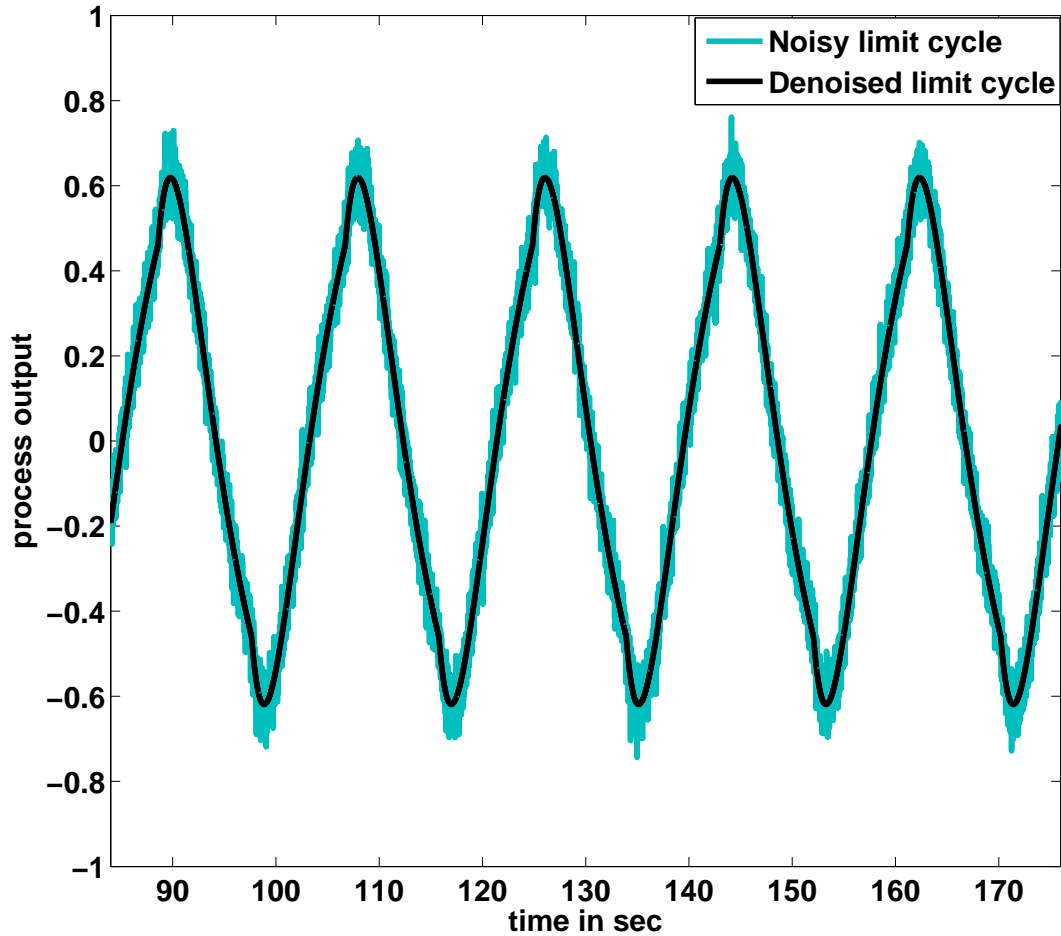


Figure 5.4: Noisy and denoised limitcycles

identified models and the model suggested by Padhy and Majhi [88] are given in Table 5.1. The % error for corresponding model parameters is given in Table 5.2.

Table. 5.1: Comparison of process models for Example 2

Method	Process model
Proposed without noise	$\frac{1.0002(-1.0s+1)e^{-1.0s}}{10.0030s^2+7.0021s+1}$
Proposed with noise	$\frac{0.9983(-1.0003s+1)e^{-0.9998s}}{10.0049s^2+6.9876s+1}$
Padhy and Majhi [88]	$\frac{1.0001(-1.0002s+1)e^{-1.0s}}{10.0079s^2+7.001s+1}$

Table. 5.2: Comparison of model parameters in % error

Model	K	z	m	n	δ
Proposed without noise	-0.02	0	-0.03	-0.03	0
Proposed with noise	0.17	-0.03	-0.049	0.1771	0.02
Padhy and Majhi [88] without noise	-0.01	-0.02	-0.079	-0.0143	0

5.4.3 Underdamped SOPDT NMP process model

Let us consider (5.1) as an underdamped SOPDT process model with $q = 1$ as given below

$$G_m(s) = \frac{K(-zs + 1)e^{-\delta s}}{ms^2 + ns + 1} \quad (5.35)$$

For underdamped processes $n^2 < 4m$, so, f_1 and f_2 become

$$f_1 = \gamma_1 + j\gamma_2; \quad f_2 = \gamma_1 - j\gamma_2 \quad (5.36)$$

where

$$\gamma_1 = \frac{-n}{2m} \quad (5.37)$$

$$\gamma_2 = \frac{\sqrt{4m - n^2}}{2m} \quad (5.38)$$

Solving γ_1 and γ_2 for m and n we get

$$m = \frac{1}{\gamma_1^2 + \gamma_2^2} \quad (5.39)$$

$$n = \frac{-2\gamma_1}{\gamma_1^2 + \gamma_2^2} \quad (5.40)$$

The below mentioned expressions are derived using (5.36) in (5.18), (5.21) and (5.26)

$$\begin{aligned} Kh \left[\frac{2e^{\gamma_1(T_p - \delta)}}{1 + e^{2\gamma_1 T_p} + 2e^{\gamma_1 T_p} \cos(\gamma_2 T_p)} \left(\frac{\gamma_1}{\gamma_2} \left(\left(\frac{f_0 + \gamma_1}{f_0} \right) (\sin(\gamma_1(T_p - \delta)) - e^{\gamma_1 T_p} \sin(\gamma_2 \delta)) \right. \right. \right. \\ \left. \left. \left. + \frac{\gamma_2}{f_0} (\cos(\gamma_2(T_p - \delta)) + e^{\gamma_1 T_p} \cos(\gamma_2 \delta)) \right) - \left(\left(\frac{f_0 + \gamma_1}{f_0} \right) (\cos(\gamma_2(T_p - \delta)) \right. \right. \right. \\ \left. \left. \left. + e^{\gamma_1 T_p} \cos(\gamma_2 \delta)) - \frac{\gamma_2}{f_0} (\sin(\gamma_2(T_p - \delta)) - e^{\gamma_1 T_p} \sin(\gamma_2 \delta)) \right) \right) + 1 \right] - \varepsilon = 0 \quad (5.41) \end{aligned}$$

$$\gamma_2(t_p - t_1) - \tan^{-1} \left[\frac{(f_0 + \gamma_1) e^{\gamma_1 T_p} \sin(\gamma_2 T_p) - \gamma_2 (1 + e^{\gamma_1 T_p} \cos(\gamma_2 T_p))}{(f_0 + \gamma_1) (1 + e^{\gamma_1 T_p} \cos(\gamma_2 T_p)) + \gamma_2 e^{\gamma_1 T_p} \sin(\gamma_2 T_p)} \right] = 0 \quad (5.42)$$

$$\frac{Kh [2e^{\gamma_1 T_p} (\gamma_1^2 + \gamma_2^2 + \gamma_1 f_0) \sin(\gamma_2 T_p) - \gamma_2 f_0 (e^{2\gamma_1 T_p} - 1)]}{\gamma_2 f_0 [1 + e^{2\gamma_1 T_p} + 2e^{\gamma_1 T_p} \cos(\gamma_2 T_p)]} - A_d = 0 \quad (5.43)$$

Expressions (5.42) and (5.43) are utilized to get

$$\frac{Kh [2e^{\gamma_1 T_p} (\gamma_1^2 + \gamma_2^2 + \gamma_1 f_0) \sin(\gamma_2 T_p) - \gamma_2 f_0 (e^{2\gamma_1 T_p} - 1)] (t_p - t_1)}{f_0 A_d [1 + e^{2\gamma_1 T_p} + 2e^{\gamma_1 T_p} \cos(\gamma_2 T_p)]} - \tan^{-1} \left[\frac{(f_0 + \gamma_1) e^{\gamma_1 T_p} \sin(\gamma_2 T_p) - \gamma_2 (1 + e^{\gamma_1 T_p} \cos(\gamma_2 T_p))}{(f_0 + \gamma_1) (1 + e^{\gamma_1 T_p} \cos(\gamma_2 T_p)) + \gamma_2 e^{\gamma_1 T_p} \sin(\gamma_2 T_p)} \right] = 0 \quad (5.44)$$

The parameters K , f_0 , γ_1 and γ_2 are estimated by solving (5.41) - (5.44) simultaneously. From f_0 , γ_1 and γ_2 the remaining process model parameters z , m and n are calculated and δ is obtained from measurements of t_1 and t_0 as $\delta = (t_1 - t_0)$ as explained in subsection 4.3.4.

Example 3

Let us consider the following underdamped SOPDT NMP process [66, 89]

$$G(s) = \frac{(-4s + 1) e^{-s}}{9s^2 + 2.4s + 1}.$$

Application of relay with hysteresis as an input to this process generates limit cycles in the absence of measurement noise. The relay parameters used are $h = 1$, $\varepsilon = 0.4$ and measured limit cycle parameters are $A_d = 0.9964$, $T_p = 9.1399$, $t_0 = 0.5831$, $t_1 = 1.5831$ and $t_p = 4.2412$. These relay and limit cycle parameters are substituted in (5.41) - (5.44) and solved simultaneously to obtain $K = 1.0001$, $f_0 = -0.250$, $\gamma_1 = -0.1333$ and $\gamma_2 = 0.3055$. From these f_0 , γ_1 and γ_2 the remaining process model parameters z , m and n are estimated. The process time delay δ is found as $\delta = (t_1 - t_0) = 1.0$. The proposed method is tested in the presence of measurement noise of 20 dB SNR, Fig. 5.5 shows the noisy process output and denoised limit cycles. Now, the measured limit cycle parameters are $A_d = 0.9964$, $T_p = 9.14$, $t_0 = 0.5831$, $t_1 = 1.5831$ and $t_p = 4.2413$ which are again substituted in (5.41) - (5.44) and $\delta = (t_1 - t_0)$ to identify the process dynamics. Hence, the identified process models in transfer function form and the models suggested by Liu and Gao [89] and Wang et al. [66] are given in Table 5.3 and the corresponding

% error for model parameters is mentioned in Table 5.4.

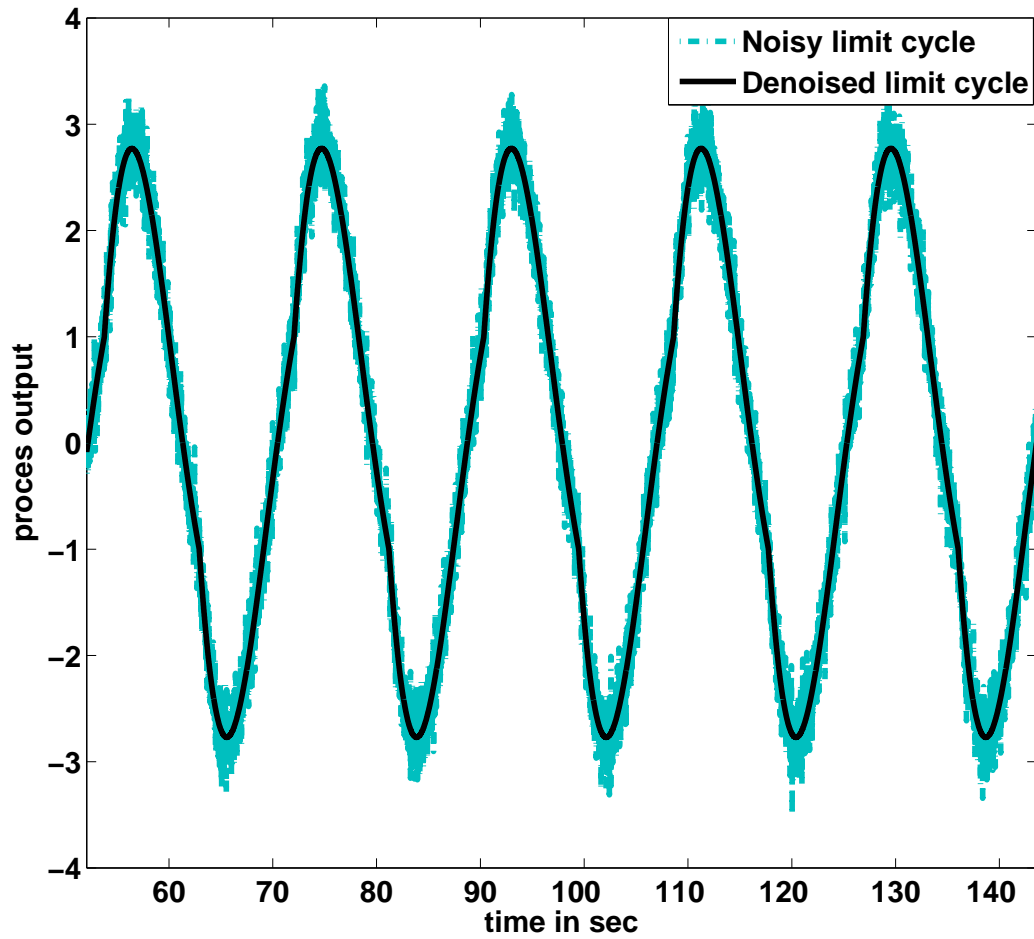


Figure 5.5: Noisy and denoised limitcycles

Table. 5.3: Comparison of process models for Example 3

Method	Process model
Proposed without noise	$\frac{1.0001(-4.0s+1)e^{-1.0s}}{9.0009s^2+2.3997s+1}$
Proposed with noise	$\frac{0.9999(-3.9984s+1)e^{-1.0s}}{9.0009s^2+2.3997s+1}$
Liu and Gao [89] without noise	$\frac{0.9998(-3.9997s+1)e^{-1.0s}}{9.0183s^2+2.3951s+1}$
Wang et al. [66] without noise	$\frac{1.0(-3.98s+1)e^{-1.07s}}{8.86s^2+2.39s+1}$

Table. 5.4: Comparison of model parameters in % error

Model	K	z	m	n	δ
Proposed without noise	-0.01	0	-0.01	0.0125	0
Proposed with noise	0.01	0.04	-0.01	0.0125	0
Liu and Gao [89] without noise	0.02	0.0075	-0.2033	0.2042	0
Wang et al. [66] without noise	0	0.5	1.5556	0.4167	-7.0

5.4.4 Critically damped SOPDT NMP process model

A critically damped SOPDT process model is represented as

$$G_m(s) = \frac{K(-zs+1)e^{-\delta s}}{(ms+1)^2} \quad (5.45)$$

The expressions obtained in subsection 5.4.3 are used here to derive the equations for critically damped process model. Hence, comparing (5.45) with (5.35), γ_1 and γ_2 in (5.37) and (5.38) are modified to

$$\gamma_1 = -1/m \quad ; \quad \gamma_2 = 0 \quad (5.46)$$

Using above values of γ_1 and γ_2 along with f_0 in (5.41) - (5.44) the below mentioned expressions are obtained

$$\frac{\varepsilon}{Kh} - \frac{2e^{\delta/m}}{m^2(1+e^{T_p/m})^2} \left[mz(1+e^{T_p/m}) + (m+z)e^{T_p/m}((\delta-m)(1+e^{-T_p/m}) - T_p) \right] - 1 = 0 \quad (5.47)$$

$$\left(\frac{1}{z} + \frac{1}{m} \right) \left[\frac{T_p}{1+e^{T_p/m}} - t_p + t_1 \right] + 1 = 0 \quad (5.48)$$

$$Kh \left[1 - e^{2T_p/m} + 2T_p e^{T_p/m} (z+m)/m^2 \right] + A_d \left(1 + e^{T_p/m} \right)^2 = 0 \quad (5.49)$$

$$Kh(t_p - t_1) \left[2T_p e^{T_p/m} (z+m) + m^2 \left(1 - e^{2T_p/m} \right) \right] + m^2 A_d \left[T_p \left(1 + e^{T_p/m} \right) + zm \left(1 + e^{T_p/m} \right)^2 / (z+m) \right] = 0 \quad (5.50)$$

Simultaneous solution of Eqs. (5.47) - (5.50) leads to estimation of critically damped process model parameters K , δ , z and m .

Example 4

Now, a second order critically damped NMP process without time delay studied by Padhy and Majhi [88] is considered as

$$G(s) = \frac{5(-3s+1)}{(2s+1)^2}.$$

The relay with $h = 1$ and $\varepsilon = 0.4$ generates limit cycle with parameters $A_d = 0.4$, $T_p = 5.4098$, $t_1 = 0.2559$ and $t_p = 1.795$. Similarly, in the presence of measurement noise of 25 dB SNR, the limit cycle parameters measured are $A_d = 0.3999$, $T_p = 5.4099$, $t_1 = 0.2558$ and $t_p = 1.795$. These parameters are substituted in (5.48) - (5.50) and solved simultaneously to estimate the process model parameters K , z and m with and without noise effect. The proposed models are given in Table 5.5 along with the model suggested by Padhy and Majhi [88], where the authors have not considered the effect of measurement noise. The % error of model parameters is given in Table 5.6.

Table. 5.5: Comparison of process models for Example 4

Method	Process model
Proposed without noise	$\frac{5.0001(-3.0s+1)}{(2.0s+1)^2}$
Proposed with noise	$\frac{5.0002(-2.9994s+1)}{(2.0s+1)^2}$
Padhy and Majhi [88] without noise	$\frac{5.0002(-2.9999s+1)}{(2.002s+1)^2}$

Table. 5.6: Comparison of model parameters in % error

Model	K	z	m
Proposed without noise	-0.002	0	0
Proposed with noise	-0.004	0.02	0
Padhy and Majhi [88] without noise	-0.004	0.0033	-0.1

5.4.5 Integrating SOPDT NMP process model

Let us assume $Kq = \bar{K}$ in (5.1) which is represented as

$$G_m(s) = \frac{\bar{K}(-zs + 1)e^{-\delta s}}{ms^2 + ns + q} \quad (5.51)$$

which is converted to the following integrating SOPDT process model by making $n = 1$ and $q = 0$

$$G_m(s) = \frac{\bar{K}(-zs + 1)e^{-\delta s}}{s(ms + 1)} \quad (5.52)$$

With reference to (5.52) the following expressions are derived assuming $f_1 \rightarrow 0$, $f_2 = -1/m$, $f_0 = (-1/z)$ and $K = \bar{K}$ in (5.18), (5.21), (5.23) and (5.26)

$$\bar{K}h(0.5T_p + t_1 - t_p + z) - A_p = 0 \quad (5.53)$$

$$m \left(1 + e^{T_p/m} \right) - 2(m + z) e^{(T_p + t_1 - t_p)/m} = 0 \quad (5.54)$$

$$(\delta + z - 0.5T_p + \varepsilon/\bar{K}h)/m - e^{(t_p - t_0 - T_p)/m} + 1 = 0 \quad (5.55)$$

$$0.5\bar{K}h \left[T_p + m \left(e^{(t_p - t_1 - T_p)/m} - e^{(t_p - t_1)/m} \right) \right] - A_d = 0 \quad (5.56)$$

Hence, the process model parameters \bar{K} , δ , z and m are estimated by solving (5.53) - (5.56) simultaneously.

Example 5

In this example a second order integrating NMP process without time delay [48] is considered as

$$G(s) = \frac{0.25(-s+1)}{s(2s+1)}.$$

Again, from simulation test, the limit cycle quantities $A_p = 0.8921$, $A_d = 0.45$, $T_p = 9.4970$, $t_1 = 1.8804$ and $t_p = 4.0604$ are measured utilizing a relay with height $h = 1$ and hysteresis width $\varepsilon = 0.45$. The process dynamics are identified from simultaneous solution of (5.53), (5.54) and (5.56). Similarly, the process model parameters are estimated in the presence of measurement noise of 10 dB SNR, where the measured quantities of limit cycle are $A_p = 0.8921$, $A_d = 0.45$, $T_p = 9.4969$, $t_1 = 1.8804$ and $t_p = 4.0604$. The identified process models and the model proposed by Panda et al. [48] are mentioned in Table 5.7 and the corresponding % error in model parameters are given in Table 5.8.

Table. 5.7: Comparison of process models for Example 5

Method	Process model
Proposed without noise	$\frac{0.250(-1.0s+1)}{s(2.0s+1)}$
Proposed with noise	$\frac{0.250(-1.0001s+1)}{s(2.0s+1)}$
Panda et al. [48] without noise	$\frac{0.252(-1.0s+1)}{s(2.0s+1)}$

Table. 5.8: Comparison of model parameters in % error

Model	\bar{K}	z	m
Proposed without noise	0	0	0
Proposed with noise	0	-0.01	0
Panda et al. [48] without noise	-0.8	0	0

Example 6

This example considers an integrating SOPDT NMP process [88] with the transfer function

$$G(s) = \frac{(-s+1)e^{-3s}}{s(2s+1)}.$$

Repeating the procedure of above examples, the relay is set to $h = 1$ and $\varepsilon = 0.7$, the limit cycle parameters measured are $A_p = 5.4711$, $A_d = 3.6734$, $T_p = 13.3316$, $t_0 = 0.7147$, $t_1 = 3.7147$ and $t_p = 5.9094$. Substituting these parameters in (5.53) -(5.56) and solved simultaneously to estimate the process model parameters K , δ , z and m . Similarly in the presence of measurement noise of 20 dB SNR the model parameters are obtained using the limit cycle quantities $A_p = 5.4711$, $A_d = 3.6734$, $T_p = 13.3316$, $t_0 = 0.7147$, $t_1 = 3.7147$ and $t_p = 5.9094$. The process models identified and the model suggested by Padhy and Majhi [88] are given in Table 5.9. Similar to above examples, Table 5.10 indicates the % error in process model parameters.

Table. 5.9: Comparison of process models for Example 6

Method	Process model
Proposed without noise	$\frac{1.0(-1.0s+1)e^{-3.0s}}{s(2.0s+1)}$
Proposed with noise	$\frac{1.0(-1.0s+1)e^{-3.0s}}{s(2.0s+1)}$
Padhy and Majhi [88] without noise	$\frac{1.0(-1.0s+1)e^{-3.0s}}{s(1.9992s+1)}$

Table. 5.10: Comparison of model parameters in % error

Model	K	z	m	δ
Proposed without noise	0	0	0	0
Proposed with noise	0	0	0	0
Padhy and Majhi [88] without noise	0	0	0.04	0

5.5 Summary

State space based analytical expressions are derived to identify the process dynamics of NMP processes with and without time delay. A single relay with hysteresis is applied as an input to the process in closed loop to extract process information. The novelty of presented technique lies in generalizing a SOPDT NMP process model and its derived expressions to identify the process dynamics of FOPDT, SOPDT overdamped, underdamped, critically damped and integrating NMP processes. The derived expressions are employed to estimate four accurate parameters at a time. Efficacy of the proposed method is shown with the help of examples taken from the recent literature. Results are tabulated and compared using the percentage error of process model parameters. Robustness of the suggested algorithms is illustrated in the presence of measurement noise.

CHAPTER 6

CONCLUSIONS AND FUTURE WORK

6.1 Conclusions

In recent years, many research work on relay based process identification are presented in the literature. Still there is much scope for improvements and extensions of this method. Briefly, the results are summarized as follows

A. Off-line and on-line identification of SISO processes

A single relay with hysteresis is used in closed loop, to get process information. Using DF method explicit expressions are derived to estimate the SISO process model parameters during off-line and on-line mode of operation. Expressions are derived for generalized process model as well as individual process models. For on-line identification, controller parameters are initially chosen and once the process model is known, suitable controller can be designed. Since measurement noise is a critical issue in process industries, validity of the proposed method is illustrated even under noisy environment. Results are verified with the help of estimation errors and Nyquist plots. These plots indicate good match neighboring the critical point. To test the robustness of the method, process dynamics are identified for different relay settings.

B. Off-line and on-line identification of TITO processes

An attempt is made to identify the process dynamics of TITO processes using DF technique and relay with hysteresis. Identification methods are proposed for on-line as well as off-line mode of operation. The TITO processes are modeled in terms of two SISO process models.

Simulation results are illustrated to show the general usefulness of proposed method.

C. Relay with hysteresis and state space based identification As DF method gives approximate results and estimation of two process model parameters. The corresponding time domain based state space technique is used to derive the expressions ensuring accurate results. Expressions are derived for off-line identification of SISO process dynamics. A generalized SOPDT process model is realized in terms of class of process models and accordingly analytical expressions are derived. As relay with hysteresis reduces the effect of measurement noise, further noise elimination is achieved by using a denoising block in the closed loop with the process and relay. Well known examples are considered to show the efficacy of the presented work. Results are compared using estimation error values and Nyquist plots.

D. Identification of processes with non-minimum phase characteristics

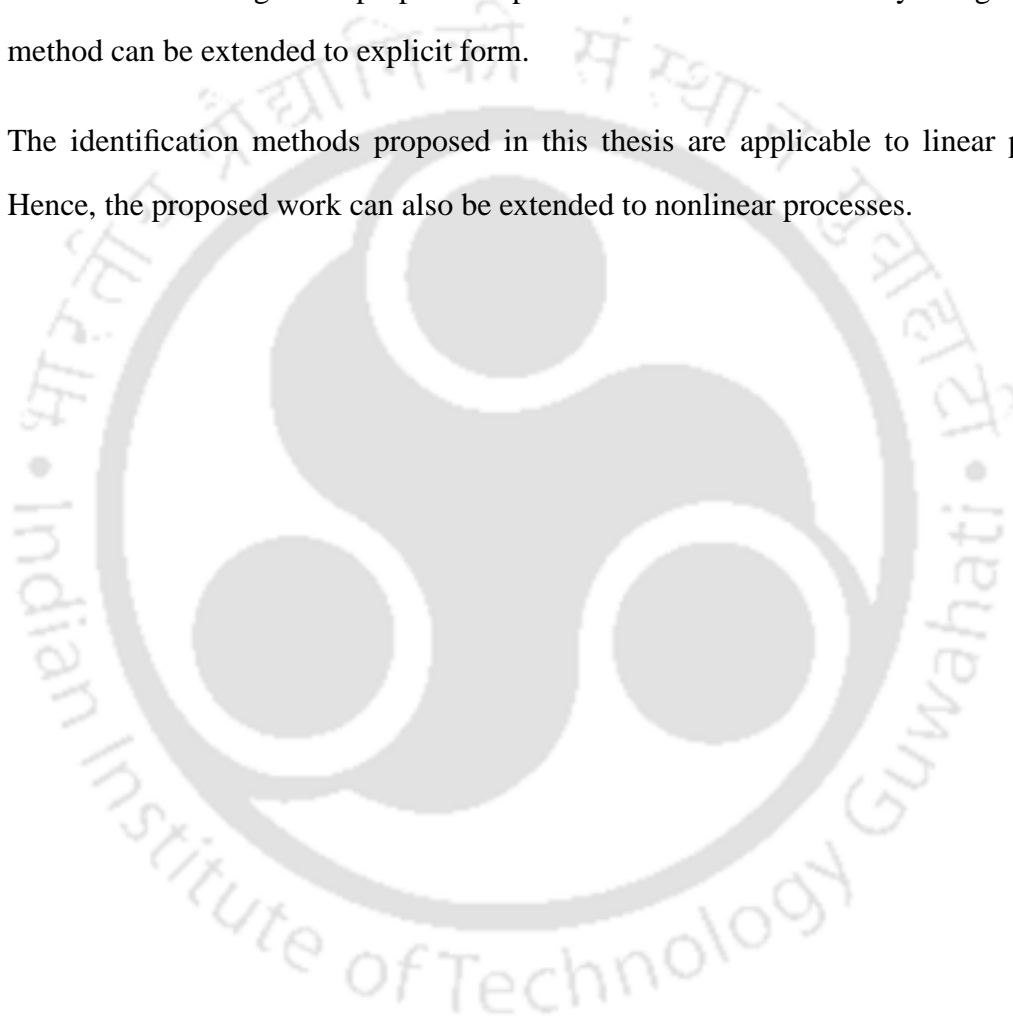
State space technique is extended to identify the process dynamics of SISO NMP processes during off-line mode of operation. Mathematical expressions are derived for stable SOPDT NMP process model which is realized in terms of FOPDT, SOPDT overdamped, underdamped, critically damped and integrating NMP process models. Proposed method is tested even in the face of measurement noise. Simulation results are compared with recent methods using % error of process model parameters.

6.2 Suggestions for further work

Following the design methods described in this thesis, there are several directions in which the presented work can be extended and further investigated. Some of them are enumerated below:

- In the proposed work DF technique is used to identify the process dynamics during off-line and on-line mode of operation and state space method is used for off-line identification. Hence, state space method can be extended for on-line identification so that accurate process dynamics are identified.

- Similarly, presented work can be extended to identify TITO processes using time domain approach.
- In the present work for on-line identification, initial controller parameters are chosen based on many simulation results. Hence, a model based controller design can be carried out.
- It will be interesting if the proposed expressions which are derived by using state space method can be extended to explicit form.
- The identification methods proposed in this thesis are applicable to linear processes. Hence, the proposed work can also be extended to nonlinear processes.



APPENDIX A

SUPPLEMENTARY MATERIALS

A.1 Detailed derivation of the expression (2.1)

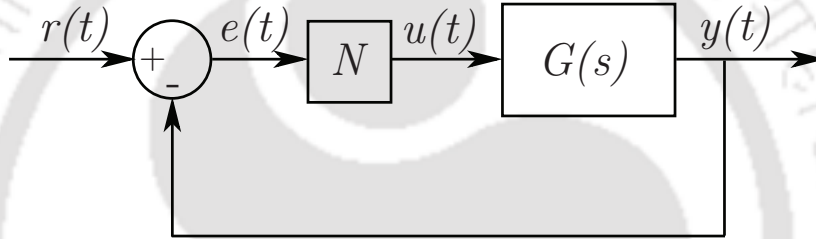


Figure A.1: Nonlinear feedback scheme

Let us consider a nonlinear feedback scheme as shown in Fig. A.1 which consists of a linear transfer function $G(s)$ and a nonlinear element N (relay with hysteresis). If the input signal to the nonlinear element is a sinusoidal wave then,

$$e(t) = A_p \sin(\omega t) \quad (\text{A.1})$$

or

$$e(t) = A_p \sin(\theta) \quad (\text{A.2})$$

where A_p is the peak amplitude and ω the fundamental frequency of the relay input signal. The presence of hysteresis in the relay, makes the output $u(t)$ to get the value of $\pm h$ according to whether $e > \varepsilon$, or $e < -\varepsilon$ on the last instant when $|e| > \varepsilon$. Then, the output of the relay is given

by

$$u(\theta) = \begin{cases} -h & 0 < \theta < \theta_0 \\ +h & \theta_0 < \theta < \pi + \theta_0 \\ -h & \pi + \theta_0 < \theta < 2\pi \end{cases} \quad (\text{A.3})$$

where

$$\theta_0 = \sin^{-1} \left(\frac{\varepsilon}{A_p} \right) \quad (\text{A.4})$$

As the describing function analysis provides a tool for frequency domain analysis of the non-linear system hence, the DF is obtained with the consideration of only the principal harmonic of the relay output signal. Therefore the relay with hysteresis is approximated by a gain of

$$N = \frac{1}{\pi A_p} \int_0^{2\pi} u(\theta) (\sin \theta + j \cos \theta) d\theta \quad (\text{A.5})$$

or

$$N = \frac{1}{\pi A_p} \left[\int_0^{2\pi} u(\theta) \sin \theta d\theta + j \int_0^{2\pi} u(\theta) \cos \theta d\theta \right] \quad (\text{A.6})$$

let

$$\lambda_1 = \int_0^{2\pi} u(\theta) \cos \theta d\theta \quad (\text{A.7})$$

and

$$\lambda_2 = \int_0^{2\pi} u(\theta) \sin \theta d\theta \quad (\text{A.8})$$

in (A.6) which is represented as

$$N = \frac{1}{\pi A_p} [\lambda_2 + j\lambda_1] \quad (\text{A.9})$$

The solution of the constants λ_1 and λ_2 are found by using (A.3) as given below

$$\lambda_1 = \int_0^{\theta_0} -h \cos \theta d\theta + \int_{\theta_0}^{\pi+\theta_0} h \cos \theta d\theta + \int_{\pi+\theta_0}^{2\pi} -h \cos \theta d\theta \quad (\text{A.10})$$

on further simplification we get

$$\lambda_1 = -4h \sin \theta_0 \quad (\text{A.11})$$

Similarly

$$\lambda_2 = \int_0^{\theta_0} -h \sin \theta d\theta + \int_{\theta_0}^{\pi+\theta_0} h \sin \theta d\theta + \int_{\pi+\theta_0}^{2\pi} -h \sin \theta d\theta \quad (\text{A.12})$$

resolving the above equation one obtains

$$\lambda_2 = 4h \cos \theta_0 \quad (\text{A.13})$$

Substituting (A.11) and (A.13) in (A.9) to get

$$N = \frac{4h}{\pi A_p} [\cos \theta_0 - j \sin \theta_0] \quad (\text{A.14})$$

Using the corresponding value of θ_0 from (A.4) in the above equation and resolving we get the DF of relay with hysteresis as

$$N = \frac{4h \left(\sqrt{A_p^2 - \varepsilon^2} - j\varepsilon \right)}{\pi A_p^2} \quad (\text{A.15})$$

A.2 Detailed derivation of the expressions (4.7) and (4.8)

Let us represent the transfer function given in (4.2) as

$$\frac{y(s)}{u(s)e^{-\delta s}} = \frac{\pm K f_1 f_2}{(s - f_1)(s - f_2)} \quad (\text{A.16})$$

Taking partial fractions of the above equation and resolving we get

$$\frac{y(s)}{u(s)e^{-\delta s}} = a \left[\frac{1}{(s - f_1)} - \frac{1}{(s - f_2)} \right] \quad (\text{A.17})$$

where

$$a = \frac{\pm K f_1 f_2}{f_1 - f_2} \quad (\text{A.18})$$

Representing (A.17) in the following form

$$\frac{y_1(s)}{u(s)e^{-\delta s}} + \frac{y_2(s)}{u(s)e^{-\delta s}} = \frac{a}{(s - f_1)} - \frac{a}{(s - f_2)} \quad (\text{A.19})$$

or

$$y_1(s)(s - f_1) = au(s)e^{-\delta s} \quad (\text{A.20})$$

$$y_2(s)(s - f_2) = -au(s)e^{-\delta s} \quad (\text{A.21})$$

Taking inverse Laplace transform of (A.20) and (A.21), following two equations are obtained, respectively

$$\dot{y}_1(t) - f_1 y_1(t) = au(t - \delta) \quad (\text{A.22})$$

$$\dot{y}_2(t) - f_2 y_2(t) = -au(t - \delta) \quad (\text{A.23})$$

Let

$$x_1(t) = y_1(t); \quad x_2(t) = y_2(t) \quad (\text{A.24})$$

Hence, (A.22) and (A.23) are modified to

$$\dot{x}_1(t) = f_1 x_1(t) + au(t - \delta) \quad (\text{A.25})$$

$$\dot{x}_2(t) = f_2 x_2(t) - au(t - \delta) \quad (\text{A.26})$$

which can be represented in the following state space equations

$$\begin{bmatrix} \dot{x}_1(t) \\ \dot{x}_2(t) \end{bmatrix} = \begin{bmatrix} f_1 & 0 \\ 0 & f_2 \end{bmatrix} \begin{bmatrix} x_1(t) \\ x_2(t) \end{bmatrix} + \begin{bmatrix} a \\ -a \end{bmatrix} u(t - \delta) \quad (\text{A.27})$$

$$y(t) = y_1(t) + y_2(t) = x_1(t) + x_2(t) \quad (\text{A.28})$$

or

$$y(t) = \begin{bmatrix} 1 & 1 \end{bmatrix} \mathbf{x}(t) \quad (\text{A.29})$$

Representing (A.27) and (A.29) in the following state space form

$$\dot{\mathbf{x}}(t) = \mathbf{A}\mathbf{x}(t) + \mathbf{b}u(t - \delta) \quad (\text{A.30})$$

$$y(t) = \mathbf{c}\mathbf{x}(t) \quad (\text{A.31})$$

Hence,

$$\mathbf{A} = \begin{bmatrix} f_1 & 0 \\ 0 & f_2 \end{bmatrix}; \mathbf{b} = \begin{bmatrix} a \\ -a \end{bmatrix}; \mathbf{c} = \begin{bmatrix} 1 & 1 \end{bmatrix} \quad (\text{A.32})$$

A.3 Detailed derivation of the expressions (5.11) and (5.12)

Let us reconsider the transfer function given in (5.7) in the following form

$$\frac{y(s)}{u(s)e^{-\delta s}} = \frac{K f_1 f_2 (s + f_0)}{f_0 (s - f_1) (s - f_2)} \quad (\text{A.33})$$

Taking partial fractions of the above equation and further simplifying we get

$$\frac{y(s)}{u(s)e^{-\delta s}} = a \left[\frac{(f_0 + f_1)}{(s - f_1)} - \frac{(f_0 + f_2)}{(s - f_2)} \right] \quad (\text{A.34})$$

where

$$a = \frac{K f_1 f_2}{f_0 (f_1 - f_2)} \quad (\text{A.35})$$

Representing (A.34) as

$$\frac{y_1(s)}{u(s)e^{-\delta s}} + \frac{y_2(s)}{u(s)e^{-\delta s}} = \frac{a(f_0 + f_1)}{(s - f_1)} - \frac{a(f_0 + f_2)}{(s - f_2)} \quad (\text{A.36})$$

or

$$y_1(s)(s - f_1) = a(f_0 + f_1)u(s)e^{-\delta s} \quad (\text{A.37})$$

$$y_2(s)(s - f_2) = -a(f_0 + f_2)u(s)e^{-\delta s} \quad (\text{A.38})$$

Taking inverse Laplace transform of (A.37) and (A.38), we get following two equations, respectively

$$\dot{y}_1(t) - f_1 y_1(t) = a(f_0 + f_1)u(t - \delta) \quad (\text{A.39})$$

$$\dot{y}_2(t) - f_2 y_2(t) = -a(f_0 + f_2)u(t - \delta) \quad (\text{A.40})$$

Let

$$x_1(t) = y_1(t); \quad x_2(t) = y_2(t) \quad (\text{A.41})$$

Hence, (A.39) and (A.40) are modified to

$$\dot{x}_1(t) = f_1 x_1(t) + a(f_0 + f_1)u(t - \delta) \quad (\text{A.42})$$

$$\dot{x}_2(t) = f_2 x_2(t) + a(f_0 + f_2)u(t - \delta) \quad (\text{A.43})$$

or representing in the following state space equations

$$\begin{bmatrix} \dot{x}_1(t) \\ \dot{x}_2(t) \end{bmatrix} = \begin{bmatrix} f_1 & 0 \\ 0 & f_2 \end{bmatrix} \begin{bmatrix} x_1(t) \\ x_2(t) \end{bmatrix} + \begin{bmatrix} a(f_0 + f_1) \\ -a(f_0 + f_2) \end{bmatrix} u(t - \delta) \quad (\text{A.44})$$

or

$$\begin{bmatrix} \dot{x}_1(t) \\ \dot{x}_2(t) \end{bmatrix} = \begin{bmatrix} f_1 & 0 \\ 0 & f_2 \end{bmatrix} \begin{bmatrix} x_1(t) \\ x_2(t) \end{bmatrix} + \begin{bmatrix} \frac{K f_1 f_2 (f_0 + f_1)}{f_0 (f_1 - f_2)} \\ -\frac{K f_1 f_2 (f_0 + f_2)}{f_0 (f_1 - f_2)} \end{bmatrix} u(t - \delta) \quad (\text{A.45})$$

$$y(t) = y_1(t) + y_2(t) = x_1(t) + x_2(t) \quad (\text{A.46})$$

or

$$y(t) = \begin{bmatrix} 1 & 1 \end{bmatrix} \mathbf{x}(t) \quad (\text{A.47})$$

A.4 Procedure to use *fsolve* function

Fsolve is a MATLAB [90] function, which solves a set of nonlinear equations simultaneously as explained below with an example.

Fsolve is used to solve a problem specified by $F(x) = 0$, for x , where x is a vector and $F(x)$ a function that returns a vector value. The following syntax is used in our presented work

$$x = fsolve(fun, x0, options)$$

which solves the equations with the optimization options specified in the structure options. To set these options, the below mentioned syntax is used

$$options = optimset('Display', 'iter')$$

which displays the output.

In *fsolve* syntax, *fun* is a function that accepts a vector x and returns a vector F , the nonlinear equations evaluated at x . The function *fun* can be specified as a function handle for a file

```
 $x = fsolve(@myfun, x0),$ 
```

where *myfun* is a MATLAB function such as

```
function F = myfun(x)
```

```
F = ...
```

to compute function values at x .

The *fsolve* function applied in Example 3 of Chapter 4 to estimate the FOPDT process model parameters τ_1 and K is explained below.

First we write a file that computes F , the values of the equations at x . The MATLAB code is given below:

```
function F = myfun(x)
```

```
h = 1; Ap = 0.2631; Tp = 5.3897; δ = 2.0; ε = 0.1;
```

```
F = [x(2) * h * tanh(0.5 * Tp / (x(1))) - Ap;
```

```
x(2) * h * (1 - (2 * exp(δ / x(1)) / (1 + exp(Tp / x(1)))) - ε];
```

where $x(1) = \tau_1$ and $x(2) = K$.

The above function file is saved as *myfun.m* on MATLAB path. Then, the initial point and options are set up and *fsolve* is called as given in the following code

```
 $x0 = [2; 1];$  make a starting guess at the solution
```

```
options = optimset('Display', 'iter');
```

```
[x, fval] = fsolve(@myfun, x0, options); call solver
```

The above code is run to calculate the parameters τ_1 and K . After several iterations, *fsolve* finds an answer as:

```
 $x(1) = 9.9957$ 
```

```
 $x(2) = 0.9994$ 
```

hence, $\tau_1 = 9.9957$ and $K = 0.9994$ are estimated.

Regarding choosing initial values for $x0$, the values are varied from $[1; 1]$ to $[20; 20]$ and it is observed that $x(1)$ varied from 9.9954 to 9.9957 but for most of the values it is 9.9957 and $x(2)$

remained at 0.9994. Or the explicit expressions proposed in Chapter 2 can be used to select the initial values.

Fsolve may converge to a non-zero point and generate the following message:

Optimizer is stuck at a minimum that is not a root, try again with a new starting guess.

In this case, *fsolve* is run again with other starting values.

Similarly, *fsolve* is used in other examples where a set of nonlinear equations need to be solved simultaneously.



REFERENCES

- [1] S. Majhi, "Relay-based identification of a class of nonminimum phase SISO processes," *IEEE Transactions on Automatic Control*, vol. 52, pp. 134–139, 2007.
- [2] K. Lavanya, B. Umamaheswari, and R. C. Panda, "Identification of second order plus dead time systems using relay feedback test," *Indian Chemical Engineer*, vol. 48(2), pp. 94–102, 2006.
- [3] T. Thyagarajan and C. C. Yu, "Improved auto tuning using shape factor from relay feedback," *Ind. Eng. Chem. Res.*, vol. 42, pp. 4425–4440, 2003.
- [4] P. K. Padhy, S. Majhi, and D. P. Atherton, "PID-P controller for TITO systems," *Proceedings of the 16th IFAC World Congress, Czech Republic*, vol. 16, no. 1, pp. 54–59, 2005.
- [5] T. Liu and F. Gao, "Alternative identification algorithms for obtaining a first-order stable/unstable process model from a single relay feedback test," *Ind. Eng. Chem. Res.*, vol. 47, pp. 1140–1149, 2008.
- [6] S. Vivek and M. Chidambaram, "An improved relay auto tuning of PID controllers for unstable FOPTD systems," *Comp. Chem. Eng.*, vol. 29, pp. 2060–2068, 2005.
- [7] C. C. Yu, *Autotuning of PID controllers - A relay feedback approach*. Second ed., Springer-Verlag, London, 1999.
- [8] Q. G. Wang, T. H. Lee, and L. Chong, *Relay feedback: Analysis, Identification and Control*. Springer-Verlag, London, 2003.
- [9] S. Majhi, *Advanced control theory - A relay feedback approach*. Cengage Learning India Pvt. Ltd., India, 2009.
- [10] K. J. Åström and T. Hägglund, "Automatic tuning of simple regulators with specifications on phase and amplitude margins," *Automatica*, vol. 20, no. 5, pp. 645–651, 1984.

- [11] W. L. Luyben, "Derivations of transfer functions for highly non-linear distillation columns," *Ind. Eng. Chem. Res.*, vol. 26, pp. 2490–2495, 1987.
- [12] S. H. Shen, J. S. Wu, and C. C. Yu, "Use of biased-relay feedback for system identification," *AIChE Journal*, vol. 42, pp. 1174–1180, 1996.
- [13] G. Marchetti, C. Scali, and D. R. Lewin, "Identification and control of open loop unstable processes by relay methods," *Automatica*, vol. 37, pp. 2049–2055, 2001.
- [14] P. K. Padhy and S. Majhi, "Relay based PI-PD design for stable and unstable FOPDT processes," *Comp. Chem. Eng.*, vol. 30, pp. 790–796, 2006.
- [15] K. K. Tan, T. H. Lee, S. Huang, K. Y. Chua, and R. Ferdous, "Improved critical point estimation using a preload relay," *Journal of Process Control*, vol. 16, no. 5, pp. 445–455, 2006.
- [16] W. K. Ho, E. B. Feng, and O. P. Gan, "A novel relay auto-tuning technique for processes with integration," *Control Engineering Practice*, vol. 4, no. 7, pp. 923–928, 1996.
- [17] R. C. Chang, S. H. Shen, and C. C. Yu, "Derivations of transfer functions from relay feedback systems," *Ind. Eng. Chem. Res.*, vol. 31, pp. 855–860, 1992.
- [18] W. Li, E. Eskinat, and W. L. Luyben, "An improved auto tune identification method," *Ind. Eng. Chem. Res.*, vol. 30, pp. 1530–1541, 1991.
- [19] T. Liu, Q. G. Wang, and H. P. Huang, "A tutorial review on process identification from step or relay feedback test," *Journal of Process Control*, vol. 23, no. 10, pp. 1597–1623, 2013.
- [20] D. P. Atherton, "Relay autotuning: an overview and alternative approach," *Ind. Eng. Chem. Res.*, vol. 45(12), pp. 4075–4080, 2006.
- [21] C. C. Hang, K. J. Åström, and Q. G. Wang, "Relay feedback auto-tuning of process controllers - a tutorial review," *Journal of Process Control*, vol. 12, no. 1, pp. 143–162, 2002.
- [22] D. Kumanan and B. Nagaraj, "Tuning of proportional integral derivative controller based on firefly algorithm," *Systems Science & Control Engineering*, vol. 1, no. 1, pp. 52–56, 2013.
- [23] Q. G. Wang, B. Zou, T. H. Lee, and Q. Bi, "Auto tuning of multi variable PID controller from decentralized relay feedback," *Automatica*, vol. 33, pp. 319–330, 1997.

- [24] P. Nordfeldt and T. Hägglund, "Decoupler and PID controller design of TITO systems," *Journal of Process Control*, vol. 16, no. 9, pp. 923–936, 2006.
- [25] B. T. Jevtović and M. R. Mataušek, "PID controller design of TITO system based on ideal decoupler," *Journal of Process Control*, vol. 20, no. 7, pp. 869–876, 2010.
- [26] J. Y. Choi, J. Lee, J. H. Jung, M. Lee, and C. Han., "Sequential loop closing identification of multivariable process model," *Comp. Chem. Eng.*, vol. 24, pp. 809–814, 2000.
- [27] P. K. Padhy and S. Majhi, "Closed loop identification of TITO systems," *Proceedings of SICPRO, Moscow*, pp. 846–856, 2005.
- [28] P. Grosdidier and M. Morari, "Interaction measures for systems under decentralized control," *Automatica*, vol. 22, no. 3, pp. 309–319, 1986.
- [29] S. H. Shen and C. C. Yu, "Use of relay feedback test for automatic tuning of multivariable systems," *AIChE journal*, vol. 40, pp. 627–646, 1994.
- [30] S. Tavakoli, I. Griffin, and P. J. Fleming, "Tuning of decentralised PI (PID) controllers for TITO processes," *Control Engineering Practice*, vol. 14, no. 9, pp. 1069–1080, 2006.
- [31] Z. J. Palmor, Y. Halevi, and N. Krasney, "Automatic tuning of decentralized PID controllers for TITO processes," *Automatica*, vol. 31, no. 7, pp. 1001–1010, 1995.
- [32] A. P. Loh, C. C. Hang, C. K. Quek, and V. U. Vasnani, "Autotuning of multiloop proportional-integral controllers using relay feedback," *Ind. Eng. Chem. Res.*, vol. 32, pp. 1102–1107, 1993.
- [33] D. K. Maghade and B. M. Patre, "Decentralized PI/PID controllers based on gain and phase margin specifications for TITO processes," *ISA Transactions*, vol. 51, no. 4, pp. 550–558, 2012.
- [34] K. J. Åström and P. Eykhoff, "System identification-a survey," *Automatica*, vol. 7, no. 2, pp. 123–162, 1971.
- [35] Q. G. Wang, C. C. Hang, and B. Zou, "Low order modeling from relay feedback," *Ind. Eng. Chem. Res.*, vol. 36, pp. 375–381, 1997.
- [36] A. Jahanmiri and H. R. Fallahi, "New methods for process identification and design of feedback controller," *Chemical Engineering Research and Design*, vol. 75, pp. 519–522, 1997.

- [37] S. Majhi and D. P. Atherton, "Autotuning and controller design for processes with small time delays," *IEE Proceedings on Control Theory and Applications*, vol. 146, pp. 415–425, 1999.
- [38] S. Majhi, "On-line PI control of stable processes," *Journal of Process Control*, vol. 15, pp. 859–867, 2005.
- [39] —, "Relay based identification of processes with time delay," *Journal of Process Control*, vol. 17, pp. 93–101, 2007.
- [40] S. Majhi and C. Mahanta, "Tuning of controllers for integrating time delay processes," *Proceedings of the IEEE TENCON, Singapore*, pp. 317–320, 2001.
- [41] K. Srinivasan and M. Chidambaram, "Modified relay feedback method for improved system identification," *Comp. Chem. Eng.*, vol. 27, pp. 727–732, 2003.
- [42] S. Vivek and M. Chidambaram, "Identification using single symmetrical relay feedback test," *Comp. Chem. Eng.*, vol. 29, pp. 1625–1630, 2005.
- [43] R. C. Panda and C. C. Yu, "Shape factor of relay response curves and its use in autotuning," *Journal of Process Control*, vol. 15, no. 8, pp. 893–906, 2005.
- [44] R. C. Panda, "Estimation of parameters of under-damped second order plus dead time processes using relay feedback," *Comp. Chem. Eng.*, vol. 30, pp. 832–837, 2006.
- [45] U. Mehta and S. Majhi, "On-line identification of cascade control systems based on half limit cycle data," *ISA Transactions*, vol. 50, pp. 473–478, 2011.
- [46] S. Majhi and D. P. Atherton, "Online tuning of controllers for an unstable FOPDT process," *IEE Proceedings on Control Theory and Applications*, vol. 147, pp. 421–427, 2000.
- [47] T. Liu and F. Gao, "Identification of integrating and unstable processes from relay feedback," *Comp. Chem. Eng.*, vol. 32, pp. 3038–3056, 2008.
- [48] R. C. Panda, V. Vijayan, V. Sujatha, P. Deepa, D. Manamali, and A. B. Mandal, "Parameter estimation of integrating and time delay processes using single relay feedback test," *ISA Transactions*, vol. 50, pp. 529–537, 2011.

- [49] G. Fedele, "A new method to estimate a first-order plus time delay model from step response," *Journal of the Franklin Institute*, vol. 346, no. 1, pp. 1–9, 2009.
- [50] B. A. L. D. L. Barra and M. Mossberg, "Identification of under-damped second-order systems using finite duration rectangular pulse inputs," *Proceedings of American Control Conference (ACC), New York City, USA*, pp. 834–839, 2007.
- [51] H. Mei and S. Li, "Decentralized identification for multivariable integrating processes with time delays from closed-loop step tests," *ISA Transactions*, vol. 46, no. 2, pp. 189–198, 2007.
- [52] T. Liu and F. Gao, "Closed-loop step response identification of integrating and unstable processes," *Chemical Engineering Science*, vol. 65, no. 10, pp. 2884–2895, 2010.
- [53] U. Mehta and S. Majhi, "Identification of a class of Wiener and Hammerstein-type nonlinear processes with monotonic static gains," *ISA Transactions*, vol. 49, pp. 501–509, 2010.
- [54] D. G. Padhan and S. Majhi, "A new control scheme for PID load frequency controller of single-area and multi-area power systems," *ISA Transactions*, vol. 52, no. 2, pp. 242–251, 2013.
- [55] S. Vivek and M. Chidambaram, "An improved relay auto tuning of PID controllers for critically damped SOPTD systems," *Chemical Engineering Communications*, vol. 199, pp. 1437–1462, 2012.
- [56] I. Ananth and M. Chidambaram, "Closed-loop identification of transfer function model for unstable systems," *Journal of the Franklin Institute*, vol. 336, no. 7, pp. 1055–1061, 1999.
- [57] E. Cheres, "Parameter estimation of an unstable system with a PID controller in a closed loop configuration," *Journal of the Franklin Institute*, vol. 343, no. 2, pp. 204–209, 2006.
- [58] R. PadmaSree and M. Chidambaram, "Improved closed loop identification of transfer function model for unstable systems," *Journal of the Franklin Institute*, vol. 343, no. 2, pp. 152–160, 2006.
- [59] W. L. Luyben, "Getting more information from relay-feedback tests," *Ind. Eng. Chem. Res.*, vol. 40, pp. 4391–4402, 2001.
- [60] I. Boiko, "Autotune identification via the locus of a perturbed relay system approach," *IEEE Transactions on Control Systems Technology*, vol. 16, no. 1, pp. 182–185, 2008.

- [61] E. Sivakumar, S. Vivek, and M. Chidambaram, "Improved saturation relay test for systems with large dead time," *Ind. Eng. Chem. Res.*, vol. 44, pp. 2183–2190, 2005.
- [62] D. P. Atherton and S. Majhi, "Plant parameter identification under relay control," *Proceedings of the 37th IEEE Conference on Decision & Control Tampa, Florida USA*, pp. 1272–1277, 1998.
- [63] R. Zhang, Y. Chen, Z. Sun, F. Sun, and H. Xu, "Path control of a surface ship in restricted waters using sliding mode," *IEEE Transactions on Control Systems Technology*, vol. 8, no. 4, pp. 722–732, 2000.
- [64] S. H. Shen, H. D. Yu, and C. C. Yu, "Autotune identification for systems with right-half-plane poles and zeros," *Journal of Process Control*, vol. 9, pp. 161–169, 1999.
- [65] P. Balaguer, V. Alfaro, and O. Arrieta, "Second order inverse response process identification from transient step response," *ISA Transactions*, vol. 50, no. 2, pp. 231–238, 2011.
- [66] Q. G. Wang, Y. Zhang, and X. Guo, "Robust closed-loop identification with application to auto-tuning," *Journal of Process Control*, vol. 11, no. 5, pp. 519–530, 2001.
- [67] T. Liu and F. Gao, "A generalized relay identification method for time delay and non-minimum phase processes," *Automatica*, vol. 45, no. 4, pp. 1072–1079, 2009.
- [68] V. Ramakrishnan and M. Chidambaram, "Estimation of a SOPTD transfer function model using a single asymmetrical relay feedback test," *Comp. Chem. Eng.*, vol. 27, pp. 1779–1784, 2003.
- [69] S. Vivek and M. Chidambaram, "Estimation of five parameters of an unstable SOPTD model with a zero using a single relay feedback test," *Indian Chemical Engineer*, vol. 54, pp. 79–96, 2012.
- [70] J. Lee, J. S. Kim, J. Byeon, S. W. Sung, and T. F. Edgar, "Relay feedback identification for processes under drift and noisy environments," *AIChE Journal*, vol. 57, no. 7, pp. 1809–1816, 2011.
- [71] C. L. Chen, "A simple method for on-line identification and controller tuning," *AIChE Journal*, vol. 35, no. 12, pp. 2037–2039, 1989.
- [72] I. Kaya and D. P. Atherton, "Parameter estimation from relay autotuning with asymmetric limit cycle data," *Journal of Process Control*, vol. 11, pp. 429–439, 2001.

- [73] C. Scali, G. Marchetti, and D. Semino, "Relay with additional delay for identification and autotuning of completely unknown processes," *Ind. Eng. Chem. Res.*, vol. 38, pp. 1987–1997, 1999.
- [74] A. Leva, "Model-based proportional-integral-derivative autotuning improved with relay feedback identification," *IEE Proceedings on Control Theory and Applications*, vol. 152, no. 2, pp. 247–256, 2005.
- [75] M. R. Mataušek and T. B. Šekara, "A fast closed-loop process dynamics characterization," *ISA Transactions*, vol. 53, no. 2, pp. 489–496, 2014.
- [76] H. P. Huang, J. C. Jeng, C. H. Chiang, and W. Pan, "A direct method for multi-loop PI/PID controller design," *Journal of Process Control*, vol. 13, no. 8, pp. 769–786, 2003.
- [77] S. Y. Li, W. J. Cai, H. Mei, and Q. Xiong, "Robust decentralized parameter identification for two-input two-output process from closed-loop step responses," *Control Engineering Practice*, vol. 13, no. 4, pp. 519–531, 2005.
- [78] Q. G. Wang, B. Huang, and X. Guo, "Auto tuning of TITO decoupling controllers from step tests," *ISA Transactions*, vol. 39, no. 3, pp. 407–418, 2000.
- [79] M. Zhuang and D. P. Atherton, "PID controller design for a TITO system," *IEE Proceedings on Control Theory and Applications*, vol. 141, pp. 111–120, 1994.
- [80] S. W. Sung and J. Lee, "Relay feedback method under large static disturbances," *Automatica*, vol. 42, no. 2, pp. 353–356, 2006.
- [81] R. C. Panda and C. C. Yu, "Analytical expressions for relay feedback responses," *Journal of Process Control*, vol. 13, pp. 489–501, 2003.
- [82] T. Liu, F. Gao, and Y. Wang, "A systematic approach for on-line identification of second order process model from relay feedback test," *AIChE Journal*, vol. 54, no. 6, pp. 1560–1578, 2008.
- [83] J. Lee, S. W. Sung, and T. F. Edgar, "Integrals of relay feedback responses for extracting process information," *AIChE Journal*, vol. 53, no. 9, pp. 2329–2338, 2007.
- [84] J. S. Kim, J. Byeon, D. Chun, S. W. Sung, and J. Lee, "Relay feedback methods for noisy processes," *ICCAS-SICE International Joint Conference, Fukuoka International Congress Center, Japan*, pp. 2793–2796, 2009.

- [85] S. Majhi, V. Kotwal, and U. Mehta, "FPAA-based PI controller for DC servo position control system," *IFAC Conference on Advances in PID Control, Brescia Italy*, pp. 1–5, 2012.
- [86] K. J. Åström and R. D. Bell, "Drum-boiler dynamics," *Automatica*, vol. 36 (3), pp. 363–378, 2000.
- [87] D. Gu, L. Ou, P. Wang, and W. Zhang, "Relay feedback autotuning method for integrating processes with inverse response and time delay," *Ind. Eng. Chem. Res.*, vol. 45 (9), pp. 3119–3132, 2006.
- [88] P. K. Padhy and S. Majhi, "Exact analysis for the identification of non-minimum phase processes," *Journal of The Franklin Institute*, vol. 348, no. 10, pp. 2734–2743, 2011.
- [89] T. Liu and F. Gao, "A frequency domain step response identification method for continuous-time processes with time delay," *Journal of Process Control*, vol. 20, no. 7, pp. 800–809, 2010.
- [90] "MATLAB," *The Mathworks Inc.*, 2013.